**Projecte Final d'Estudis
MÀSTER
EN
ENGINYERIA BIOMÈDICA**

EB

A NEW KINEMATIC AND DYNAMIC MODEL FOR CLINICAL EVALUATION OF THE UPPER EXTREMITY MOTION DURING AN ACTIVITY OF DAILY LIVING IN SUBJECTS WITH NEUROLOGICAL DISORDERS

Barcelona, 5 de Setembre del 2011

Autor: Joan Lobo Prat

Directors: Dr. Josep Maria Font Llagunes
            Dra. Rosa Angulo Barroso
            Dr. Josep Medina Casanovas

Realitzat a: Institut Guttmann

UNIVERSITAT POLITÈCNICA
DE CATALUNYA

UNIVERSITAT DE BARCELONA

Data de registre: 09/05/11

MÀSTER ENGINYERIA BIOMÈDICA

Registre Projecte Final d'Estudis

NOM DE L'ALUMNE: JOAN LOBO PRAT

TÍTOL DEL PROJECTE: A new kinematic and dynamic model for clinical evaluation of the upper extremity motion during an Activity of Daily Living in subjects with neurological disorders.

N DNI: 11501331
DNI: 47799716

DIRECTOR/S DEL PROJECTE:
(Indiqueu Centre, Departament, Empresa, Hospital, etc. on està vinculat el director)

Dra. Rosa Angulo Barroso.
Dep. de Salut i Ciències Aplicades.
Institut Nacional d'Educació Física de Catalunya (INEFC).

Dr. Josep Medina Casanovas
Cap de Rehabilitació Funcional
Institut Guttmann Hospital de Neurorehabilitació

Dr. Josep Mª Font Llagunes
Departament d'Enginyeria Mecànica.
Universitat Politècnica de Catalunya (UPC).

Dra. Rosa Angulo Barroso   Dr. Josep Medina Casanovas   Dr. Josep Mª Font Llagunes

Signatura de l'alumne
Joan Lobo Prat

Dr. Pere Caminal   Dr. Josep Samitier
Coordinador UPC   Coordinador UB
Màster Enginyeria Biomèdica   Màster Enginyeria Biomèdica

To Subjects 04, 05 and 06.

Resum

Les lesions del sistema nerviós tenen un impacte considerable en els aspectes bio-psico-socials del pacient perquè poden provocar grans discapacitats i dèficits funcionals i cognitius. Les Lesions Medul·lars Cervicals i el Dany Cerebral Adquirit acostumen a causar una reducció notable de la funcionalitat de l'extremitat superior, la qual cosa complica o fins i tot limita la realització d'Activitats de la Vida Diària bàsiques. La neurorehabilitació en hospitals especialitzats és, avui en dia, l'única alternativa pel tractament de pacients amb lesions d'origen neurològic com ara la Lesió Medul·lar i el Dany Cerebral Adquirit. L'evolució dels pacients durant el complex procés de rehabilitació ha d'estar sistemàticament avaluada. La valoració clínica de la funcionalitat de les extremitats superiors està, malauradament, menys desenvolupada que la de les extremitats inferiors i, actualment, és massa depenent de l'observació subjectiva i qualitativa del moviment i basada en una comprensió intuïtiva del moviment humà. La quantificació objectiva del procés de rehabilitació és necessària per tal de millorar els mètodes de tractament i les estratègies de rehabilitació, i també per a prevenir lesions. Aquesta memòria presenta una metodologia pràctica per a la valoració objectiva i quantitativa de l'extremitat superior en subjectes amb lesions d'origen neurològic i en especial en subjectes tetraplègics amb lesió medul·lar completa o incompleta al nivell cervical C5-C6 i que han estat sotmesos a una transposició tendinosa. El nucli del projecte és l' elaboració d'un nou model biomecànic de sòlids rígids per a portar a terme anàlisis cinemàtiques i dinàmiques del moviment de l'extremitat superior, durant la realització d'una Activitat de la Vida Diària i a partir de dades obtingudes amb un sistema optoelectrònic. A més a més del model, la memòria descriu una nova metodologia adequada per a l'adquisició de les dades del moviment de l'extremitat superior, i una cadena de processat i anàlisi dissenyades per a la presentació d'informació de la biomecànica rellevant als especialistes de la rehabilitació.

El nou model biomecànic de l'extremitat superior està format per 10 segments amb un total de 20 graus de llibertat. El model de marcadors combina els avantatges dels marcadors dels segments i dels marcadors de les articulacions per a la definició dels centres articulars i la determinació de les rotacions dels segments. El model biomecànic fa possible una anàlisi cinemàtica i dinàmica integral que millora la valoració de la funcionalitat de l'extremitat superior. A diferència dels models descrits prèviament en la literatura, el model presentat és capaç d'analitzar la pinça entre la primera falange del dit polze i la primer falange del dit índex, la qual és considerada un moviment crucial pels clínics.

Les mesures biomecàniques resultants (cinemàtica i dinàmica dels segments i articulacions, trajectòries de les articulacions i dels centres de massa), són presentades en un informe seguint estàndards clínics i proporcionen valuosa informació als clínics per tal d'aconseguir una entesa rigorosa del moviment de l'extremitat superior dels pacients. Les anàlisis cinemàtiques i dinàmiques de la fexió-extensió del colze i de la espatlla, portades a terme per mitjans d'Anàlisi Gràfic Exploratori, han estat adequades per tal de destacar diferències biomecàniques entre subjectes sans i patològics.

Abstract

Injuries of the nervous system have a considerable impact on the bio-psycho-social aspects of patients because of their potential for resulting life-long disabilities and functional and cognitive deficits. Cervical Spinal Cord Injury and Acquired Brain Injury commonly imply a reduction of of the upper extremity functionality which complicate or even preclude the performance of basic Activities of Daily Living. Neurological rehabilitation of patients in specialized hospitals is currently the only alternative for treating patients with neurological disorders such as Acquired Brain Injury and Spinal Cord Injury. The progression of the patients through the complex rehabilitation process has to be systematically evaluated. Unfortunately, clinical assessment of functional capacity in the upper extremities is less advanced than that of lower extremities, and currently too dependent on subjective, qualitative observational motion analysis, which is highly based on intuitive understanding of human motion. Objective quantification of rehabilitation progress is necessary for the improvement of clinical treatment methods and rehabilitation strategies, and to prevent injury.

This dissertation presents a practical methodology for the objective and quantitative evaluation of the upper extremity motion in subjects with neurological disorders, with particular focus on tetraplegic subjects with complete or incomplete Spinal Cord Injury (SCI) at the C5-C6 cervical level and who have undergone tendon transfer surgery. The core of the dissertation is a new rigid body biomechanical model to carry out a kinematic and dynamic analysis of the upper extremity motion during an Activity of Daily Living through data acquired by an opto-electronic system. In addition to the model, this dissertation describes a new dedicated set-up for the acquisition of motion data of the upper extremity, and a new processing and analysis chain designed to present relevant summaries of biomechanical information to rehabilitation specialists.

The upper extremity biomechanical model consists of 10 segments with 20 Degrees of Freedom. The marker set-up combines the advantages of joint and segment markers to determine the joint centers of rotation and the segments' motions. The model makes possible a comprehensive kinematic and dynamic analysis, improving the evaluation of the upper extremity motion. In contrast to previous upper extremity models, the presented model is able to analyze the grasp motion between the first phalange of the thumb and the first phalange of the index finger, a motion considered as crucial by clinicians.

The resulting set of biomechanical measurements (joint and segment kinematics and dynamics, and trajectories of the joints and segment Centers of Mass), which are reported according to clinical standards, provides valuable information for clinicians to achieve a thorough understanding of the upper extremity motion of the patients. Furthermore, the Kinematic and Dynamic analyses of the elbow and shoulder flexion-extensions carried out by means of Exploratory Graphical Analysis are suitable to highlight biomechanical differences between healthy and pathological subjects.

Contents

Table of Acronyms

1D	One-dimensional
2D	Two-dimensional
3D	Three-dimensional
ABI	Acquired Brain Injury
ADL	Activity of Daily Living
ARA	Action Research Arm
ASIA	American Spinal Injury Association Score
C-SCI	Cervical Spinal Cord Injury
CoM	Center of Mass
CNS	Central Nervous System
DoF	Degrees of Freedom
EFE	Elbow Flexion-Extension
EPS	Elbow Pronation-Supination
EXT	External
Fc	Cut-off Frequency
GO	Global Optimization
GRF	Ground Reaction Forces
H1	Height 1
H2	Height 2
H3	Height 3
ISB	International Society of Biomechanics
LS	Left Shoulder
MOI	Moment of Inertia
NRMSD	Normalized Root Mean Square Deviation
PNS	Peripheral Nervous System
RMSD	Root Mean Square Deviation
ROM	Range of Motion
RS	Right Shoulder
SABD	Shoulder Abduction-Adduction
SCI	Spinal Cord Injury
SFE	Shoulder Flexion-Extension
SEIR	Shoulder Internal External Rotation
SNR	Signal to Noise Ratio
TBI	Traumatic Brain Injury

Introduction

Clinical assessment of functional capacity in the upper extremities is currently based on subjective, qualitative observational motion analysis. One-dimensional (1D), non-functional diagnostic movement tests are used to examine the range of motion and the associated movements of the bones of a joint. Such assessment is highly dependent on the physician's experience but based on intuitive understanding of human motion (Williams et al., 2006).

Basing physician's experience on an objective quantification of rehabilitation progress is necessary to improve clinical treatment methods and rehabilitation strategies, and to prevent injury. Recent work shows that 3-dimensional (3D) biomechanical models are useful clinical and research tools to achieve a thorough understanding of human motion and forces. For the past few decades, human motion analysis has largely been focused on the lower extremity, but recent clinical interests fuel research on the upper extremity also (Slavens and Harris, 2008).

The study of the motion of the upper extremity is challenging. The complex nature of the upper body movements complicate (or even preclude) the definition of standard movement patterns (Slavens and Harris, 2008), which have facilitated the development of generalized biomechanical models in the case of lower extremities (Rau et al., 2000). As a consequence, biomechanical models of the upper extremities are most often specifically designed for a particular task and/or patient population (Slavens and Harris, 2008), and a consensus has not been reached in critical technical aspects such as joint and segment coordinate system orientation, definition and nomenclature of motions, anatomical joints to be modeled and joint angle description. A significant step towards standards to define joint coordinate systems of various joints for the reporting of human joint motion has been made by the International Society of Biomechanics (ISB) (Wu et al., 2005). In addition, Kontaxis et al. (2009) presented a proposal of a framework for the definition of standardized protocols for upper extremity motion analysis.

The framework of the project was defined from an existing clinical requirement of the *Institut Guttmann - Hospital de Neurorehabilitació* exposed by Dr. Frederic Dachs Cardona (head of the Neuro-Orthopedics Department) and Manel Ochoa (physical therapist coordinator of the Functional Rehabilitation Department): a method to carry out objective and quantitative evaluations of the upper extremity motion of their patients, using the current facilities and equipments of the Institute. I accepted this challenging project and this dissertation summarizes my work to provide a solution. After an exciting and intense period during which I was introduced to virtually all departments and activities of the *Institut Guttmann*, the core of my project has been the development of an upper extremity rigid body model specifically designed for the particular patient population and particular motion capture system of the *Institut Guttmann*. In order to fulfill standardization requirements, and thanks to the interaction with the Functional Rehabilitation Department, I also designed an specific Activity of Daily Living (ADL), and its corresponding markers set-up, suitable for recording the motion of the upper extremity motion with an optoelectronic system and relevant for the systematic assessment of rehabilitation progress. The ADL is based on experience gained by participating on test sessions currently used in observational motion analysis (e.g. Action Research Arm (ARA) test), and the marker set-up on a set of tests of previous studies by other authors. Finally, the biomechanical output of the model had to be converted into practical information for rehabilitation specialists, demonstrating the relevance of the whole method through the comparison of a reduced set of healthy and pathological subjects.

Overall, I think I have provided a useful response to the challenging expectations of the project, but the reader should judge on his own. What I do know for sure is the success on the fulfillment of my most important expectations: getting to understand people with disabilities and the institutions and professionals who work with them, and putting my engineering skills to their service.

Organization

The organization of the dissertation is as follows. Parts I to III introduce the subject. Part I presents a very simplified description of the injuries of the nervous system with which the highly qualified personnel of *Institut Guttmann* are confronted every day. Part II summarizes the basic knowledge of biomechanics that is needed to understand this work, with particular emphasis on motion analysis of the upper extremity. Part III puts the problem in the context of the current specialized literature. All three parts are based on extensive literature review and made me realize how little a grain of sand is my contribution in the beach of international efforts in this field.

The core of my contribution is described in Parts IV to VI. Part IV on methods intends to compatibilize detail with brevity. Detail is necessary to fully understand the experimental approach and thus facilitate repeatability as required by rigorous scientific communication. Brevity is mandatory in this type of dissertations and recommended to alleviate the tedious of the reader. I have thus moved to the appendices a considerable amount of material that I hope will be valuable for practitioners, including the slightest line of code which is contributed under an open license. Several different software packages have been used, taking advantage of the particular features of each one to best address the different tasks that are involved in the transversal and methodologically heterogeneous processing and analysis chain that I have set up.

It is perhaps not immediately obvious to the reader of Part IV the rewarding difficulty of working with the 6 persons who participated in the study as subjects of analysis. Designing specific set-ups for them has been an opportunity for me to apply my background as Industrial Design Engineer and an invaluable human experience.

Part V presents the results, making extensive use of statistical graphics. Results include the clinical report that I have designed through the continuous interaction with rehabilitation specialists of the *Institut Guttmann*, as well as the kinematic, dynamic and energetic analyses. Results from the healthy subjects provide the reference background for each pathological subject.

Part VI summarizes conclusions, accomplishments and future work.

Objectives

The general goal was defined in accordance with the departments of Research, Neuro-Orthopedics and Functional Rehabilitation of the *Institut Guttmann* as the development of a practical methodology for the objective and quantitative evaluation of the upper extremity motion in patients with neurological disorders, and especially in tetraplegic subjects with a complete or incomplete spinal cord injury (SCI) at the C5-C6 cervical level which have been submitted to a tendon transfer surgery (deltoid-triceps or biceps-triceps). In order to achieve this general goal, we defined the following specific objectives:

- Design of a set-up for the acquisition of motion data of the upper extremity, which included:
  - Development of a suitable marker set-up (in particular, clinically practicable) for the specific patient population and particular motion capture system.
  - Development of a suitable motion task for the specific clinical assessment.

- Development of a suitable biomechanical model in terms of segments, joints and local frames definition and subsequent calculation of angles (kinematics), joint forces and moments (dynamics), and muscular powers (energetics).

- Development of a processing and analysis chain, to present relevant summaries of biomechanical information to the consideration of physicians and rehabilitation specialists.

- In order to demonstrate the interest of the method, the resulting sets of biomechanical measurements of pathological subjects are compared to those of healthy subjects to highlight biomechanical differences.

Part I.

Injuries of the Nervous System

1. Introduction

It is of major importance to know about the injuries that this study deals with, in order to understand how they affect on the human motion. This chapter describes two main acquired injuries of the nervous system: Acquired Brain Injury (ABI) and Spinal Cord Injury (SCI). For each injury, a general definition, classification and epidemiology is described.

The human nervous system consists of two basic parts: the central nervous system (CNS), composed by the brain and the spinal cord, and the peripheral nervous system (PNS), composed by the peripheral nerves (Figure1.0.1). The CNS integrates the information and coordinates the activity of all parts of the body. Its role is so crucial in human movement control that any minimal alteration implies a significant change in the performance of the basic Activities of Daily Living.

Injuries of the nervous system are particularly frightening to patients and families because of the many unknowns that still revolve around nervous system function, and because of the potential for resulting life-long disabilities and functional deficits.
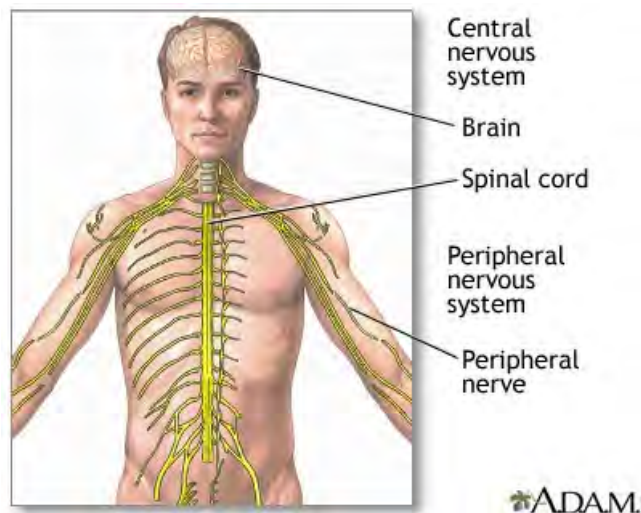
Figure 1.0.1.: Nervous system diagram.

2. Acquired Brain Injury

The brain is the most complex structure of the human body and the center of the nervous system. Different brain areas coordinate movement, sensations, perceptions, emotions and behavior. The brain is also the home of higher mental functions such as attention, memory, language and intelligence (Figure 2.0.1). Any damage to the brain can affect these functions to a greater or a lesser extent. According to the World Health Organization the definition of Acquired Brain Injury (ABI) is a "Damage to the brain that occurs after birth and is not related to a congenital or a degenerative disease. These impairments may be temporary or permanent and cause partial or functional disability or psychological maladjustment (Geneva, 1996)".
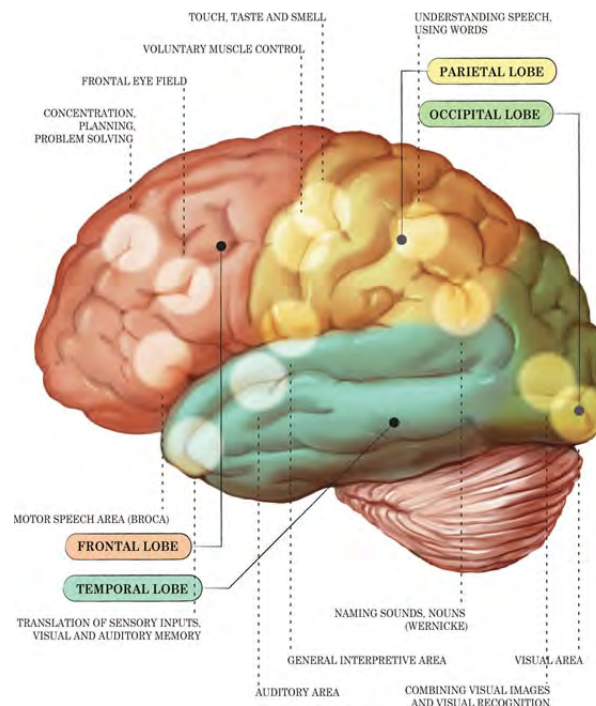
Figure 2.0.1.: Brain cortex regions (Adapted from The Gordon-Pomares Centre (2011)).

2.1. Classification of Acquired Brain Injury

The two most common mechanisms of injury to the brain are the application of a mechanical force (internal or external) or the interruption of the normal supply of oxygen (internal). Occasionally these two mechanisms occur together (Elbaum and Benson, 2007). According to these authors, ABI can be classified as follows:

2.1.1. Mechanical Force Injuries

External Mechanical Force Injuries:

The External Mechanical Force Injuries, also known as Traumatic Brain Injury (TBI), can be open or closed injuries. Blows to the head are most common type of force associated with ABI, and may be as simple as a bump on the head. The blow may be forceful, as in a fall striking the head against the ground or falling off a bicycle. Even greater forces are transmitted to the brain in any accident where speed is involved and a rapid deceleration occurs. Penetrating injuries are also considered as external mechanical force injuries.

Internal Mechanical Force Injuries:

Occasionally mechanical force is applied to the brain from within. Such forces are caused by spontaneous hemorrhages into or around the brain which may result from a ruptured aneurysm, a weak spot on an artery around the base of the brain, or from a ruptured arterio-venous malformation (Hemorrhagic or Vascular Brain Injury). Bleeding may also occur from a brain tumor or because of the use of blood-thinning medications that can also worsen any bleeding resulting from a blow to the head.

The type of injury suffered by the brain after a blow to the head or following a spontaneous hemorrhage depends on its intensity, location and site and size of the hemorrhage. Associated factors intervene as well in determining the effect of the injury, such as age, coexisting disease or illness, nutritional state, fitness, and use of medications or illicit drugs.

2.1.2. Interruption of Oxygen Supply

The brain does not store any oxygen, yet it is totally dependent on oxygen to function. If the brain is totally deprived of oxygen for two minutes, the brain dies. Many situations occur where oxygen is deprived to parts of the brain (focal anoxia) or where the oxygen supply is diminished but not totally cut off (hypoxia). Focal anoxia or hypoxia (Anoxic Brain Injury) may occur without mechanical blows to the head but are frequently associated with internal mechanical force injuries.

2.2. Signs and Symptoms

Brain injury causes signs and symptoms related to levels of consciousness, breathing, vital signs, pupillary function, motor function, sensory function, and autonomic function. The pattern of deficits seen in ABI varies greatly from person to person, based on the severity of injury, location and nature of the brain injury, and medical complications (Elbaum and Benson, 2007). Regardless of the etiology of the brain injury, many patients share a similar clinical course. Focusing on motor function alterations, these follow a similar progression reflecting a worsening condition, starting with weakness, then paralysis on one side of the body, opposite the side of the brain injury (hemiparesis/hemiplegia). Weakness or paralysis of both sides reflects bilateral brain injury (tetraparesis/tetraplegia). As pressure in the skull increases, abnormal reflexive movements develop, known as decorticate or decerebrate posturing. In the former the arm flexes over the chest and the hand turns inward. In the latter the arm extends stiffly by the side, inwardly rotated. In both conditions, the leg extends stiffly with the foot and toes pointing downward. In some patients, seizures or convulsions represent an irritation of the surface of the brain as a result of the injury (Elbaum and Benson, 2007).

2.3. Epidemiology

TBI, according to the World Health Organization, will surpass many diseases as the major cause of death and disability by the year 2020. The incidence is estimated at 10 million people affected annually by TBI , that is a global rate of 106 per 100,000 inhabitants per year (Hyder et al., 2007). Despite this high incidence, the mortality rate has declined from 24.6 per 100,000 population in 1979 to an estimated 17.5 per 100,000 in 2003 thanks to improved acute medical care and injury-prevention strategies. Although the majority of injuries are mild and cause no lasting impairment, TBI of any severity can lead to significant long-term disability. Severe disability from TBI has an incidence rate estimated at 2 % per 100,000 inhabitants per year, and moderate disability at 4 % per 100,000 inhabitants per year. The community at highest risk is young adults between the ages of 15 and 24 (917.5/100,000), the risk of TBI for men is still almost twice that for women and the main cause is traffic accidents (Brown et al., 2008).

3. Spinal Cord Injury

The spinal cord is a nerve cord protected by the spine and running from the base of the brain to the lumbar area. It is the main pathway for the brain to receive information from the rest of the body and to send away movement regulating signals. The spinal nerves come out of the spinal cord along its length and, depending on the spinal site they emerge from, they are called cervical, thoracic, lumbar or sacral nerves (Figure 3.0.1).
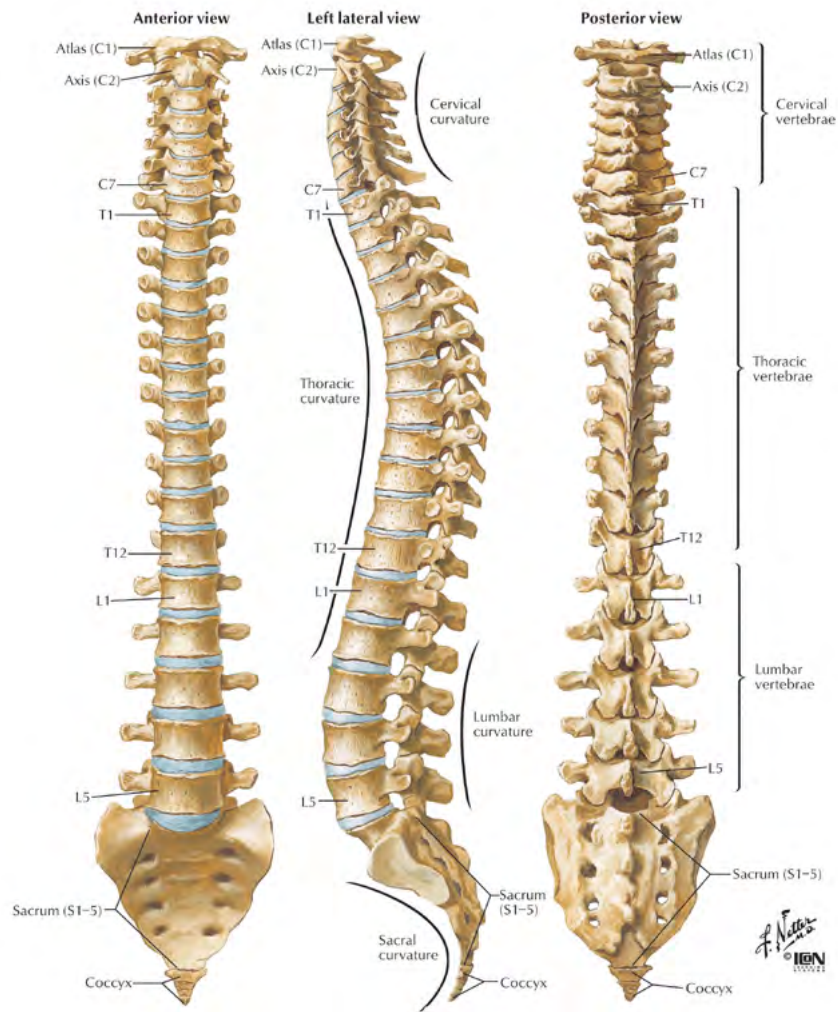
Figure 3.0.1.: Spinal cord structure.

The SCI refers to any injury to the spinal cord that is caused by trauma instead of a disease or medical causes. When a SCI takes place the transmission of the motor and sensitive signals are affected and the neurological signals below the injury are blocked (Table 3.1). SCI often results in severe motor dysfunction, such as complete paralysis. Typically, these patients not only cannot walk, but also lose bowel, bladder, and sexual functions.

3.1. Classification of SCI.

Disrupted cervical nerve pathways result in *tetraplegia*. This involves a loss or decrease in sensation and/or voluntary movement of all four limbs and the entire trunk. Affected thoracic and lumbar nerves result in *paraplegia*. This involves absence of sensation and/or complete or partial paralysis of the lower limbs and of the trunk below the injury. The effects of injuries known as Conus Medullaris and Cauda Equina on sensation and voluntary movements are less severe. Patients can still walk in most cases.

Severity of injury may be classified using the American Spinal Injury Association Score (ASIA) for quantitative assessment of motor and sensory function, and the ASIA/Frankel grading system A–E for clinical grading (see Appendix A *Standard Neurological Classification of Spinal Cord Injury* for details):

- **A - Complete:** the most severe with no motor or sensory function below the level of the lesion with no preservation of sensation in sacral dermatomes S4–S5;

- **B - Incomplete:** Sensory, but not motor, function is preserved below the neurologic level and extends through sacral segments S4-S5

- **C - Incomplete:** Motor function is preserved below level of lesion (MRC <3);

- **D - Incomplete:** Motor function is preserved below level of the lesion with 50% muscles MRC grade 3 or above;

- **E - Normal:** Sensory and motor functions are normal.

Definitions of complete and incomplete SCI are based on the above ASIA definition with sacral-sparing (evidence of the physiologic continuity of spinal cord long tract fibers)

- **Complete:** Absence of sensory and motor functions in the lowest sacral segments

- **Incomplete:** Preservation of sensory or motor function below the level of injury, including the lowest sacral segments

With the ASIA classification system, the terms paraparesis and quadriparesis have become obsolete. The ASIA classification using the description of the neurologic level of injury is employed in defining the type of SCI (Waring et al., 2010).

3.2. Signs and symptoms

SCI is a devastating event that results in motor dysfunction below the level of lesion (Table3.1), as well as development of chronic pain syndromes. Depending on where the spinal cord and nerve roots are damaged, the symptoms can vary widely, from pain to paralysis to incontinence. Since the Spinal cord is not only the connexion between the brain and the extremities, but is a structure that acts as a regulator entity of different vital functions as urination, sexual, digestive, and vascular functions as well as temperature regulation and involuntary and voluntary movements.

To all this symptomatology the psychological disorders that a person can suffer from facing the new situation have to be added. After a SCI the person and the family have to learn how to live a new style of life. Few survivable injuries have as much impact on a patient's life as acute spinal cord trauma, and its associated human and social cost. The most common cause is vehicle accidents, followed by violent assault, falls and sports injury, especially high board diving (Belanger and Levi, 2000).

Persons with cervical spinal cord injury (C-SCI) demonstrate, in addition to the loss of function in the lower extremities and trunk, motor and sensory loss in arms and hands. The level of functioning in these persons is, for the most part, determined by the impairments of the arm and hand.

Table 3. Key Muscles According to the American Spinal Injury Association

Key muscle groups	Roots	Movement	Muscles
1	C5	Elbow flexion	Biceps, brachialis
2	C6	Wrist extension	Extensor carpi radialis longus and brevis
3	C7	Elbow extension	Triceps
4	C8	Finger flexion, middle finger	Flexor digitorum profundus
5	T1	Small finger abductors	Abductor digiti minimi
6	L2	Hip flexor	Iliopsoas
7	L3	Knee extensors	Quadriceps
8	L4	Ankle dorsiflexion	Tibialis anterior
9	L5	Long toe extensors	Extensor hallucis longus
10	S1	Ankle plantar flexion	Gastrocnemius, soleus

Table 3.1.: Key muscles according to the American Spinal Injury Association (Adapted from Belanger and Levi (2000))

3.2.1. Tendon Transfer Surgery

A tendon transfer is a surgical procedure where a functioning healthy tendon is shifted from its original attachment to a new one to restore the action that has been lost. (American Society for Surgery of the Hand, 2011)

Tendon transfer surgery is sometimes convenient when a certain muscle function is lost because of a nerve injury. When a nerve is injured, then the nerve no longer sends signals to certain muscles leading to a paralysis and loss of function of those muscles. Tendon transfer surgery can be used to attempt to replace that muscle function. Thus it is appropriate in some cases to restore elbow extension in tetraplegic subjects with a complete or incomplete C-SCI at the C5–C6 vertebral level, which are unable to actively extend the elbow due to a paralysis of the triceps brachii muscle Robinson et al. (2010).

3.3. Epidemiology

The annual incidence of SCI varies widely among countries and ranges from 6 per million to 57.8 per million. In Spain the incidence is estimated to be around 25 per million of inhabitants per year (approximately 1,000 people per year) and in Catalonia between 140 and 160 new cases of spinal injury are reported every year.

The most common mechanisms of injury reported among the 2,814 cases in the National Spinal Cord Injury Statistical Center database are motor vehicle accidents, accounting for 35.9% of injuries, followed by violence, falls, and sports-related injuries, which account for 29.5%, 20.3%, and 7.3%, respectively.

The prevalence of SCI is increasing steadily because of improved survival in both the acute and chronic stages of the disease. The acute mortality rate for cervical SCI within the first 3 months is approximately 21%, after the acute period mortality rate decreases even thought SCI patients still have a shortened life expectancy compared with their uninjured peers (Belanger and Levi, 2000).

Pain impact following SCI has been reported 37% of higher-level SCI patients and 23% of lower-level SCI patients (Nakae et al., 2011).

4. Treatment: Neurorehabilitation

The consequences of a SCI and ABI are currently irreversible. This is due to the fact that the spinal cord and the brain do not regenerate. In addition, the complexity of the structure make surgical repair impossible with current techniques. Despite this, research is being carried out worldwide to find a future cure. Currently, great efforts are being made in the field of prevention (Guttmann, 2011). New surgical and technological procedures are being developed to improve the patients prognosis and quality of life. Neurological rehabilitation of patients in a specialized hospital is the only present choice for treating these patients appropriately. Neurorehabilitation is a complex medical process which aims to aid recovery from a nervous system injury, and to minimize and/or compensate for any functional alterations resulting from it (Guttmann, 2011). The neurorehabilitation process must be guided by a large group of professionals from the health care sphere, and carried out in a center with specific facilities aimed to realize the different activities that take place during the neurorehabilitation process.

This dissertation has been carried out at the *Institut Guttmann - Hospital de Neurorehabilitació*, which is a leading hospital in the medical treatment, surgery and full rehabilitation of patients with spinal cord injury, acquired brain injury or any other serious neurological disorders.

During the first month at the *Institut Guttmann* I had the opportunity to participate to most of the activities of the Function Rehabilitation Department. During this period I could get a comprehensive idea of how functional rehabilitation works. The activities are divided into two groups (4.1): (i) *fundamental activities* and (ii) *additional activities*.

FUNDAMENTAL ACTIVITIES	
Activity/Therapy	**Definition**
Activities of Daily Living (ADLs)	active training of basic ADLs as: personal hygiene and grooming, dressing and undressing, self feeding, functional transfers, bowel and bladder management and bed mobility.
Transfer- therapy	active therapy that aims to train the transference of the patient from the wheelchair to the bed, bath, car, and other common life facilities. This transference's are putted into practice during the ADLs activities at the hospital.
Occupational therapy	active therapy that aims to improve functional patters of the upper extremities and train cognitive functions (e.g. attention, memory etc.). This therapy use robotic systems such as *Mit-Manus*® and *Reo-Go*®
Manual-therapy	active or passive treatment that is based on the use of the hands of the physical therapist to stimulate/stretch/exercise body functional structures.
Gait therapy	active therapy that aims to reeducate gait. This therapy takes advantage of assistive devices and robotic systems such as *Lokomat*® and *Gait Trainer*®.

ADDITIONAL ACTIVITIES	
Activity/Therapy	**Definition**
Hydro-therapy	active or passive treatment that is based on using the properties and effects of watter such as flotation, temperature, density and pressure to exercise or stimulate body function of the patient.
Sling Exercise therapy	active and/or assistive training based on basic elements such springs, weights, pulleys, elastic bands and a *Rocher cage* to increase muscular power.
Sport	activity that is based on playing games that require physical exercise
Fitness	activity that is based on performing physical exercise (cycling, elliptical machine, oriented exercises)

Table 4.1.: Functional rehabilitation activities. Top) Complementary activities. Bottom) Additional activities

Part II.

Biomechanics of the Upper Extremity

5. Introduction

Biomechanics is a contraction of the words 'biology' and 'mechanics', thus is the study of the application of the laws of physics and in particular the laws of mechanics, on biological systems. Traditionally, the field of biomechanics has been roughly divided in 3 sectors: (i) Fluid biomechanics,(ii) tissue biomechanics and (iii) motion biomechanics. Motion biomechanics analyze the motions of the neuromusculoskeletal system, focusing on the role of joints, bones, muscles, sensors and the central and peripheral nervous system (van der Kooij et al., 2008).

Biomechanics has a number of application fields. In clinical applications, biomechanics is attempted to improve the diagnosis, treatment and prevention of disorders to the musculoskeletal and cardiovascular system. In sport biomechanics the aim is to improve performance by a thorough understanding of the biomechanical principles of the movements. In ergonomic applications the behavior of human in interaction with the environment is studied to improve performance (van der Kooij et al., 2008).

Biomechanics is a multidisciplinary field of research, in which medical researchers and practicians (orthopedics, neurology, rehabilitation, morphology, physiology) collaborate with engineers (mechanical, electrical and control engineers), and with researchers of biophysics and human movement science. Therefore communication among them is challenging.
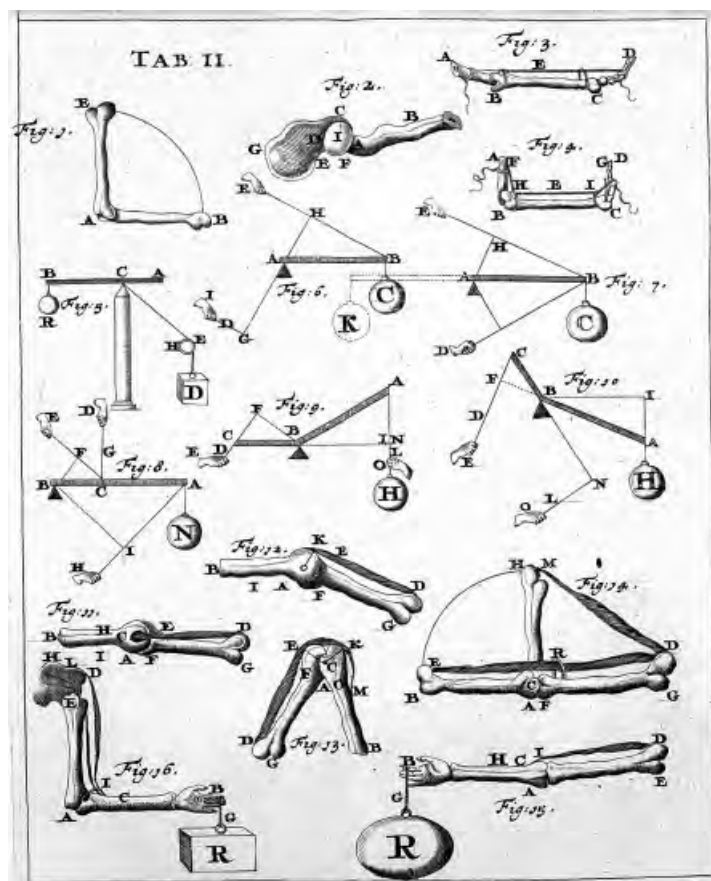

Figure 5.0.1.: Page of one of the first works of Biomechanics (De Motu Animalium of Giovanni Alfonso Borelli)

6. Anatomy of the upper extremity

The upper extremity is composed of the *shoulder girdle, the upper arm, the forearm and the hand.* The only joint in the upper limb between the axial skeleton and the shoulder girdle is the *sternoclavicular joint* between the sternum and the clavicule. This is a ball and socket synovial joint with an articular disk. Moving distally the next joint is the *acromioclavicular joint* which is a sliding synovial joint between the acromion process on the scapular and the clavicule. The next joint is the *glenohumeral joint* between the head of the humerus and the glenoid fossa of the scapula. This is a highly mobile ball and socket joint and a large number of muscles are needed to cope with this mobility.

The *elbow joint* is actually a complex of 3 joints that share the same synovial sheath: *humeroradial, humeroulnar, and superior radioulnar joints.* The humeroradial and humeroulnar joints allow flexion-extension at the elbow while the superior radioulnar, humeroradial, and the more distal inferior radioulnar joints allow the specialized actions of supination-pronation. This action is a rolling of the radius around the ulna that produces an apparent rotation of the wrist around the longitudinal axis of the forearm (Netter, 1997).

The *wrist joint* which connects the forearm (radius and ulna) with the hand, consists of 10 small carpal bones, but it can be divided into only two functional components: *the radiocarpal and midcarpal joints.* The wrist complex is usually described as a condyloid synovial joint allowing ulnar and radial deviation, flexion and extension. The exact ways that the wrist bones move to produce these composite movements is complex but flexion occurs mostly at the midcarpal joint and extension is mostly at the radiocarpal joint. The radiocarpal joint also provides most of the ulnar and radial deviation. The *carpometacarpal joints* that are numbered from 1 to 5 between the distal row of carpal bones and the five metacarpals are saddle joints which allow flexion-extension and adduction and abduction of the first ray. More distally the *phalanges (proximal, middle and distal)* are connected by simple hinge joints which only allow flexion-extension (Snell, 2000).
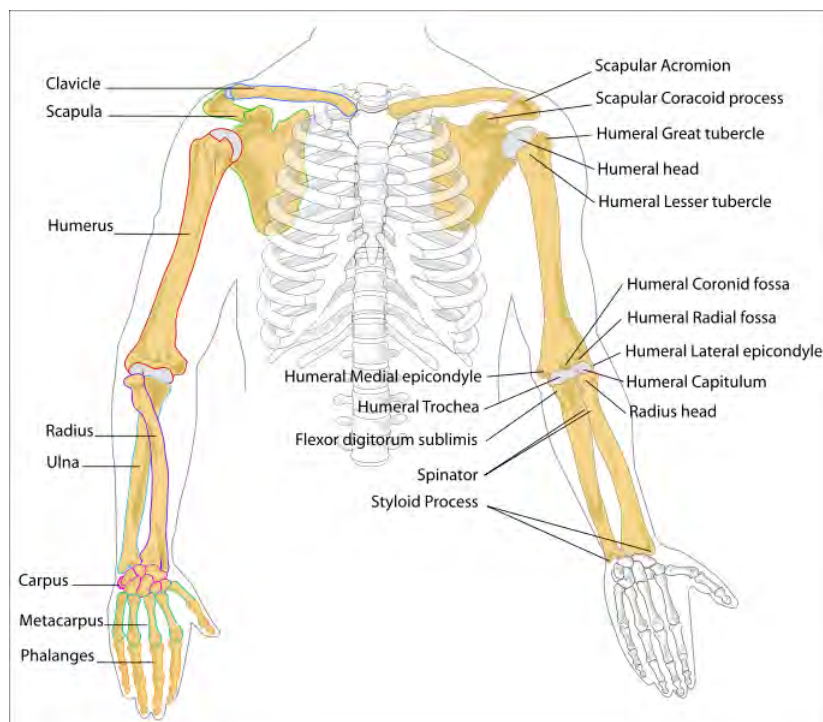

Figure 6.0.1.: Upper extremity anatomy (adapted from Dentalarticles (2011)).

7. Motion analysis

7.1. Biomechanical model

The design of a biomechanical model requires a simplification of the body. This is done by dividing the body into segments that are assumed to behave as rigid elements and connected with joints. The concept of modeling the body as a number of linked, rigid segments is based on the anatomical fact that the skeleton is composed of bones (rigid elements), which are linked by different kinds of articulations or joints. More complex models also include assistive devices such as walkers or crutches (Slavens and Harris, 2008).

In principle, an unconstrained bone has 6 Degrees of Freedom (DoF) of motion with respect to the next bone: 3 rotations and 3 translations. The relative motions of the bone are limited by passive structures such as articular surfaces and ligaments. Even though motion in the direction of the restraint is still possible (e.g. cartilage can be compressed few millimeters), this fact is neglected and the motion is said to be constrained (van der Kooij et al., 2008). For each constraint, the number of DoF decreases by one. Typically, the human arm, involves 3 major joints: shoulder, elbow and wrist, and contains 7 DoF (Yang et al., 2002). The shoulder is modeled as a ball and socket joint allowing 3 DoF (flexo-extension, abduction-adduction, internal-external rotation), the elbow is modeled as a rotating hinge joint allowing 2 DoF (flexo-extension, pronation-supination) and the wrist is modeled as a saddle joint allowing 2 DoF (flexo-extension, ulnar-radial rotation) (Figure 7.1.1).
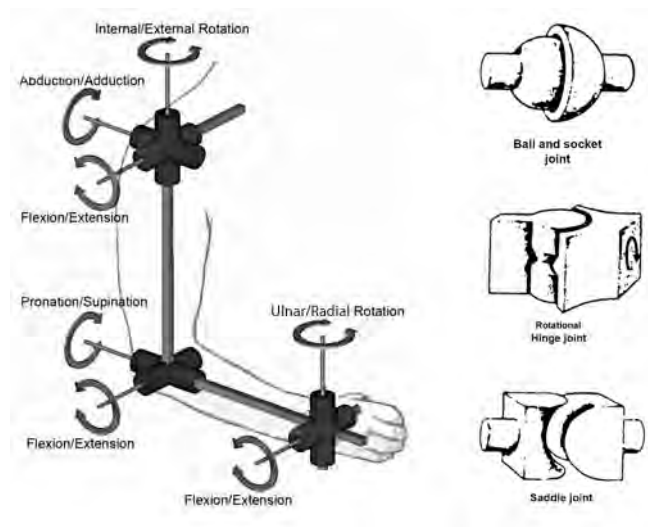
Figure 7.1.1.: DoF of the upper extremity (Shoulder, elbow and hand) and joint models of the shoulder, elbow and wrist joint (adapted from van der Kooij et al. (2008)).

7.2. Kinematics

Kinematics describes the motion of body segments or groups of body segments without consideration of the forces that cause the motion. The motion of the bodies depends on the geometry of the links between them (articulation or joint). Joint motion is actually the relative motion of the distal segment with respect to the proximal one which are connected with a joint. This section deals with the medical and technical motion definitions regarding the kinematics of human movement.

7.2.1. Medical motion definitions

Since physicians were the first to study joint motions, medical definitions are still prevalent. Medical definitions aim to distinguish between pathological and normal motion, to evaluate the outcome of treatments. In order to standardize the motion description, the *anatomical position* is officially and internationally defined in the Nomina Anatomica (Anatomists, 1961) as the reference body position from where motion is described (Figure 7.2.1).
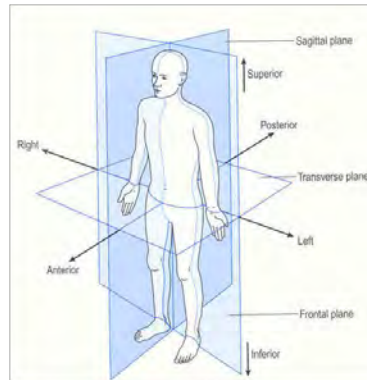

Figure 7.2.1.: Anatomical Position (adapted from Whittle (2007)).

From the anatomical position, motion is defined for each single rotation apart (Figure 7.2.2):

- Flexion-Extension: rotation in the *sagital plane.*

- Abduction-Adduction: rotation in the *frontal plane.*

- Internal-External Rotation: rotation in the *transverse plane.*

- Pronation-Supination: rotational movement of the forearm at the radioulnar joint in the *transversal plane.*

- Ulnar-Radial rotation: rotational movement of the hand at the wrist joint in the *frontal plane.*
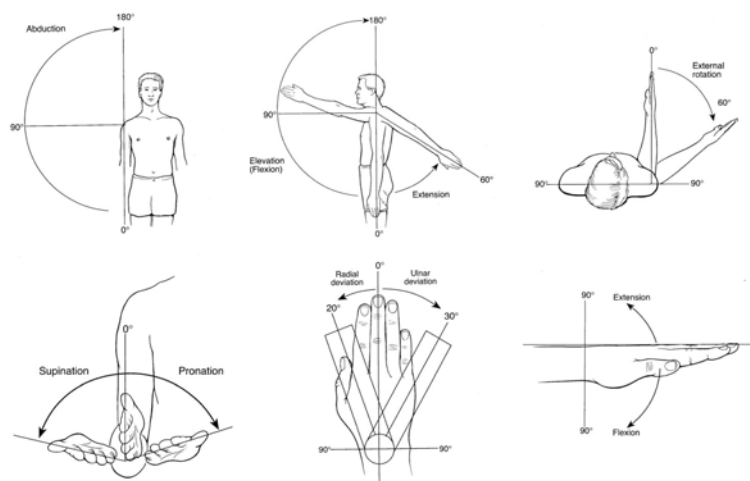
Figure 7.2.2.: Rotations of the upper extremity (adapted from Jenkins (1991)).

A problem occurs if the motion is not in just one of the standardized axis but is a combination of rotations. In this case, the order of rotations is not defined and thus, it is not clear whether the rotation axes move with the bone. This still results in much confusion when describing rotation angles, and often complicates the comparison between studies. An accurate definition of complex joint motion is essential for understanding normal and pathological bone and joint kinematics. Technical motion definitions fulfill this requirement.

7.2.2. Technical motion definitions

Body Segment Kinematics

Global and Local Reference Frame: Kinematic techniques, in the analysis of human motion, have been used to study body movements in both two-dimensional (2D) and 3D space. While there are potentially many kinds of kinematic measurements that can be used, relative segmental angular motions are used most frequently. The configuration of a body segment in the 3D space is determined by the orientation and position of one of its points with respect to the *reference frame*. A reference frame is a particular perspective used by the analyst to describe and/or observe a motion effectively. There are different types of reference frames: the *global frame* is a fixed reference frame which is fixed to the environment (not to the moving subject) and is commonly used for describing the motions of different body segments. The *local frames* are all the reference frames fixed to the moving body segments and are used for describing the relative motion between body segments.

Position and Orientation: The vector that defines the inertia center of the segment (G) with respect to the origin of the global reference frame (O) $\vec{r}_{OP}$ is commonly used to determine the *position* of a body segment point. In many cases, the orientation of a body segment is described with respect to the local reference frame attached to the proximal adjacent segment. The body segment *orientation* with respect to the global or the local reference frame it is commonly defined by *Euler angles (ϕ, θ and Ψ)*. It is important to note that Euler rotations are not commutative and consequently, the rotational sequence has to be taken into account (Figure 7.2.3).It is important to understand that a given axis transformation determines a second axis transformation, in other words: a rotation around the first axis will change the orientation of the second and third axes and a rotation around the second axis will change the orientation of the third axis, and rotation about the third axis will result in the final orientation of the coordinate system. As a consequence for a targeted rotational sequence, the axis with the most motion should be rotated first, and the one with least amount of motion should be rotated last (Slavens and Harris, 2008).
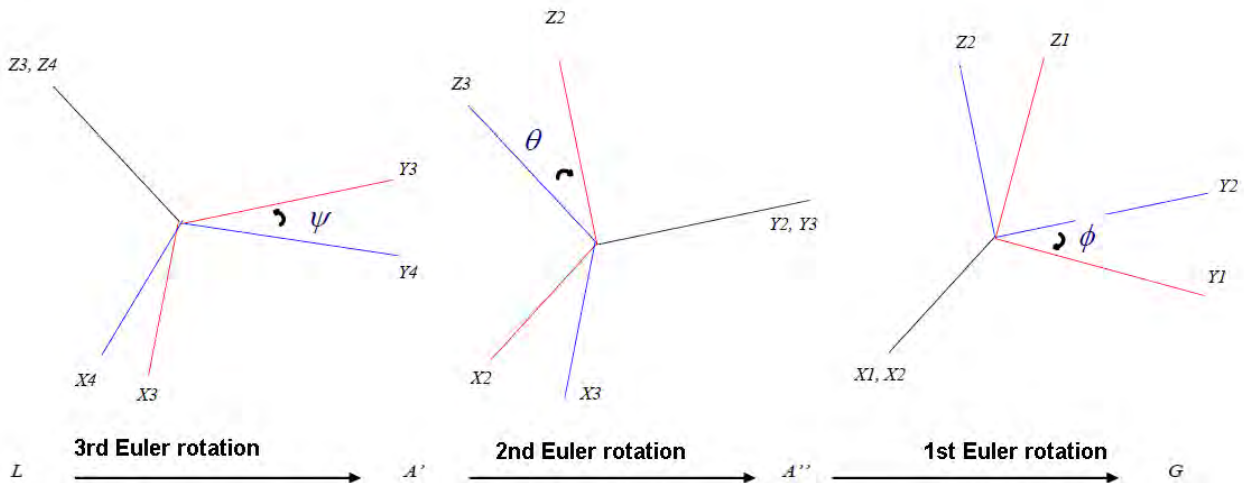

Figure 7.2.3.: Rotational sequence of Euler angles where the local coordinate system L is defined by *X4, Y4, Z4* and the global coordinate system G by *X1, Y1, Z1* (adapted from van der Kooij et al. (2008)).

Given a local coordinate system defined by axes *X4, Y4, Z4* and a global coordinate system defined by axes *X1, Y1, Z1* the rotation of the local coordinate system relative to the global coordinate system ($\mathbf{R}_G^L$) can be defined in terms of the 3 successive rotations ($^x\mathbf{R}_G^{A''}$ $^y\mathbf{R}_{A''}^{A'}$ $^z\mathbf{R}_{A'}^L$, where A' and A'' are intermediate coordinate systems) and their 3 Euler angles (ϕ, θ and Ψ) (Figure 7.2.3):

$$\mathbf{R}_G^L = {}^x\mathbf{R}_G^{A''}\ {}^y\mathbf{R}_{A''}^{A'}\ {}^z\mathbf{R}_{A'}^L =$$

$$= \begin{bmatrix} 1 & 0 & 0 \\ 0 & cos\phi & -sin\phi \\ 0 & sin\phi & cos\phi \end{bmatrix} \begin{bmatrix} cos\theta & 0 & sin\theta \\ 0 & 1 & 0 \\ -sin\theta & 0 & cos\theta \end{bmatrix} \begin{bmatrix} cos\Psi & -sin\Psi & 0 \\ sin\Psi & cos\Psi & 0 \\ 0 & 0 & 1 \end{bmatrix} =$$

$$= \begin{bmatrix} cos\theta cos\Psi & -cos\theta sin\Psi & sin\theta \\ sin\Psi cos\phi + sin\theta cos\Psi sin\phi & cos\Psi cos\phi - sin\theta sin\Psi sin\phi & -cos\theta sin\phi \\ sin\Psi sin\phi - sin\theta cos\Psi cos\phi & cos\Psi sin\phi - sin\theta sin\Psi cos\phi & cos\theta sin\phi \end{bmatrix} \quad (7.2.1)$$

In most cases, the reverse of this operation will take place: the rotation matrix ^{GL}R reconstructed from measurements will be decomposed into 3 rotation matrices with the respective Euler angles. From Equation 7.2.1, angles ϕ, θ and Ψ can be found:

$$\theta = arcsin\left({}^{1,3}R_G^L\right)$$
$$\Psi = atan2\left(\frac{-{}^{1,2}R_G^L}{-{}^{1,1}R_G^L}\right)$$
$$\phi = atan2\left(\frac{-{}^{2,3}R_G^L}{-{}^{3,3}R_G^L}\right) \quad (7.2.2)$$

A pitfall of using Euler angles is the gimbal lock position. If the second rotation is 0° or 180°, the first and third axis coincide resulting into a singular position. Furthermore, the calculated angles become very sensitive to measurement noise near the gimbal lock position. In order to avoid the gimbal lock a proper definition of the rotation order must be used, such that the second rotation is not likely to become 0° or 180°. Other methods for describing technically 3D rotations include *direction cosines*, *helical axes* and the *method of Grood and Suntay* (Slavens and Harris, 2008).

In conclusion, the *position* and the *orientation* of a body segment are defined unambiguously by 6 coordinates: the point position described by 3 coordinates (x, y and z) and the orientation of the *local frame* described by 3 Euler angles (ϕ, θ and Ψ).

Point Velocity and Angular Velocity: The *point velocity* $\vec{v}_P$ of a point P respect to a reference frame is the time derivative of the position vector $\vec{r}_{OP}$:

$$\vec{v}_P = \frac{d\vec{r}_{OP}}{dt} \quad (7.2.3)$$

The *angular velocity* $\vec{\omega}_R^S$ of a segment S respect to a reference frame R is the time derivative of the segment Euler angles :

$$\vec{\omega}_R^S = \dot{\vec{\phi}} + \dot{\vec{\theta}} + \dot{\vec{\Psi}} \quad (7.2.4)$$

In Equation 7.2.4 the angular velocity vector of an Euler rotation (e.g., $\dot{\vec{\phi}}$) has the scalar time derivative as modulus, its direction follows the axis direction and its attitude follows the rotation attitude.

The angular velocity of a local frame relative to a global frame can be expressed as the time derivatives of the orientation angles that define the orientation of the local frame relative to the global frame. Care should be taken to transform these independent velocity vectors into a common reference frame. Assuming a rotating local frame L that is rotating with respect to a global frame G. The angular velocity vector of L is a vector addition of the derivatives of Euler orientation angles projected into a common basis. For example, the angular velocity vector of L relative to G ($\vec{\omega}_G^L$) can be expressed in the global reference frame as:

$$\vec{\omega}_G^L = \begin{bmatrix} \dot{\phi} \\ 0 \\ 0 \end{bmatrix} + {}^x\mathbf{R}_G^{A''} \begin{bmatrix} 0 \\ \dot{\theta} \\ 0 \end{bmatrix} + {}^x\mathbf{R}_G^{A''}\, {}^y\mathbf{R}_{A''}^{A'} \begin{bmatrix} 0 \\ 0 \\ \dot{\Psi} \end{bmatrix} \tag{7.2.5}$$
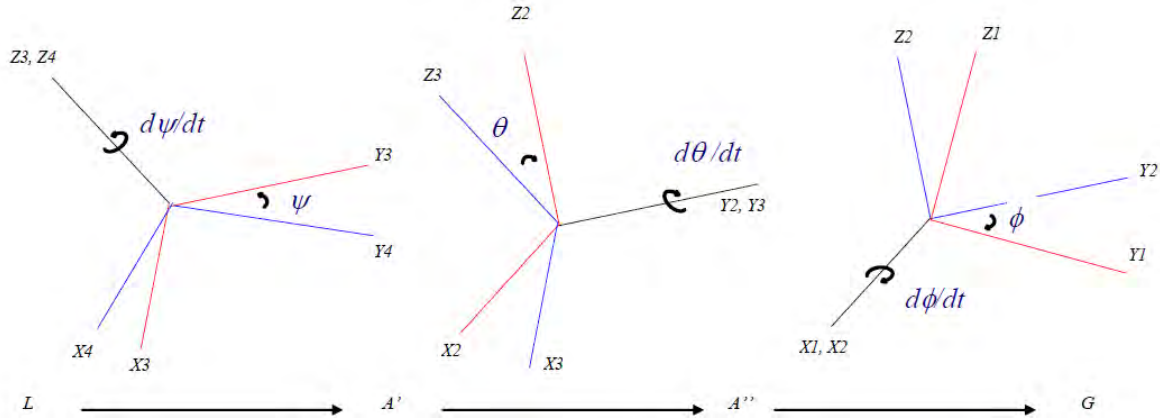
Figure 7.2.4.: Angular Velocity of the local frame L relative to the global frame G. The 3 successive rotations change the local frame *X4, Y4, Z4* into the global frame *X1, Y1, Z1*. Note that the sign of Ψ is negative since its associated rotation is counter clockwise. By taking the time-derivatives of the orientation angles 3 independent angular velocities are obtained around the *Z3=Z4* axis, the *Y2=Y3* axis, and the *X1=X2* axis (adapted from van der Kooij et al. (2008)).

Point Acceleration and Angular Acceleration: In the same way, the *point acceleration* $\vec{a}_P$ is the time derivative of the point velocity vector $\vec{v}_P$ and the *angular acceleration* $\vec{\alpha}_R^S$ is the time derivative of the angular velocity $\vec{\omega}_R^S$:

$$\vec{a}_P = \frac{d\vec{v}_P}{dt} \tag{7.2.6}$$

$$\vec{\alpha}_R^S = \frac{\vec{\omega}_R^S}{dt} \tag{7.2.7}$$

Joint Kinematics

Given a set of segments connected by joints, the joint motion is defined as the motion of the distal segment relative to the proximal segment. Once the joint coordinate systems of the segments (local frames) are defined, the joint motions can be described as relative rotations between their coordinate systems using Euler angles. For a clearer *clinical interpretation* of the resulting Euler angles, the local frames of the proximal and distal body segments should be initially aligned to each other by defining the axis of the local coordinate systems in the anatomical orientations (i.e. along or perpendicular to the anatomical planes of the segment). By consensus the origin of the body segment local frame is the proximal end (or proximal joint) of the segment (Rau et al., 2000). This way, shoulder rotations are rotations of the humerus coordinate system with the origin at the shoulder joint with respect to the trunk coordinate system with the origin at the sternum. Elbow rotations are rotations of the forearm coordinate system with the origin at the elbow with respect to the humerus coordinate system. Wrist rotations are rotations of the hand coordinate system with the origin at the wrist with respect to the forearm coordinate system (Figure 7.2.5).

Origin local frame: proximal end or proximal joint of the segment.
X axis: Along the transversal plane or perpendicular to the sagital plane.
Y axis: Along the sagital plane or perpendicular to the frontal plane.
Z axis: Along the frontal plane or perpendicular to the transversal plane.

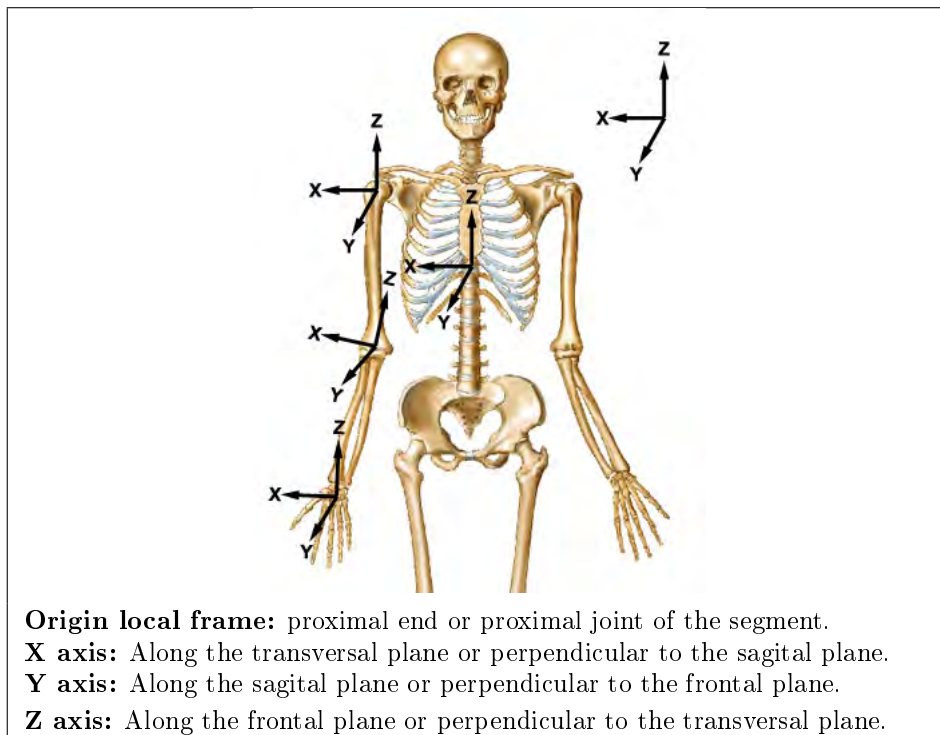Figure 7.2.5.: Local frames for the hand, forearm, upper arm and trunk segments.

Another important issue in joint kinematics is the location of the rotation center of the joints and the axis of rotation. Accurate determination of the location of the joint center is the base in the joint kinematics while the location and migration of the axis of rotation has bearings on the computation of the moment arms of the muscles.

7.3. Dynamics

Kinetics is the study of forces and moments. Kinetic assessment is particularly important to quantify force related to injury. Measures of force and its duration can provide insight into the biomechanics of how the joints are being loaded during a particular task. Dynamic analysis may be applied for prevention of arthritis, rotator cuff tears, carpal tunnel syndrome, and upper extremity joint pain (Slavens and Harris, 2008).

To study the dynamics of the human body this is modeled as a linked-segment system. The basic assumptions for a linked-segment system are:

- The joints are all spherical joints and there is no friction at the joint. Thus, the forces produced by the elements of the joint such as ligaments and joint capsules are all concentric about the joint centers. In other words, all these forces pass through the joint centers.

- Muscles are the only elements that can produce moments of force about the joint centers.

- All muscles are uni-articular and there is no intervening structure that can act as pulley. In other words, muscles are straight and directly attached to the segments through the tendons.

The process of obtaining joint forces and moments involves collecting patient segmental geometry information (i.e., dimensions, masses, and moments of inertia) and the motion.

This section is based on information from Kwon (1998).

7.3.1. Inertial Properties

Center of Mass (CoM)

The *center of mass G* represents the mean location of all the mass (m_i) in a system. In the case of a rigid body, the position of the center of mass is fixed in relation to the body. The position of center of mass $\vec{r}_{OG}$ of a system of particles is defined as the average of their positions $\vec{r}_i$ weighted by their masses m_i:

$$\vec{r}_{OG} = \frac{\sum m_i \vec{r}_i}{\sum m_i} \tag{7.3.1}$$

Moment of inertia (MOI)

The *moment of inertia* of an object about an axis is a property that depends only on the object's shape and mass distribution around this axis. This can be interpreted as the tendency of an object to maintain the current angular velocity or the difficulty in changing this velocity. It is a purely geometric characteristic of the object, as it depends only on its shape and mass. Consider a rigid body rotating with angular velocity around a certain axis. The body consists of N point masses m_i whose distances to the axis of rotation are denoted l_i. The moment of inertia is usually denoted with the capital letter I:

$$I = \sum_{i=1}^{N} m_i l_i^2 \tag{7.3.2}$$

Inertia tensor

In 3 dimensions, if the axis of rotation is not given, we need to be able to generalize the scalar moment of inertia to a quantity that allows us to compute a moment of inertia about arbitrary axes. This quantity is known as the *inertia tensor.* For a rigid object of N point masses m_i, the *inertia tensor* (with respect to a point P) has components given by:

$$\mathbf{I}_P = \begin{bmatrix} I_{11} & I_{12} & I_{13} \\ I_{21} & I_{22} & I_{23} \\ I_{31} & I_{32} & I_{33} \end{bmatrix} \tag{7.3.3}$$

where

$$
\begin{aligned}
I_{11} = I_{xx} &= \sum_{i=1}^{N} m_i(y_i^2 + z_i^2) \\
I_{22} = I_{yy} &= \sum_{i=1}^{N} m_i(x_i^2 + z_i^2) \\
I_{33} = I_{zz} &= \sum_{i=1}^{N} m_i(x_i^2 + y_i^2) \\
I_{12} = I_{xy} &= -\sum_{k=1}^{N} m_i x_i y_i \\
I_{13} = I_{xz} &= -\sum_{i=1}^{N} m_i x_i z_i \\
I_{23} = I_{yz} &= -\sum_{i=1}^{N} m_i y_i z_i
\end{aligned}
\tag{7.3.4}
$$

Principal moments of inertia

When aligning the local reference frame in such a way that the mass of the body evenly distribute around the axes, all the non-diagonal terms (products of inertia) become zero, and thus, the terms in the diagonal are the principal moments of inertia:

$$\mathbf{I}_P = \begin{bmatrix} I_{1'} & 0 & 0 \\ 0 & I_{2'} & 0 \\ 0 & 0 & I_{3'} \end{bmatrix} \tag{7.3.5}$$

Rigid body linear momentum

The rigid body linear momentum is the product of the mass m and velocity $\vec{v}_G$ of a rigid body:

$$\vec{p}_G = m\vec{v}_G \tag{7.3.6}$$

Linear momentum theorem states that the rate of change of the linear momentum $\vec{p}_G$ of a particle with constant mass is equal to the sum of all external forces acting on the rigid body:

$$\frac{\mathrm{d}(m\vec{v}_G)}{\mathrm{d}t} = m \cdot \vec{a}_G = \sum \vec{F}_{ext} \tag{7.3.7}$$

where m is the rigid body mass, $\vec{v}_G$ is the CoM velocity and their product is the linear momentum $\vec{p}_G$, and $\sum \vec{F}_{ext}$ is the sum of the external forces acting on the rigid body.

Rigid body angular momentum

The angular momentum $\vec{L}_O$ of a particle P with respect to some point of origin O is:

$$\vec{L}_O = \vec{r}_{OP} \times m\vec{v}_P \tag{7.3.8}$$

For a rigid body the angular momentum $\vec{L}_P$ can be expressed as the product of the body's inertia tensor $\mathbf{I}_P$ and its angular velocity $\vec{\omega}_R^S$:

$$\vec{L}_P = \mathbf{I}_P \vec{\omega}_R^S \tag{7.3.9}$$

Once the movement of system of rigid bodies (kinematics) and the inertia properties have been defined, the next step is to apply the equations of motion (dynamics). This results in either a *direct dynamic*s or an *inverse dynamics* formulation of the system, depending on the application. The direct dynamics is applied to obtain the movement of the system from the known forces that act on it. The inverse dynamics is applied to obtain the forces from the the known movement of the system. In this study, the Newton-Euler equations of motion are used to formulate the inverse dynamics of the system. Other methods to study the rigid body dynamics are the Lagrange approach or the TMT combination method (van der Kooij et al., 2008).

7.3.2. Newton-Euler equations for a single rigid body

Newton formulated the equations of motion for systems of mass particles. Euler recognized that a rigid body is a special case for such a system: the positions of the particles are constrained with respect to each other. This leads to the notion that the internal forces (the forces acting between the particles) do not contribute to the equations of motion for the entire system (rigid body). Since a rigid body has six degrees of freedom, there must be six equations describing the relation between forces and motion. This leads to the formulation of the Newton-Euler equations of motion:

$$\sum \vec{F}_{ext} = \dot{\vec{p}}_G = m {\cdot} \vec{a}_G$$

$$\sum \vec{N}_{ext}(G) = \frac{d(\vec{L}_G)}{dt} = \frac{d(\mathbf{I}_G \vec{\omega}_R^S)}{dt} \tag{7.3.10}$$

Where $\sum \vec{F}_{ext}$ is the sum of the external forces acting on rigid body S, $\dot{\vec{p}}_G$ is the the time derivative of the momentum of the CoM, which equals (with a constant mass m) the product of the mass and the acceleration of the CoM. $\sum \vec{N}_{ext}(G)$ is the sum of the moments of the external forces about the CoM *(G)*, which equals the time derivative of the rigid body angular momentum $\vec{L}_G$.

7.3.3. Newton-Euler equations for linked rigid body systems

Usually a rigid body is not moving freely in space. In general, there is some interaction with other rigid bodies. As shown in Figure the upper extremity system consists of 3 body segments (upper arm, forearm and hand) which interact with each other (Figure 7.3.1)
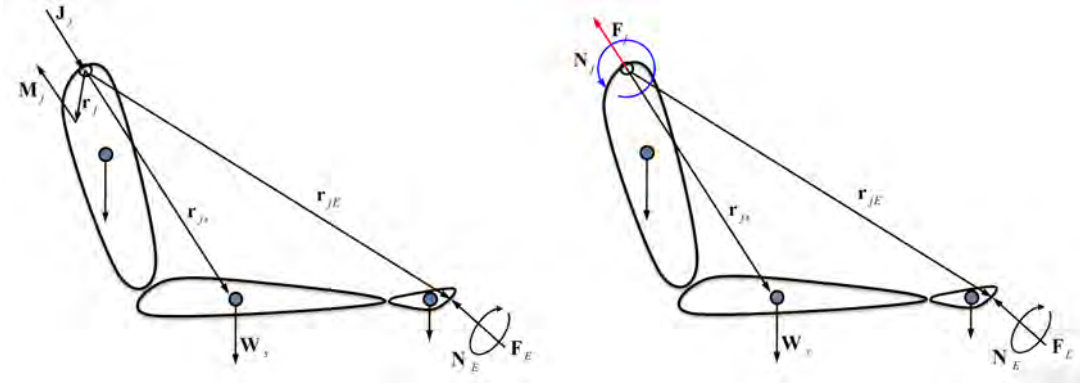

Figure 7.3.1.: Free Body Diagrams of the upper extremity linked rigid bodies. Joint forces($\vec{J}_j$), muscle force ($\vec{M}_j$), body segment weight ($\vec{W}_s$), external force ($\vec{F}_E$) , external moment ($\vec{N}_E$) and the position vector ($\vec{r}_{jS}$,$\vec{r}_{jE}$). In the B free body diagram, the resulting joint force ($\vec{F}_j$) calculated from $\vec{M}_j$ and $\vec{J}_j$, and the resulting joint moment ($\vec{N}_j$) calculated from $\vec{M}_j$ and $\vec{r}_j$ are shown.

The Newton-Euler equations of motion for the upper extremity system presented in Figure 7.3.1 are:

$$\vec{F}_j + \sum_s \vec{W}_S + \vec{F}_E = \sum_s m_S \cdot \vec{a}_{G,S}$$

$$\vec{N}_j + \sum_s (\vec{r}_{jS} \times \vec{W}_S) + \vec{r}_{jE} \times \vec{F}_E + \vec{N}_E = \sum_s \left(\frac{d\vec{L}_{j,S}}{dt} \right) \tag{7.3.11}$$

The arrangement of the Newton-Euler equations of motion (eq. 7.3.11) for the inverse dynamics approach is:

$$\vec{F}_j = \underbrace{\sum_s m_S \cdot \vec{a}_{G,S}(G)}_{Inertial} \underbrace{- \sum_s \vec{W}_S}_{Gravitational} \underbrace{- \vec{F}_E}_{External}$$

$$\vec{N}_j = \underbrace{\sum_s \left(\frac{d\vec{L}_{j,S}}{dt} \right)}_{Inertial} \underbrace{- \sum_s (\vec{r}_{jS} \times \vec{W}_S)}_{Gravitational} \underbrace{- (\vec{r}_{jE} \times \vec{F}_E + \vec{N}_E)}_{External} \tag{7.3.12}$$

Where $\vec{L}_{j,S}$ is the angular momentum of each segment S relative to the shoulder joint j and $\vec{a}_{G,S}$ is the acceleration of the CoM G for each segment S. The colors of Eq.7.3.12 indicate the origin of the component. Red indicates the *Inertial component*, green indicates the *Gravitational component* and blue indicates the *External component*. Iteratively, in a similar way the forces and moments acting on the elbow and wrist can be found.

7.4. Energetics

Power is defined as the rate of work or the rate of energy flow. The measurements of power that can be obtained from the joint kinetics are: joint power and muscle power. Since joint power does not provide any interpretable information it is not presented in this section.

7.4.1. Muscle (Angular) Power

The *muscle power* is defined as the scalar product of the joint moment and the segment's angular velocity. Precisely speaking, the *muscle power* is the rate of energy transfer through the joint caused by the angular motion of the joint. The *muscle power* of the forearm and the upper arm at the right elbow joint is:
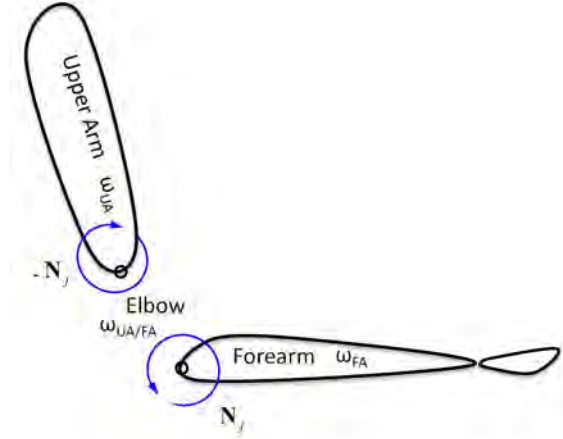

Figure 7.4.1.: The muscle power of the forearm and the upper arm at the right elbow joint.

$$P_{M_{FA}} = \vec{N}_j \bullet \vec{\omega}_R^{FA} = \vec{N}_j \bullet (\vec{\omega}_{UA}^{FA} + \vec{\omega}_R^{UA})$$
$$P_{M_{UA}} = (-\vec{N}_j) \bullet \vec{\omega}_R^{UA}$$
$$P_{M_{El}} = P_{M_{FA}} + P_{M_{UA}} = \vec{N}_j \bullet \vec{\omega}_{UA}^{FA} \tag{7.4.1}$$

Where P_M is the muscle power, $\vec{N}_j$ is the joint moment and $\vec{\omega}_{FA}^{UA}$ is the angular velocity of the upper arm relative to the forearm. $P_{M_{El}}$ is the muscular work rate done by the muscles at the elbow joint.

7.5. Interpretation of the rigid body dynamics and energetics

7.5.1. Resultant joint force

The *Resultant joint force (F_j)* is the sum of both the joint reaction force and the muscle force. Thus, it does not specifically reflect either the joint reaction force or the muscle force. It is simply the combined effect of the forces from the next segment attached through the joint and the muscle. To calculate the actual contact force at the joint a musculoskeletal modeling is needed.

7.5.2. Joint moment

The joint moment is the torque produced by the muscle force about the joint center and reflects the overall muscular efforts at the joint. It is always advantageous to describe the joint torque in the local (segmental) reference frame since the local components reflect the dominant muscle groups. For consistency, the origins of the segmental reference frames are located at the proximal ends of the segments. It must be kept in mind that the sign of the joint moment varies from one side to another (i.e. a positive torque of the z component for the right upper arm means an internal rotation dominant torque while a positive torque of the z component for the left upper arm means an external rotation dominant torque).

7.5.3. Muscle (Angular) Power - Rate of work

If the joint torque and the angular velocity of the motion have the same direction, the rate of work becomes positive, suggesting concentric contraction of the muscle while a negative power means eccentric activation of the muscle.

Part III.

State of the Art

8. Introduction: From the Lower to the Upper Extremity

The analysis of lower extremity has been well established for sports, ergonomics and clinical applications since long time (Rau et al., 2000). The breakthrough of 3D motion analysis in clinical application can be attributed to clinical *gait analysis* which is now applied to the detailed diagnosis and treatment planning of patients with difficulties in gait (Rau et al., 2000). Since gait is primarily 2D and a well defined motion type with cyclic sequences from heel strike to heel strike, its motion analysis becomes relatively simple. Even though, several pathological aspects which can modify a person's walking pattern increase the difficulty of gait analysis. Several biomechanical models of the lower extremities have been developed allowing the calculation of joint angles, joint forces and moments as well as the work, power or energy (e.g. Davis et al. (1991)). Note that for the dynamic analysis it is necessary to measure the ground reaction forces (GRF), which is usually performed using 3D force plates. For movement detection, the first applicable optoelectronic systems for gait analysis were introduced in the early seventies and have been developed into reliable tools (Rau et al., 2000). Over the last few decades, a number of gait laboratories have been established in which gait abnormalities can be examined precisely. However, sophisticated motion analysis requires technological knowledge and, nowadays, clinical applications take place mainly at those centers with tight collaboration between clinicians and engineers. Another obstacle to the clinical use of motion analysis is the lack of standardized, consistent and liable data banks that are necessary for interpreting the clinical significance of the set of biomechanical measurements.

While, human motion analysis has largely been focused on the lower extremity for the past few decades, research is nowadays including the upper extremity also, as newer clinical interests have emerged (Slavens and Harris, 2008). The study of the motion of the upper extremity is challenging. The complex nature of the upper extremity movements (3D and non-cyclic) and the difficult access to the external forces complicate (or even preclude) the definition of standard biomechanical models (Slavens and Harris, 2008). As a consequence, biomechanical models of the upper extremities are most often specifically designed for a particular task and/or patient population (Slavens and Harris, 2008), and a consensus has not been reached on some critical technical aspects such as joint and segment coordinate system orientation, definition and nomenclature of motions, anatomical joints to be modeled and joint angle description. A significant step towards standards to define joint coordinate systems of various joints for the reporting of human joint motion has been made by the International Society of Biomechanics (ISB) (Wu et al., 2005). Table 8.1 summarizes the differences between the lower extremity analysis (gait analysis) and the upper extremity analysis.

Gait analysis	Upper extremities
One standard movement	Task-dependent movements
Cyclic	Non-cyclic
Approx. 2D	3D
External forces easily measurable	External forces difficult to access
Limited range of motion	Extremely large range of motion
Standard protocols exist	No standard protocols
Ready-to-use systems available	No adapted systems available

Table 8.1.: Comparing lower extremity analysis (gait analysis) with upper extremity analysis (Adapted from Rau et al. (2000)).

9. Current Motion Measurement Methods

Several different methods have been used to detect the position and orientation of the upper extremity segments. Motion measurement methods can be divided into two categories: (i) *Optical* and (ii) *Non-optical*. Table 9.1 describes the most common tracking methods:

Tracking method	Category	Description	Commercial Brand
Movie camera Passive or Active marker	Optical	Optical systems require a minimum of 3 markers for segment to determine the position and orientation of the body segment. They experience problems with marker occlusion and marker tracking. Active optical system use light-emitting diodes.	OPTOTRAK MACREFLEX
Infrared camera Passive marker	Optical	Passive optical systems use reflective markers.	BTS VICON
Roentgen stereophotogrammetry	Optical	Tantulum balls are used as markers. Clear disadvantage of this method is the exposure of the subject to radiation. Maximal loads for experimentation are limited to a few photos or a few seconds of film. Photos have a better contrast. The contrast in films is amplified by fluorescence. The films have a very limited fieldof- view.	-
Sonic sensors Microphones	Non-Optical	Using speakers, the position of microphones can be determined using the delay time due to the limited speed of sound as a measure of the distance to each speaker	-
Electromagnetic sensor	Non-Optical	A magnetic field is generated by a transmitter, and the position and orientation of sensors can be derived by measuring the current in electric coils in the sensors. Obviously, this method is very sensitive to metallic objects interfering with the magnetic field and are limited in range.	ISOTRACK FLOCK BIRDS
Electrogoniometer	Non-Optical	Attached to the proximal and distal link, goniometers record the angle between the links in one plane (or three planes if three goniometers are placed in succession with a common rotation center). Electrogoniometers are simpler and cheaper, but have traditionally had problems with cross-talk between axes and can interfere with the movement.	BIOMETRICS Ltd
Accelerometer	Non-Optical	Accelerometers are sensitive to acceleration but also to gravity. Typically, two accelerometers rigidly attached on one link are needed to distinguish between accelerations and the orientation with respect to the gravity field. Velocities and positions can be derived by integration of the acceleration signal. However, this will often result in a static offset	KINETISENSE

Table 9.1.: Tracking methods (adapted from Anglin and Wyss (2000) and van der Kooij et al. (2008)).

10. Review of Upper Extremity models

This chapter reviews several kinematic and kinetic biomechanical models from the literature. The reviewed biomechanical models have been classified into two main groups depending on the strategy applied to define the marker set-up: (i) *Models that use joint markers and segment markers (marker cuffs)* and (ii) *Models that use joint markers.*

Models that use joint markers and segment markers (marker cuffs)

Models by R. Schmidt and N. Yang

Schmidt et al. (1999) proposed a rigid body model of the upper-extremities that consists of 3 segments: the upper-arm, the forearm and the hand, connected by two ball-and-socket joints: the elbow and the wrist. The model simplifies the elbow joint assuming that the pronation-supination of the forearm is performed in the elbow only and not in the two radioulnar joints. The required minimum of 3 non-collinear markers per segment is used to measure the all six DoF of every segment, and inter-marker motions are suppressed by connecting each 3 markers of a segment using marker cuffs. The forearm marker cuff is fixed close to the wrist in order to record most of the pronation-supination rotation. The joint centers and joint axes are defined with additional markers at the acromion, at the lateral and medial epicondyles and ulnar and radial styloids. A static reference measurement is needed to measure the locations of the joint markers and centers with respect to the segment markers and to define the neutral joint orientations. After this measurement the joint markers are removed, which avoids marker positions that are disturbed by large skin movements at the joints. After testing the model with ten subjects performing sample motions (tracking tasks) Schmidt et al. (1999) applied corrections on the surface marker data for skin and soft tissue motions in order to compare between the original signals and the corrected signals. Schmidt et al. (1999) concluded that the model assumptions were reasonable and that accurate joint rotations could be obtained, but that the skin motion corrections were essential to analyze the upper extremity motion.

Yang et al. (2002) used the model by Schmidt et al. (1999) to carry out a synergic analysis of the upper limb motion during target-reaching tasks. While Schmidt et al. (1999) assumed a fixed distance of 7 cm, Yang et al. (2002) measured the distance between the acromion marker (acr) and the shoulder center of rotation for each subject, In addition, Yang et al. (2002) did not apply any skin correction to the marker data, and recorded arm swing motions to identify and confirm the upper extremity joint centers. Yang et al. (2002) concluded that topological invariance and synergies can be found in target reaching movements of human upper limbs.
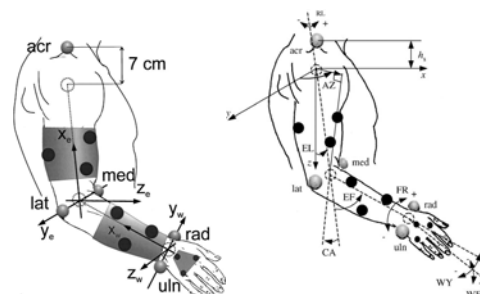

Figure 10.0.1.: Right side) an schematic representation of the marker set-up of the model proposed by Schmidt et al. (1999). Left side) an skeptical representation of the marker set-up presented by Yang et al. (2002). Note that the distance between the acromion marker (acr) and the shoulder center of rotation is in one case an anthropometric parameter (h_s) and in the other a fixed distance of 7cm.

Models by G. Rau and S. Williams

Rau et al. (2000) and Williams et al. (2006) expanded the model proposed by Schmidt et al. (1999) by adding the torso and the clavicle segments. Therefore, their model incorporates the shoulder and the sternoclavicular joints. This modification was necessary to evaluate the upper extremity motion from a clinical point of view. Williams et al. (2006) used the model to analyze the upper extremity motion during a particular ADL (removing a parking token) in patients with subcromial impingement syndrome and in healthy subjects. The results showed that it is possible to identify movement patterns of different groups and to compare the differences between populations. Rau et al. (2000) presented an example of assessing the movement disorders in children with plexus lesion to illustrate the implications and the potential of upper extremity motion analysis in clinical applications.
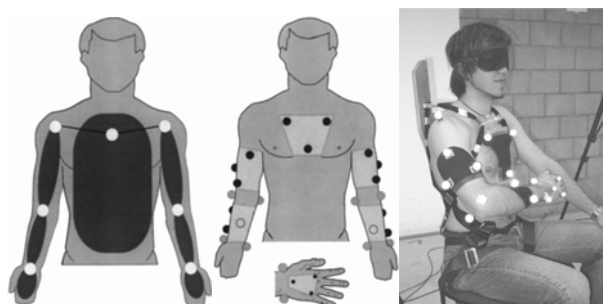

Figure 10.0.2.: Schematic representation of the marker set-up of the model presented by Rau et al. (2000) and Williams et al. (2006).

Model by E. Roux

Roux et al. (2002) assessed the performance of the global optimization (GO) method (Lu and O'Connor, 1999) that is to correct skin movement with an upper limb kinematic analysis. The GO method estimates bone position from skin marker coordinates and to decrease the skin motion artifacts that are caused by the relative motion between bone and markers. The model presented by Roux et al. (2002) consists of six segments: head, trunk, shoulder girdle, upper arm, forearm and hand. The marker set-up is similar to the one of Schmidt et al. (1999) for the acromion, forearm, elbow, wrist and hand. Four markers were attached to the upper arm segment. Elbow and wrist joint markers were used during the static trial only. On the contrary to Schmidt's model, a sphere-fitting method was used for determination of the shoulder and wrist joint centers, which is more accurate (Stokdijk et al., 2000). The elbow center was defined as the midpoint between the medial and lateral elbow markers. Results showed a significant reduction of the error and variability due to skin movement.
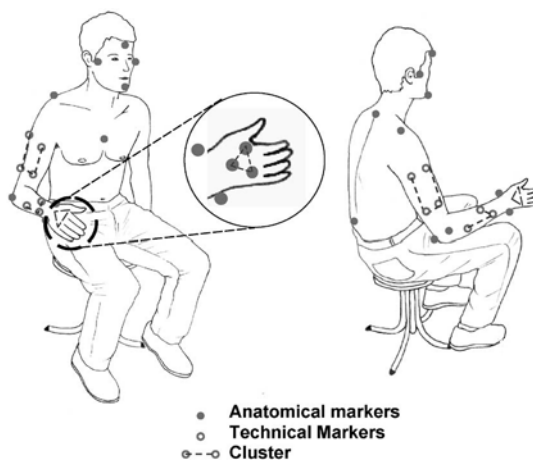

Figure 10.0.3.: Schematic representation of the marker set-up of the model presented by Roux et al. (2002).

Models that use joint markers

Model by G. Rab

The model presented by Rab et al. (2002) consists of 10 segments: head, neck, shoulder girdle, right/left upper arms, right/left forearms, right/left hands and pelvis. The wrist joint was modeled as a universal (saddle) joint with 2 DoF. In agreement with clinical convention, wrist movement was represented by movement between the hand and forearm segments, determined by a vector connecting the geometric wrist center and the calculated elbow center. The elbow joint was modeled as a rotating-hinge joint with 2 DoF, with a single joint center in the distal humerus. Forearm pronation and supination were modeled as rotation about an axis connecting the elbow center and distal ulna. The shoulder joint was modeled as a ball and socket joint with 3 DoF, located in the center of the humeral head. Movement was calculated between the humerus and the trunk, and scapular contribution to shoulder motion was ignored. Note that the upper arm segment has only 2 markers, which forces to used the wrist joint center as a third reference point to calculate the internal-external rotation of the upper arm. Problems occur if the elbow is hyperextended, because all 3 markers (shoulder, elbow and wrist) become collinear. Rab et al. (2002) verified, and quantified the sensitivity to calculation errors of the model. This biomechanical model has been applied to analyze upper extremity motions of normal children performing ADLs (Petuskey et al., 2007).
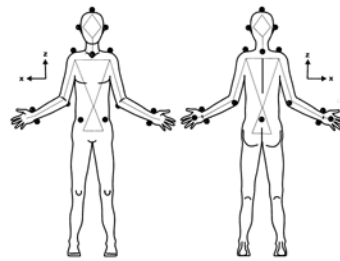

Figure 10.0.4.: Schematic representation of the marker set-up of the model presented by Rab et al. (2002).

Model by A. H. Mackey

Mackey et al. (2005) presented an upper extremity model of 7 segments, including: right/left trunk, right/ left upper arm, right/left forearm and pelvis. Marker location of this upper extremity model slightly differed from those previously described by Schmidt et al. (1999) Rau et al. (2000) and Rab et al. (2002). In contrast to Rab et al. (2002), no head markers were included. Forearm and upper arm segments contained a segment marker to register the rotational orientation of the segments. Upper limb joint centers, at the shoulder, elbow, wrist and neck, were defined as virtual markers and calculated as the middle point between external marker positions. Mackey et al. (2005) analyzed measurements of arm movement during simple upper limb tasks ('hand to head' and 'hand to mouth') and gait in 10 children with hemiplegic cerebral palsy. They concluded that the 3D kinematic analysis of movement of the hemiplegic upper limb during simple upper limb tasks had moderate to good repeatability, suggesting it may be able to be used as an outcome measure in the hemiplegic upper limb.
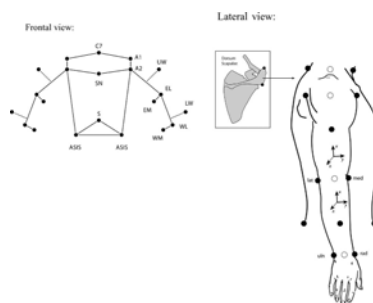

Figure 10.0.5.: Schematic representation of the marker-set up of the model presented by Mackey et al. (2005).

Models by B. Hingtgen and B. A. Slavens

The upper extremity model presented by Hingtgen et al. (2006) consists of 5 segments: trunk, right upper arm, right forearm, left upper arm, and left forearm. The segments are connected by a 3 DoF joint (glenohumeral joint) and a 2 DoF elbow joint. To determine the shoulder joint center location, the circumference of the shoulder, around the acromion and axilla was measured for each subject. From this approximately circular measurement, the radius of the shoulder was calculated. The joint center was then located inferiorly from the acromion, at the measured distance. The joint centers and joint coordinate systems were defined using subject specific anthropometric measurements and were based on standards set forth by the ISB recommendations (Wu et al., 2005). Hingtgen et al. (2006) used the model to quantify the upper extremity movement of 8 hemiparetic stroke patients with spasticity, while completing a set of reaching tasks. Results from this work indicated that the model was sufficient for detecting differences in upper extremity motion.

Slavens et al. (2010) expanded the model from Hingtgen et al. (2006) adding a right Lofstrand crutch and a left Lofstrand crutch to assess upper extremity kinematics and kinetics of children with myelomeningocele. Kinematics of model segments were calculated for use in the kinetic model. Kinetic equations were formulated according to the inverse dynamics Newton-Euler approach. The model calculates 3D joint forces and moments, bilaterally, for the proximal crutch/hand interface, wrist, elbow, and shoulder.
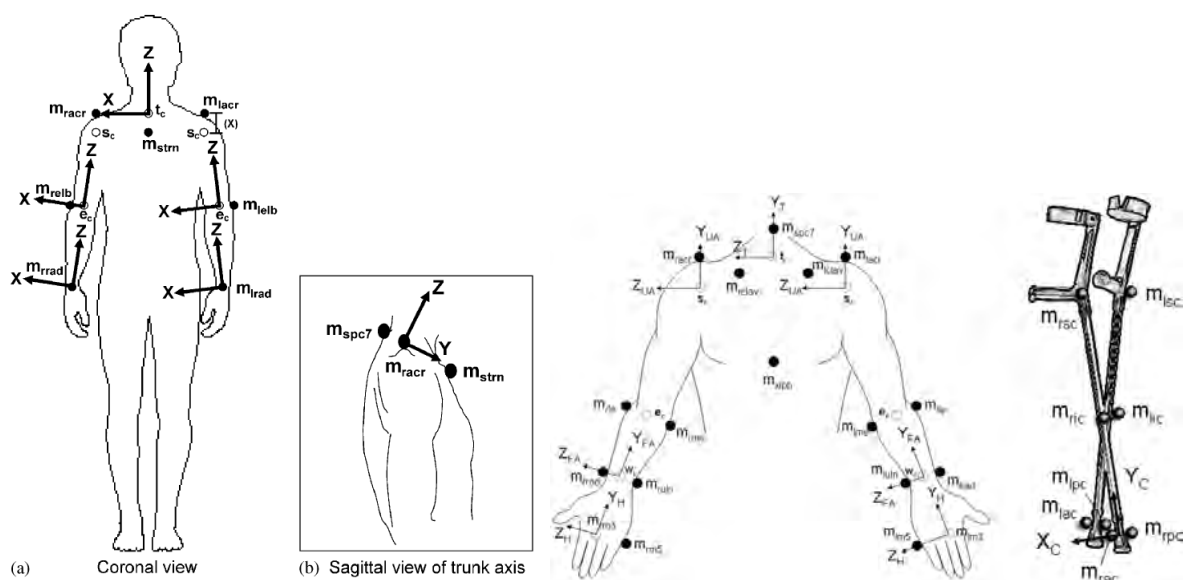

Figure 10.0.6.: Schematic representation of the marker-set up of the model presented by Hingtgen et al. (2006) and Slavens et al. (2010).

Model from O. Rettig et al. 2009

The HUX model presented by Rettig et al. (2009) consists of 7 segments: thorax, clavicles, upper arms and forearms. The sterno-clavicular joint was treated as a universal joint with 2 DoF (its axial rotation was not considered) and was used for calibration purposes only. The gleno-humeral joint was regarded as a ball and socket joint with 3 DoF. The elbow was treated as a hinge joint with 1 DoF. Translational DoF are not considered in any of the joints. After a static calibration trial for assessing thorax position and for determining parameters of the humerus segment marker, 3 independent functional trials were performed, each starting with the arm in neutral position: (i) shoulder abduction/adduction, (ii) shoulder flexion/extension and (iii) elbow flexion/extension . The method described by Gamage and Lasenby (2002) was used to determine the position of the gleno-humeral joint center and the elbow joint center. This protocol was applied to 50 subjects and they found that the variability in shoulder and elbow joint center localization in repeated measures was typically below 1 cm. Moreover, differences between the computed joint angles and the angles obtained directly with a goniometer remained below $\pm 5°$ for joint angles up to 120° and $\pm 10°$ above 120°.

Figure 10.0.7.: Schematic representation of the marker-set up of the model presented by Rettig et al. (2009).

Part IV.

Materials and Methods

11. Activity of Daily Living (ADL) to be analyzed

In order to fulfill standardization requirements, the upper extremity motion is analyzed during an specific ADL based on a test currently used in observational motion analysis (Action Research Arm (ARA) test). The actual task was defined in agreement with the clinicians of the *Institut Guttmann*. The selection of the task was a trade-off between the complexity required for a relevant biomechanical analysis, and the simplicity required for being performed by pathological subjects. The requirements for the task design were:

1. Inclusion of different levels of difficulty.

2. Adaptability to a range of anthropometric dimensions.

3. Compatibility with subjects on wheelchair and on other assistive devices.

4. Appropriate to evaluate shoulder and elbow flexion-extension motion.

5. Appropriate to evaluate grasping.

6. Being performed by one single arm.

7. Involving interaction with common life object.

11.1. Description of the motion task

Steps listed in table 11.1 schematically define 3 basic daily living functions involving the simple manipulation of a given object: (i) reaching the object, (ii) transporting the object and (iii) placing the object. Each of these functions is done in 2 depths: (i) near and (ii) far.

Steps	Function	Depth
1: Arm initial position (*)	-	-
2: Reach the object in the object initial position (**)	1	1
3: Transport the object to the target position	2	2
4: Place the object in the target position	3	1-2
5: Withdraw the arm initial position	-	-
6: Reach the object in the target position	1	2
7: Transport the object to the object initial position	2	2-1
8: Place the object in the object initial position	3	1
9: Return to the arm initial position	-	-
Arm Initial position: sitting with no shoulder flexion and with 90° of elbow flexion. The ulnar and radial styloids have to coincide with the edge of the table.		
**Object Initial position:* the object is placed at the center between both shoulders and at 10 cm from the edge of the table.		

Table 11.1.: Sequence of the analyzed task.

The task is repeated for nine target positions at the maximum distance that can be reached by the subject. Note that in the case of subjects who cannot completely extend the elbow, this distance is shorter than the actual length of the arm. The nine target positions are placed in front of the subject at 3 widths and at 3 heights (Figure 11.1.1). The 3 widths are: in front of the shoulder of the analyzed arm (LS or RS), in front of the other shoulder (LS or RS) and on the external side of the analyzed arm (EXT). The 3 heights are: elbow height (H0), shoulder height (H1) and two times the height from the elbow to the shoulder (H2). The combination of the widths and heights results into the nine target positions, which depending on the analyzed arm (right or left) have one distribution or another (Table 11.2).

In addition to the information of the sequence of the task, the subject was instructed to complete the task without flexing the trunk, and to take the bottle (object) as if he/she was going to drink from it. Each task was repeated twice.
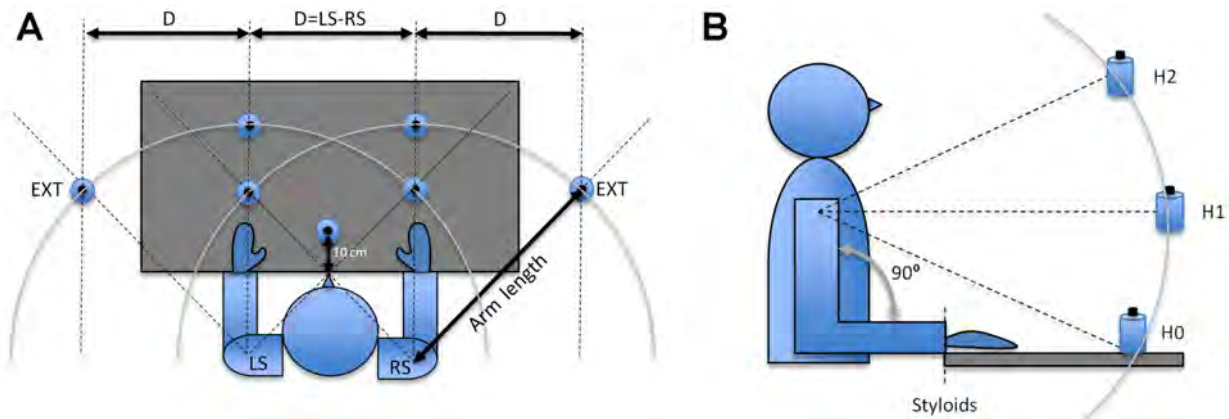

Figure 11.1.1.: Schematic representation of the nine target positions respect to the subject of study. A) transversal view of the set-up of the task. B) a sagital view of the set-up of the task.

A	EXT	LS	RS
H2	H2_EXT	H2_LS	H2_RS
H1	H1_EXT	H1_LS	H1_RS
H0	H0_EXT	H0_LS	H0_RS

B	LS	RS	EXT
H2	H2_LS	H2_RS	H2_EXT
H1	H1_LS	H1_RS	H1_EXT
H0	H0_LS	H0_RS	H0_EXT

Table 11.2.: Combination of widths and heights. A) the resulting nine reaching conditions for the left arm. B) the resulting nine reaching conditions for the right arm. Note that A and B are symmetrical.

11.2. Material for the task

The task was done using the following material (which is shown in Figure 11.2.1):

- A height adjustable table.

- An stool (in the case the subject does not use a wheelchair).

- A plastic Bottle of 33cl of capacity full of water.

- A height adjustable surface.

Figure 11.2.1.: Set-up of the task.

12. Subjects

This study has been carried out with a total of six subjects (3 healthy and 3 pathological). Healthy subjects did not have any injury on the upper body. The inclusion criteria for pathological Subject 04, 05 and 06 was that they had to be able to perform the task and to understand the task instructions. In order to provide reference values from which biomechanical differences between healthy and pathological subjects could be extracted, the set of motions described in Section 11.1 *Description of the task* were registered for both arms of healthy subjects. For pathological subjects, the motion of the most affected arm was registered. Table 12.1 summarizes the characteristics of the population.

- Subject 04 has an incomplete SCI at the C4 level classified as ASIA D with gait preserved. In order to increase his/her degree of independence when performing daily living activities, Subject 04 was submitted to a deltoid-triceps tendon transfer at the left arm to gain elbow extension.

- Subject 05 presents the same kind of SCI (incomplete SCI at the C4 level classified as ASIA D with gait preserved). Contrary to Subject 04, Subject 05 has the elbow flexion-extension preserved and thus no deltoid-triceps tendon transfer is needed. Moreover, Subject 05 has both the motor function of the right side of the body and the sensitive function of the left side of the body affected. Subject 06 is a Stroke patient with the right side of the body more affected (right hemiparesis).

- Subject 06 had a left middle cerebral artery infarction. Subject 06 presents a Broca's aphasia (non-fluent aphasia) and a Fugl-Meyer score of 20 for the right arm, which means that the functionality of the right upper extremity is very limited to perform the proposed task of this study.

Subject Nb	Age (years)	Gender (Male/Female)	Analyzed Arm	Condition (Healthy/Pathological)	Height (cm)	Weight (Kg)
01	27	Male	Right and Left	Healthy	189	82
02	43	Male	Right and Left	Healthy	190	92
03	22	Male	Right and Left	Healthy	181	64
04	34	Female	Left	Pathological (SCI)	163	77
05	34	Female	Right	Pathological (SCI)	170	61
06	25	Male	Right	Pathological (Stroke)	180	81

Table 12.1.: Population characteristics.

13. Upper Extremity Biomechanical model

13.1. Joints and Segments of interest

The aim of the proposed upper extremity biomechanical model is to analyze the motion of 10 body segments, 5 joints and 20 DoF (Table 13.1). Note that while the model considers 5 joints, the shoulder and elbow joints are the most interesting for clinicians.

Segment	Proximal / Distal Joint	Rotation of Interest	DoF
Lower Trunk	-	Flexion-extension	1
Upper Trunk	-	Flexion-extension Internal-external rotation Lateral Inclination	3
Head	-	Compensation movements (3 anatomical axis)	3
Right clavicule	Sternoclavicular joint R Shoulder	Elevation-depression Retraction-protraction	2
Left clavicule	Sternoclavicular joint L Shoulder	Elevation-depression Retraction-protraction	2
Upper arm	Shoulder Elbow	Flexion-extension Abduction-adduction Internal-external rotation	3
Forearm	Elbow Wrist	Flexion-extension Pronation-Supination	2
Palm	Wrist metaphalangeal joint	Flexion-extension Ulnar-radial deviation	2
Thumb	Wrist	First phalange Flexion-Extension	1
Fingers	metaphalangeal joint	First phalange flexion-extension	1

Table 13.1.: Joints and segments of interest. For each segment the proximal and distal joint, the rotations of interest and the DoF are shown.

13.2. Selection of the marker set-up

Selecting an appropriate marker set-up is crucial to achieve a full accurate quantitative description of the upper extremity motion. This section presents the results of the experiment carried out to select the best marker set-up for the specific reaching task and for the particular case of the motion capture system of the *Institut Guttmann*. On this regard, it is important to note that the current set-up of the capture system of the *Institut Guttmann* is designed for gait analysis and therefore the capture volume is much grater than the one necessary to capture upper extremity motions (Figure 13.2.1). It is also worth noting that the simple solution of just bringing the cameras closer to the volume of interest was not an option because the cameras are well fixed to the wall.

Figure 13.2.1.: Motion analysis laboratory.

As described in chapter *10 Review of Upper Extremity models*, there are two main strategies to define the marker set-up: (i) the use of joint markers and (ii) the use of a combination of joint markers and segment markers (marker cuffs) (Figure 13.2.2 and Table 13.2). The main advantage of the first strategy is that the segment motion measurements are more accurate because markers are placed in the joint bony landmarks (i.e., styloids or epicodyles). The disadvantage of this method is that joint markers experiment occlusion problems (i.e., medial epicondyle), which often implies that the tracking of a considerable number of segments is not possible. The second strategy implies a static reference measurement to calculate the relative locations of the joint markers with respect to the segment markers. This method has the advantage that joint markers can be removed after the static measurement, and the dynamic measurements are performed selecting those markers with good visibility, which implies that in the worst case occlusion occurs during limited periods of time only. This is an important characteristic for the analysis of the non-smooth movements of pathological subjects. The disadvantage of this method is that the signal presents higher values of noise due to relative motion between the attachment and the skin. Therefore, there is a trade-off between the accuracy of the first method and the more comprehensive but noisy register of markers of the second. Note that almost all of the placements of our joint markers follow the ISB recommendations proposed by Wu et al. (2005).
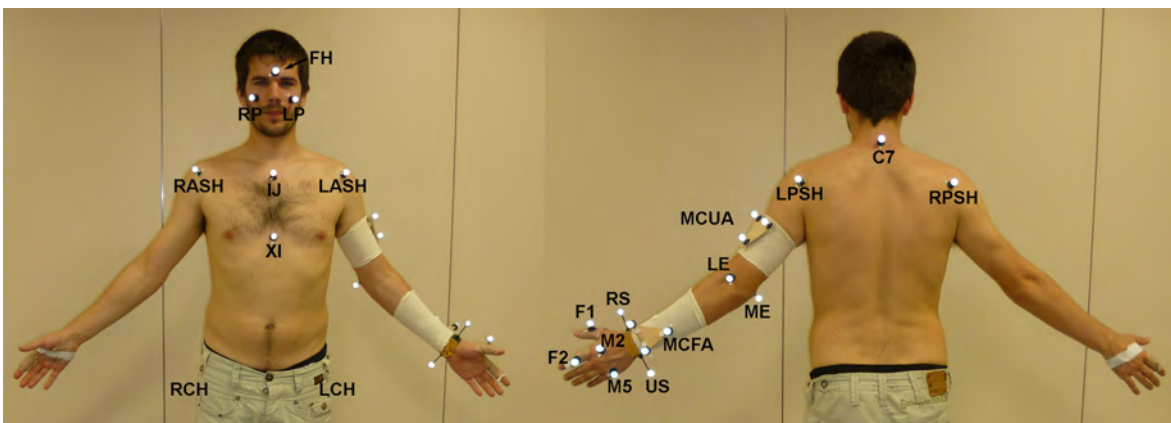

Figure 13.2.2.: Joint markers and Segment markers placed together. Each marker is labeled with an acronym.

Marker	Anatomical Location
FH	Glabella.
RP/LP	Right / Left cheekbone.
IJ	Deepest point of Incisura Jugularis.
XI	Processus Xiphoideus, most caudal point on the sternum.
C7	Processus Spinosus of the 7th cervical vertebra.
RASH/LASH	Right / Left Anterior Shoulder (acromion front).
RPSH/LPSH	Right / Left insert of the dorsum scapulae (acromion back).
MCUA	Marker Cuff placed at the lateral Upper arm.
LE/ME	Lateral / Medial Epicondyle.
MCFA	Marker Cuff placed at most distal part of the Forearm.
RS/US	Radial/Ulnar Styloids.
M2/M5	Second and Fifth Metaphalangeal joint.
F1/F2	Proximal Phalanges of Finger 1 and 2.
RCH/LCH	Projection of the right/left trocanter to the stool/wheelchair.

Table 13.2.: Marker acronyms and their anatomical location.

In order to determine the best marker set-up, five rotations of the two main arm joints (shoulder flexion-extension, abduction-adduction, internal-external rotation and elbow flexion-extension, pronation-supination) were captured with joint markers (Method 1) and segment markers (Method 2) at the same time. Each rotation was repeated 3 times for the left arm by 3 healthy subjects. The registered data was analyzed on the frequency and time domain. The first objective was to quantify and compare the signal quality (using the Signal to Noise Ratio (SNR)) of the two marker set-ups for each rotation. The second objective was to quantify the difference in the angular displacement for each rotation taking as standard the angular displacement obtained with the joint markers. Figures 13.2.3, 13.2.4 and 13.2.5 show respectively the angular displacement, angular velocity and angular acceleration of the elbow flexion-extension rotation for each subject, method and filter (see Appendix B *Figures* for the rest of joint rotations graphics, and Appendix D *Program code: Functions and scripts* for the program code used for the SNR and Angular displacement comparison).

13.2.1. Analysis on the frequency domain: SNR comparison

The first analysis was performed comparing the SNR of the angular acceleration for each rotation and each subject. Each signal was filtered using 3 different methods: (i) no filter (NF) , (ii) Butterworth filter with a cut-off frequency (Fc) of 6 Hz (F6) and (iii) Butterworth filter with a cut-off frequency of 3 Hz (F3). Note that the third filter (Butterworth Fc=3Hz) is the one that is going to be used in the study (see Section *15 Data Processing*). The SNR was calculated as:

$$\text{SNR} = \frac{P_{\text{signal}}}{P_{\text{noise}}} \tag{13.2.1}$$

where P_{signal} stands for the average power of the signal (meaningful information) which is contained between 0 and 3 Hz (Silva and Ambrósio, 2004) and P_{noise} stands for the average power of the noise (unwanted signal) which is contained from 3 Hz on. The relative SNR is calculated as:

$$SNR_{relative} = \frac{SNR_{M1} - SNR_{M2}}{SNR_{M1}} \tag{13.2.2}$$

where SNR_{M1} is the SNR of Method 1 and SNR_{M2} is the SNR of Method 2.

The results of SNR and relative SNR for each rotation, subject, method and filter are presented on Figures13.2.6 and 13.2.7 respectively. The SNR_{M1} (using joint markers) is grater than the SNR_{M2} (using segment markers) in all cases but SIER of subject 3, where SNR_{M2} is slightly larger than SNR_{M1}(probably caused by a bad data capture). The difference between both methods decreases when decreasing the Fc. Note that the relative SNR has to be interpreted with the information of the absolute SNR.
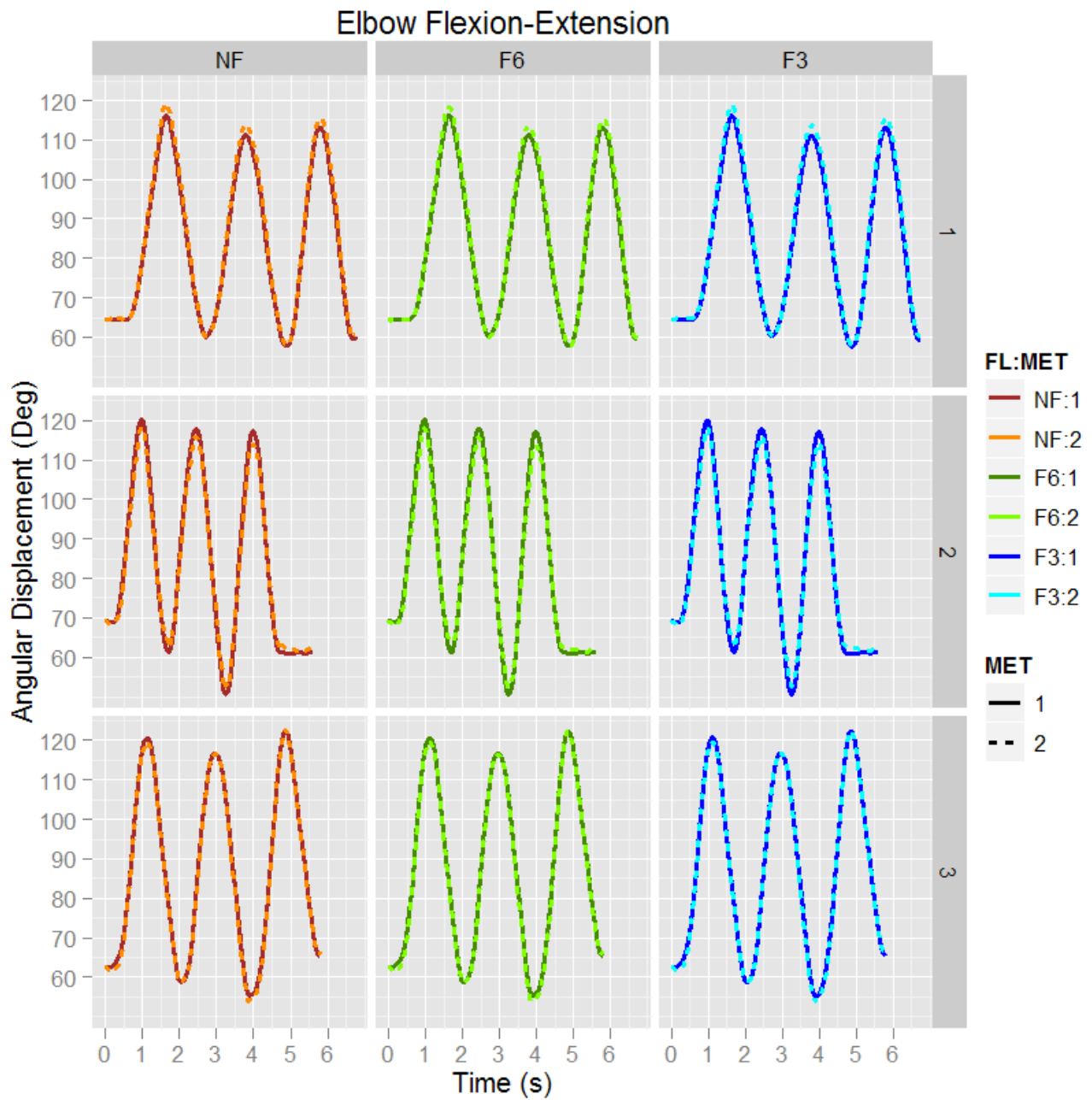
Figure 13.2.3.: Angular displacement of the elbow flexion-extension along time for each subject (1,2 and 3), method (MET) and filter (NF,F6 and F3).
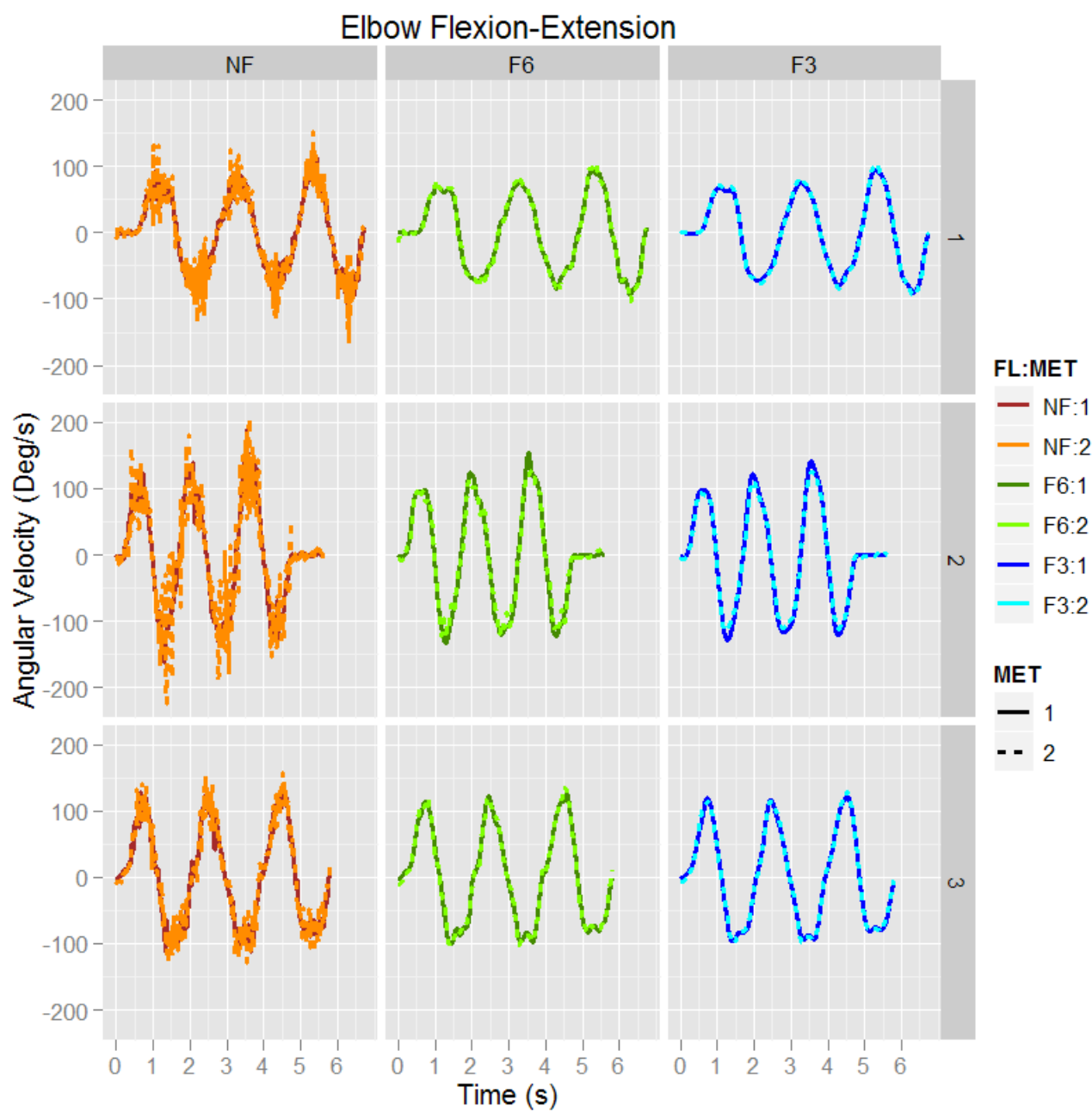
Figure 13.2.4.: Angular velocity of the elbow flexion-extension along time for each subject (1,2 and 3), method (MET) and filter (NF,F6 and F3).
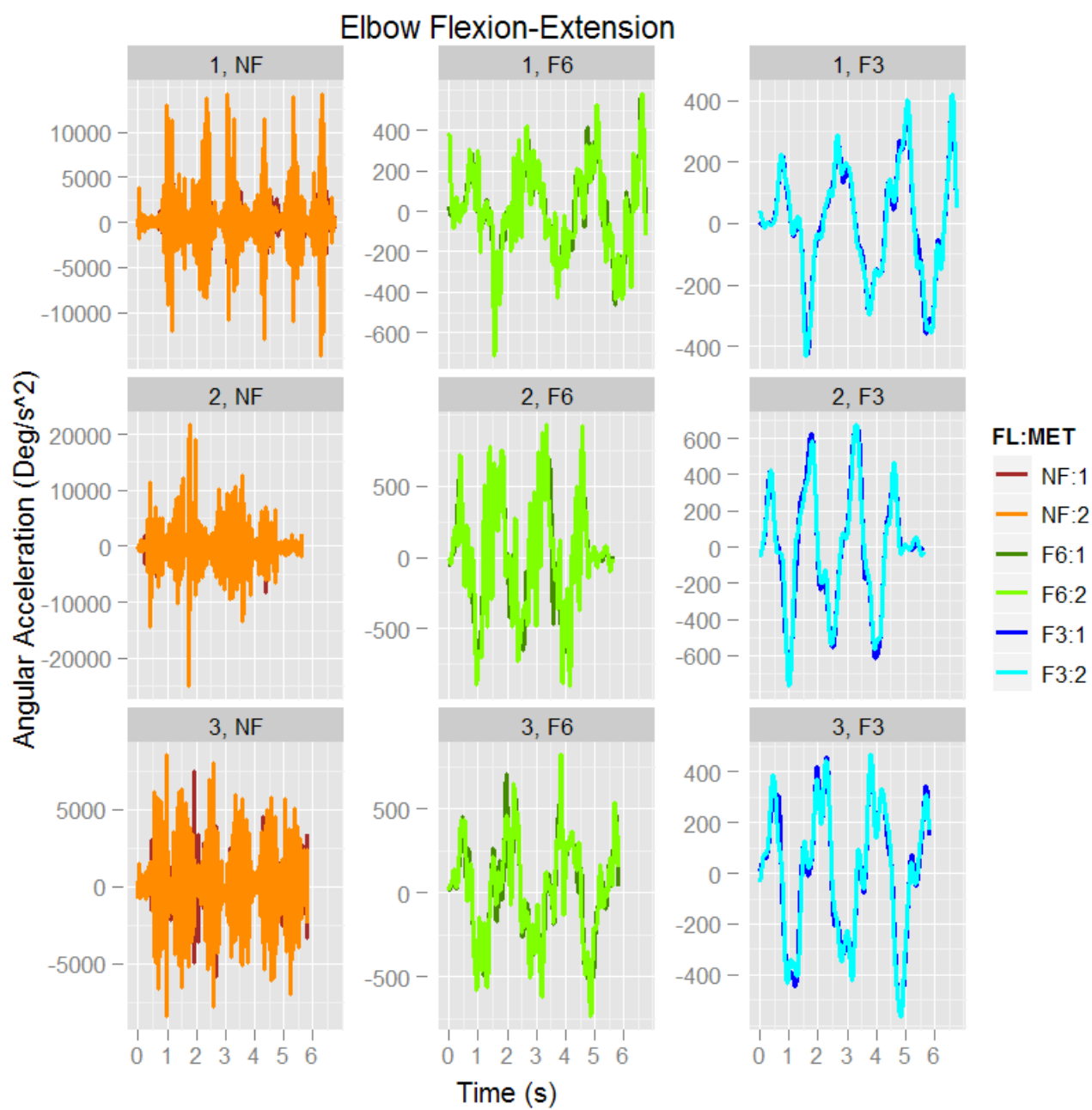
Figure 13.2.5.: Angular acceleration of the elbow flexion-extension along time for each subject (1,2 and 3), method (MET) and filter (NF,F6 and F3). Note the scale change between graphics.
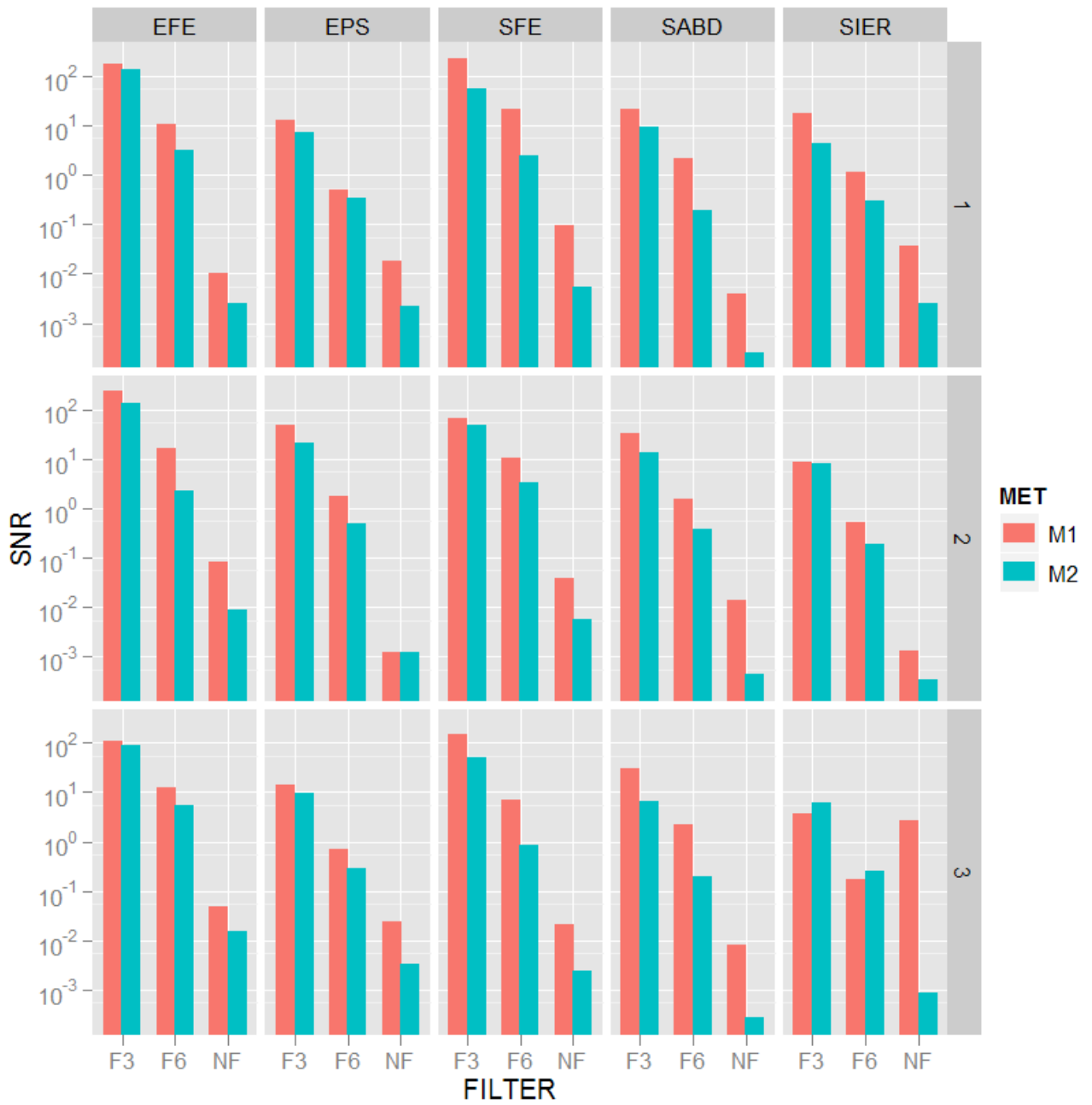
Figure 13.2.6.: SNR analysis of the angular acceleration for each rotation (EFE, EPS, SFE, SABD and SIER), subject (1,2 and 3), method (M1 and M2) and filter (NF, F6 and F3). Note the logarithmic scale in the Y axis.
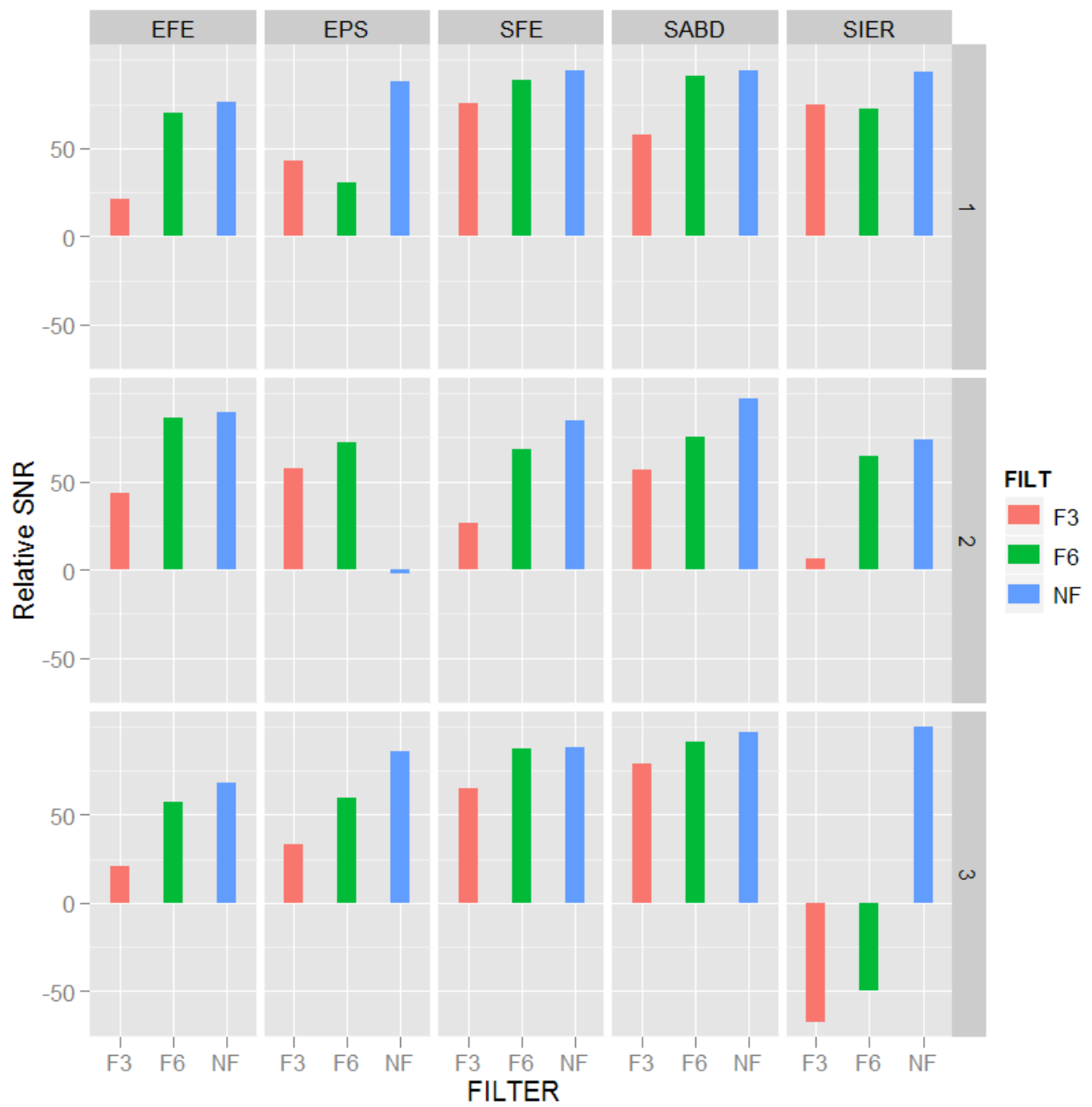
Figure 13.2.7.: Relative SNR of the angular acceleration for each rotation (EFE, EPS, SFE, SABD and SIER), subject (1,2 and 3), method (M1 and M2) and filter (NF, F6 and F3).

13.2.2. Analysis on the time domain: Angular Displacement comparison

The second analysis was performed comparing the signal of angular displacement between Method 1 (M1) and 2 (M2), applying the Butterworth filter with a cut-off frequency of 3Hz (F3). The objective of this analysis was to quantify the differences in angular displacement between methods. Method 2 used marker cuffs attached to the skin. The attachments are susceptible to intrasegment motions due to muscle contractions and to a bad capture of the segment roll (rotation around the longitudinal segment axis). This is because the skin close to the proximal joint rotates little around the longitudinal segment axis and only at the distal end of the segment the skin follows most of the segment rotation. The marker cuffs guarantee the same amount of rotation for every marker, but still they rotate less than bones. This problem can be reduced by placing the marker cuff as close as possible to the distal part of the segment (Schmidt et al., 1999). In the upper extremity there are two main segments that can roll: the upper arm and the forearm. In the latter, because of the nature of the elbow joint the problem is amplified. Figure 13.2.9 show the angular displacement difference between methods for each rotation and subject. The Root Mean Square Deviation (RMSD) and the Normalized Root Mean Square Deviation (NRMSD) is used to quantify the difference between methods:

$$RMSD(\theta_{M1}, \theta_{M2}) = \sqrt{\frac{\sum_{i=1}^{n}(\theta_{M1,i} - \theta_{M2,i})^2}{n}}$$
$$\mathrm{NRMSD} = \frac{\mathrm{RMSD}}{\theta_{M1,\mathrm{max}} - \theta_{M1,\mathrm{min}}} \cdot 100 \tag{13.2.3}$$

where θ_{M1} and θ_{M2} are the angular displacement for Method 1and 2, respectively, and n is the length of vector θ_{M1} and θ_{M2}. Note that Method 1 is used as reference method because joint markers follow better bone rotations than Method 2.

Table 13.3 presents the results of the NRMSD for each rotation and subject. As expected, elbow pronation-supination and shoulder internal-external rotation are the largest values followed by the shoulder abduction-adduction. Elbow and shoulder flexion-extension present the smallest values. These results indicate that Method 2 presents problems for capturing the roll rotations of both the upper arm and forearm segments (shoulder internal-external rotation and elbow pronation-supination).

	EFE	EPS	SFE	SABD	SIER
1	9.0%	25.2%	3.4%	24.4%	20%
2	8.3%	60.2%	9.8%	27.1%	50.6%
3	3.5%	56.5%	5.7%	18.1%	30.0%
MEAN	6.93%	47.3%	6.3%	23.2%	35.53%

Table 13.3.: NRMSD values for each rotation (EFE, EPS, SFE, SABD and SIER) and subject (1,2 and 3).

13.2.3. Selected marker set-up

The selected marker set-up is a combination of both methods (Figure 13.2.8). Because of the aforementioned problems to capture the elbow pronation-supination when using marker cuffs and taking advantage of the good visibility of the styloid markers, the latter was used to define the orientation of the forearm discarding the use of marker cuffs. On the upper arm the situation is different, the medial epicondyle had problems of occlusion and therefore it was necessary to use a marker cuff to determine the elbow joint center of rotation during the dynamic trial. This decision also takes into account the fact that the SNR values of Method 1 and Method 2 are very similar when using a FC of 3 Hz.

The static trial is done with all the markers (Figure 13.2.8A) in order to register the relative relations in position between the marker cuff and the joint markers that are removed in the dynamic trial (shoulder markers and the medial epicondyle marker) (Figure 13.2.8B). Note that even though is not seen, the medial epicondyle is placed in Figure 13.2.8A and removed in Figure 13.2.8B. In addition to the joint and segment markers, the objects of interaction (bottle, table and the height adjustable surface) had also markers to register their position in space.
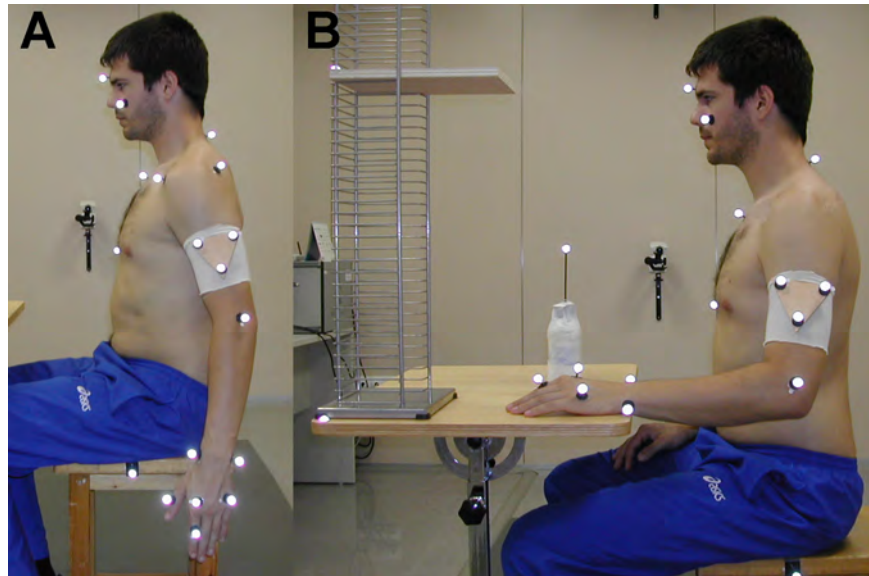
Figure 13.2.8.: Selected marker set-up. A shows the marker set-up for the static trial (22 markers) and B shows the marker set-up for the dynamic trial (19 markers).
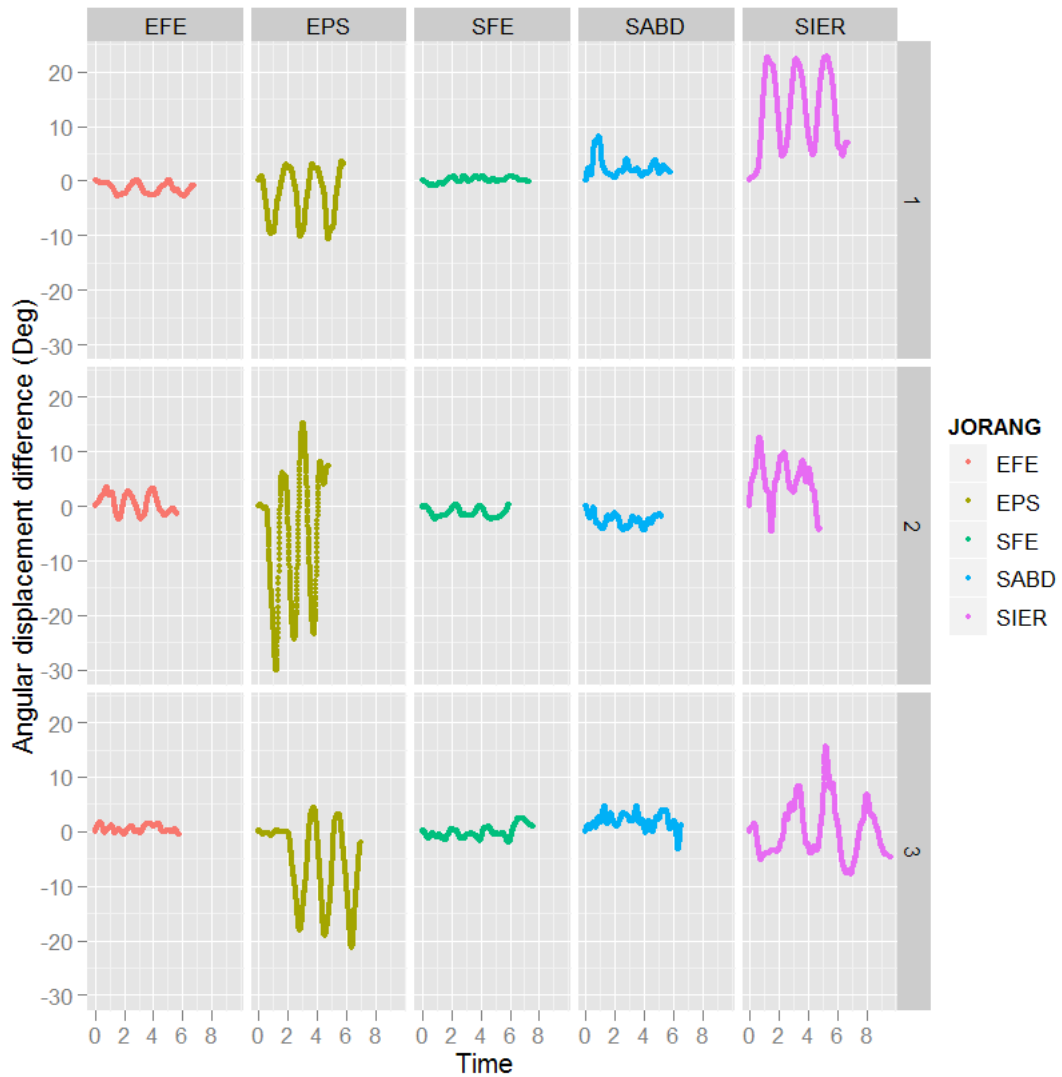

Figure 13.2.9.: Difference between Method 1 and 2 of the angular displacement along time for each rotation (EFE, EPS, SFE, SAND and SIER) and subject (1,2 and 3).

13.3. Kinematic and Dynamic Model

The proposed biomechanical model is made up of 10 segments and the joints that connect the segments are ideal ball-and-socked joints which do not permit translations between the segments, as schematically represented in Figure 13.3.1
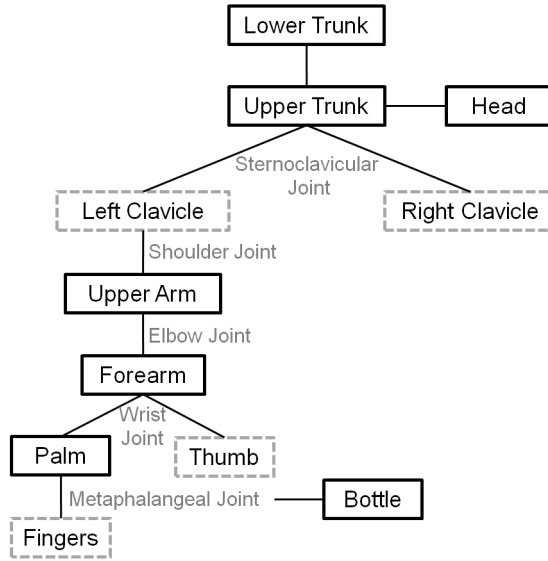
Figure 13.3.1.: Diagram of the upper extremity model (left arm). Segments are displayed in black and joints in grey. The segments with the discontinuous frame are not computed in the inverse dynamic model.

13.3.1. Joint definition

The sternoclavicular joint connects the clavicule with the upper trunk (Table 13.4). This joint is a complete simplification of the real sternoclavicular joint because the joint center coincide with the Incisura Jugularis marker *(IJ)* and both left and right clavicules share the same sternoclavicular joint. This simplification was proposed by Rau et al. (2000) and Williams et al. (2006). All the other joints (shoulder, elbow, wrist and metaphalangeal) are calculated as the mid point between two markers. The shoulder joint of the analyzed arm and the elbow are calculated using the *Rigid Body Method (Kwon, 1998)* which means that they are calculated from the position and orientation of the upper arm marker cuff combining data from the static trial and the dynamic trial.

Joint	Proximal segment	Distal segment	Position
Sternoclavicular	Upper Trunk	Right/Left Clavicule	$\vec{J}_{SC} = \vec{IJ}$
Shoulder*	Right/Left clavicule	Upper arm	$\vec{J}_{RSh} = \frac{1}{2}(\vec{RPSH} + \vec{RASH})$ $\vec{J}_{LSh} = \frac{1}{2}(\vec{LPSH} + \vec{LASH})$
Elbow*	Upper Arm	Forearm	$\vec{J}_{El} = \frac{1}{2}(\vec{LE} + \vec{ME})$
Wrist	Forearm	Palm and Thumb	$\vec{J}_{Wr} = \frac{1}{2}(\vec{RS} + \vec{US})$
Metaphalangeal	Palm	Fingers	$\vec{J}_{Meta} = \frac{1}{2}(\vec{M1} + \vec{M5})$

Table 13.4.: Joint Definition. Proximal and distal segments and the joint calculation. The (*) indicates that the joint has been calculated using the *Rigid Body Method* (Kwon, 1998).

13.3.2. Segment definition

The markers placed on the left and right side of the stool (Figure 13.2.8) are used to define the anchor of the system ($\vec{P}_{LTrunk}$) which is the most proximal point of the system. This is calculated as the middle point between the Right Chair marker (RCH) and the Left Chair marker (LCH):

$$\vec{P}_{LTrunk} = \frac{1}{2}(R\vec{C}H + L\vec{C}H)$$

To define a body segment the distal and proximal point/s and its coordinate system ($\vec{X}$,$\vec{Y}$ and $\vec{Z}$ and the origin $\vec{O}$) have to be defined. As described in chapter 7.2.2 *Joint Kinematics,* the first axis (which can be either $\vec{X}$,$\vec{Y}$ or $\vec{Z}$) is aligned with the longitudinal axis of the moving segment. The second axis is by definition perpendicular to the anatomical plane defined by the first axis and an anatomical vector, and the third axis is by definition perpendicular to the first and second axis. By consensus the origin of the body segment local frame is always the proximal end (or proximal joint) of the segment (Rau et al., 2000). Table 13.5 shows the distal and proximal points and equations of the segment coordinate systems and Figure 13.3.2 shows all the segment coordinate systems of the left upper extremity biomechanical model.

Segment	Distal point	proximal point (Origin)	X-axis	Y-axis	Z-axis
Lower Trunk	$\vec{XI}$	$\vec{O}_{LT} = \vec{P}_{LTrunk}$	$\vec{X}_{LT} = \vec{Y}_{LT} \times \vec{Z}_{LT}$	$\vec{Y}_{LT} = \frac{(R\vec{C}H - L\vec{C}H)}{|R\vec{C}H - L\vec{C}H|} \times \vec{Z}_{LT}$	$\vec{Z}_{LT} = \frac{(\vec{XI} - \vec{P}_{LTrunk})}{|\vec{XI} - \vec{P}_{LTrunk}|}$
Upper Trunk	$\vec{C7} and \vec{IJ}$	$\vec{O}_{UT} = \vec{XI}$	$\vec{X}_{UT} = \frac{(\vec{C7} - \vec{XI})}{|\vec{C7} - \vec{XI}|} \times \vec{Z}_{UT}$	$\vec{Y}_{UT} = \vec{Z}_{UT} \times \vec{X}_{UT}$	$\vec{Z}_{UT} = \frac{(\vec{IJ} - \vec{XI})}{|\vec{IJ} - \vec{XI}|}$
Head	$\vec{FH}$	$\vec{O}_H = \frac{(\vec{LP} - \vec{RP})}{2}$	$\vec{X}_H = -\frac{(\vec{LP} - \vec{RP})}{|\vec{LP} - \vec{RP}|}$	$\vec{Y}_H = \frac{(\vec{FH} - \vec{LP})}{|\vec{FH} - \vec{LP}|} \times \vec{X}_H$	$\vec{Z}_H = \vec{X}_H \times \vec{Y}_H$
Right Clavicule	$\vec{J}_{RSh}$	$\vec{O}_{RC} = \vec{IJ}$	$\vec{X}_{RC} = \frac{(\vec{J}_{RSh} - \vec{IJ})}{|\vec{J}_{RSh} - \vec{IJ}|}$	$\vec{Y}_{RC} = \vec{Z}_{UT} \times \vec{X}_{RC}$	$\vec{Z}_{RC} = \vec{X}_{RC} \times \vec{Y}_{RC}$
Left Clavicule	$\vec{J}_{LSh}$	$\vec{O}_{LC} = \vec{IJ}$	$\vec{X}_{LC} = -\frac{(\vec{J}_{RSh} - \vec{IJ})}{|\vec{J}_{RSh} - \vec{IJ}|}$	$\vec{Y}_{LC} = \vec{Z}_{UT} \times \vec{X}_{LC}$	$\vec{Z}_{LC} = \vec{X}_{LC} \times \vec{Y}_{LC}$
Upper arm	$\vec{J}_{El}$	$\vec{O}_{UA} = \vec{J}_{LSh}$	$\vec{X}_{UA} = \vec{Y}_{UA} \times \vec{Z}_{UA}$	$\vec{Y}_{UA} = \frac{(\vec{J}_{El} - L\vec{E})}{|\vec{J}_{El} - L\vec{E}|} \times \vec{Z}_{UA}$	$\vec{Z}_{UA} = \frac{(\vec{J}_{LSh} - \vec{J}_{El})}{|\vec{J}_{LSh} - \vec{J}_{El}|}$
Forearm	$\vec{J}_{Wr}$	$\vec{O}_{FA} = \vec{J}_{El}$	$\vec{X}_{FA} = \vec{Y}_{FA} \times \vec{Z}_{FA}$	$\vec{Y}_{FA} = \frac{(\vec{US} - \vec{RS})}{|\vec{US} - \vec{RS}|} \times \vec{Z}_{FA}$	$\vec{Z}_{FA} = \frac{(\vec{J}_{El} - \vec{J}_{Wr})}{|\vec{J}_{El} - \vec{J}_{Wr}|}$
Palm	$\vec{J}_{Meta}$	$\vec{O}_P = \vec{J}_{Wr}$	$\vec{X}_P = \vec{Y}_P \times \vec{Z}_P$	$\vec{Y}_P = \frac{(\vec{M5} - \vec{M2})}{|\vec{M5} - \vec{M2}|} \times \vec{Z}_P$	$\vec{Z}_P = \frac{(\vec{J}_{Wr} - \vec{J}_{Meta})}{|\vec{J}_{Wr} - \vec{J}_{Meta}|}$
Thumb	$\vec{F1}$	$\vec{O}_{UA} = \vec{J}_{Wr}$	$\vec{X}_T = \vec{Y}_F \times \vec{Z}_F$	$\vec{Y}_T = \vec{Z}_T \times \vec{X}_P$	$\vec{Z}_T = \frac{(\vec{F1} - \vec{J}_{Wr})}{|\vec{F1} - \vec{J}_{Wr}|}$
Fingers	$\vec{F2}$	$\vec{O}_{UA} = \vec{J}_{Meta}$	$\vec{X}_F = \vec{Y}_F \times \vec{Z}_F$	$\vec{Y}_F = \vec{Z}_F \times \vec{X}_P$	$\vec{Z}_F = \frac{(\vec{F2} - \vec{J}_{Meta})}{|\vec{F2} - \vec{J}_{Meta}|}$

Table 13.5.: Segments definition. Distal and proximal point and equations of the segment coordinate systems.
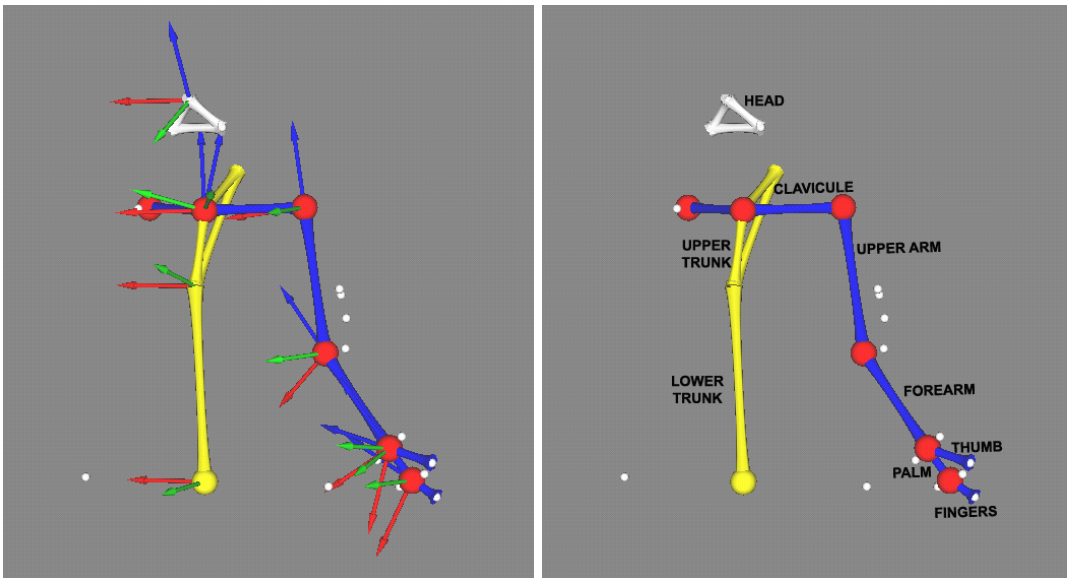

Figure 13.3.2.: Representation of the left upper extremity biomechanical model with all the segment coordinate systems in anatomical position.

13.3.3. Angles definition

As described in section 7.2.2 *Joint Kinematics,* for a clearer *clinical interpretation* of the resulting Euler angles, the local frames of the proximal and distal body segments should be initially aligned to each other by defining the axis of the local coordinate systems in the anatomical orientations. In this study, the initial position of the subject does not fulfill this requirement (i.e. the initial position of the task is not the anatomical position) due to the limitations of the capturing system. Only the coordinate systems of the lower trunk, upper trunk, head, clavicules and upper arm segments are initially aligned and therefore the resultant Euler angles can be directly clinically interpreted. Since flexion-extension rotation, which is produced around the X axis, is the rotation with most motion, the rotational sequence used to calculate the Euler angles is *X-Y-Z*. For clinical interpretation of the joint kinematics of the rest of the segments, *User Angles (Kwon, 1998)* are employed (Table 13.6). A User Angle is defined as the angle between two vectors, which can be projected to a plane in order to prevent that other joint rotations interfere in the calculation of the angle. All the User Angles defined are projected to a plane, with the exception of the *grasp angle* which is defined as the angle between two vectors ($\vec{Z}_F$ and $\vec{Z}_T$) without plane of projection. In the case of the grasp angle it is interesting to calculate the angle between vectors without their projection, due to the complex motions of the thump. Note that even though for clinical interpretation of some joint kinematics, User Angles are employed, for the computation of rigid body dynamics and energetics the time derivatives of the computed Euler angles are used as described in Chapter *7 Motion Analysis.*

Rotation	1st vector	2nd vector	Projection plane
Elbow Flexion-Extension	$\vec{Z}_{UA}$	$\vec{Z}_{FA}$	$\vec{Y}_{UA}\vec{Z}_{UA}$
Elbow Pronation-Supination	$\vec{X}_{UA}$	$\vec{X}_{FA}$	$\vec{Z}_{UA}\vec{X}_{UA}$
Wrist Flexion-Extension	$\vec{Z}_{FA}$	$\vec{Z}_P$	$\vec{Y}_{FA}\vec{Z}_{FA}$
Wrist Ulnar-Radial deviation	$\vec{Z}_{FA}$	$\vec{Z}_P$	$\vec{Z}_{FA}\vec{X}_{FA}$
Grasp angle	$\vec{Z}_F$	$\vec{Z}_T$	-

Table 13.6.: User Angles definition

13.3.4. Body Segment Parameters (BSPs)

The *Body Segment Parameters (BSPs)* refer to the inertial parameters of the body segments, such as mass, CoM location and the 3 principal moments of inertia (I_x, I_y and I_z) (Table 13.7). It has to be taken into account that the accuracy in the kinetic analysis partially depends on the accuracy of the BSPs. The BSPs that we have taken are from de Leva (1996) and are expressed as a percentage of the body mass (in the case of the segment mass) or as a percentage of the segment length (in the case of the CoM and the principal moments of inertia). Therefore, knowing the body mass and the segment lengths of the subjects BSPs can be calculated. Note that as described in Figure 13.3.1 the segments left and right clavicule, the fingers and the thumb are not computed in the inverse dynamic model due to the lack of BSPs for these segments.

Body Segment	Mass(%)		CoM(%)		I_x (%)		I_y (%)		I_z (%)	
	Male	Female	Male	Female	Male	Female	Male	Female	Male	Female
Lower trunk	11.17	12.47	38.85	50.80	55.10	40.20	61.50	43.30	58.70	44.40
Upper Trunk	15.96	15.45	57.90	64.5	35.55	57.38	59.22	38.62	54.50	55.23
Head	6.94	6.68	59.76	59.76	73.20	70.18	72.40	66.00	62.40	63.60
Upper Arm	2.71	2.55	57.72	57.54	26.90	26.00	28.50	27.80	15.80	14.80
Fore Arm	1.62	1.38	45.74	45.59	26.50	25.70	27.60	26.10	12.10	9.40
Palm	0.61	0.56	79	74.74	51.30	45.40	62.80	53.10	40.10	33.50
Bottle	0.33 Kg	0.33 Kg	6 cm	6 cm	4.71 $Kg\cdot cm^2$	$4.71 Kg\cdot cm^2$	$1.41 Kg\cdot cm^2$	$1.41 Kg\cdot cm^2$	$4.71 Kg\cdot cm^2$	$4.71 Kg\cdot cm^2$

Table 13.7.: Body Segment Parameters for males and females (de Leva, 1996).

14. Motion Recording

The upper extremity motions were recorded with a BTS SMART-D® opto-electronic system (BTS Bio-engineering S.P.A, Italy) with 6 cameras. The cameras sample rate was 140 Hz, the mean precision was 0.466 mm (SD =0.442mm) and the calibrated volume was $1504.7m^3$ (3.85m*1.87m*2.09m) (Figure 14.0.1).
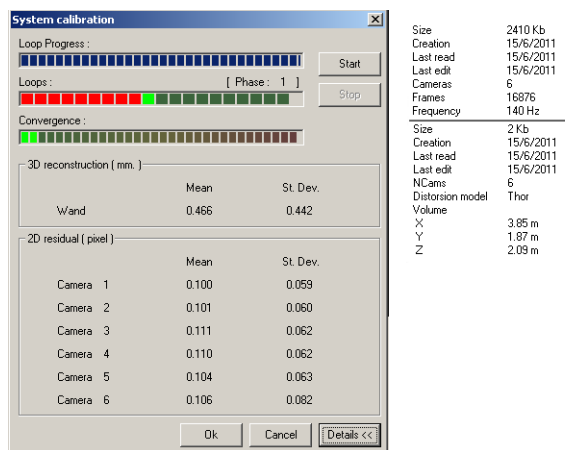

Figure 14.0.1.: Details of the system calibration.

14.1. Protocol

We set the following protocol for the motion recording of the upper extremity movement:

1. System calibration

   a) *Axis Calibration:* Definition of the global coordinate system by a 5 s capture of a static Cartesian space built with three orthogonal wands with 4, 2 and 3 markers for, respectively, x, y and z axis.

   b) *Wand Calibration:* Settings of the optical parameters of the cameras, definition of the volume of work and precision of the system were defined by a 190 s capture of a manual random movement of the wand with three markers within the volume of interest.

2. Markers set-up

   a) Placement of the 21 body markers (Joint and segment markers and marker cuffs), in positions according to the results of the preliminary study (see Figures 13.2.2 and 13.2.8 and Table 13.2).

   b) Placement of the object markers (bottle, shelf and table; Figure 13.2.8).

3. Static trial

   a) Placement of the subject and objects of interaction in the calibrated volume.

   b) Five seconds capture of the subject in the static position (Figure 13.2.8).

   c) Data checking to ensure all markers have been captured by the cameras. Repeat the capture otherwise.

4. Dynamic trials

    a) Remove the shoulder joint markers of the arm to be analyzed, and the medial epicondyle marker (ME).

    b) Set the target positions (RS, LS and EXT) for height H0, according to the arm length of the Subject (Figure 11.1.1).

    c) Explain the task to the Subject and perform a test before the actual capture.

    d) Capture the reaching motions defined in Table 11.1, with 2 repetitions, for the 3 target positions H0.

    e) Set the target positions (RS, LS and EXT) for height H1, according to both arm length and shoulder height of the Subject (Figure 11.1.1).

    f) Capture the reaching motions defined in Table 11.1, with 2 repetitions, for the 3 target positions H1.

    g) Set the target positions (RS, LS and EXT) for height H2, equal to twice the length from the elbow to the shoulder joints of the Subject (Figure 11.1.1).

    h) Capture the reaching motions defined in Table 11.1, with 2 repetitions, for the 3 target positions H2.

14.2. Output of the motion recording

The output of the motion recording consists of the marker trajectories as 25 tables (one for each marker) with spatial (x, y, z) and time coordinates, in C3D format (C3D.ORG, 2011).

15. Data Processing

Figure 15.0.1 summarizes the data processing chain, which has been implemented in BTS SMART D® (BTS Bioengineering S.P.A, Italy), KWON3D XP® (VISOL, Inc., Korea), MATLAB® (The Math-Works, Inc., Natick, MA) and R (R Development Core Team, 2011) according to the suitability of each tool for the different tasks. First, the registered 3D marker trajectories have to be tracked to form the stick figure for each trial using a program from the BTS SMART D system. Second, the trials have to be exported to C3D format and imported to the KWON3D XP software to perform all the motion analysis (filter, interpolation and kinematic and dynamic computation) and create the clinical report. For further data analysis the desired biomechanical variables are exported as CSV table, which is subsequently imported into MATLAB and/or R, where the core of the processing took place through functions specifically developed by the author for this study and provided in Appendix (REF). Functions for Exploratory Graphic Analysis (Wilkinson, 2005) were developed in R using package ggplot2 (Wickham, 2009). See Figure 15.0.1 for details on the data processing flow.
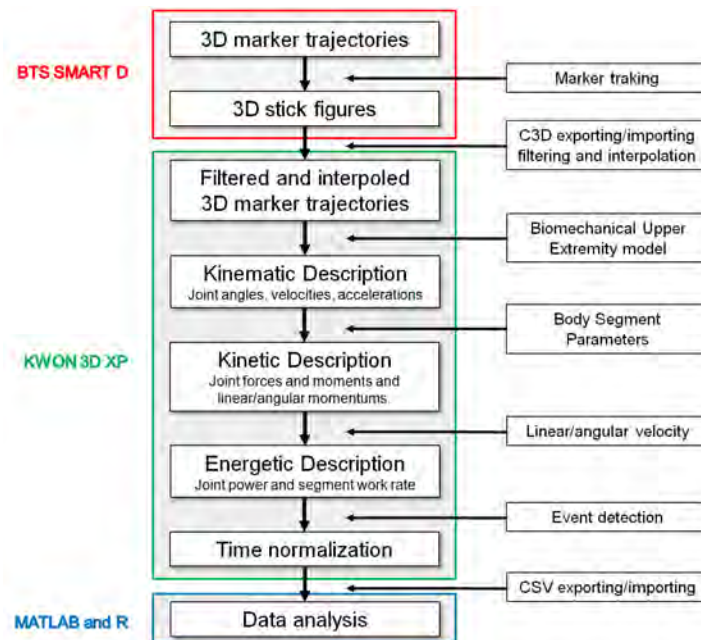
Figure 15.0.1.: Diagram of the steps of the data processing.

The tracked data sets of markers position along time captured at 140 Hz for each trial were pre-processed within KWON3D XP. Pre-processing consisted of a Butterworth filter with a cut-off frequency of 3 Hz, which was subsequently interpolated using Cubic Spline in case the windows with missing data were smaller than or equal to 20 frames. The kinematic, kinetic and energetic description resulted from the application of the equations presented in Chapter 7 *Motion Analysis* and the time normalization and was conducted in KWON3D XP as well. MATLAB was used to carry out the signal analysis (SNR analysis) that was required for the selection of the marker set-up (Section D.1 *Selection of the marker set-up*). R was used to carry out the Exploratory Graphic Analysis of the data computed with KWON3D XP. The Angular Displacement, Angular Velocity, Joint Moment and Muscle Power of elbow and shoulder flexion-extension were exported as CSV tables. Subsequently the CSV tables were imported into R, reshaped, and plotted using the functions provided in Appendix D *Program code: Functions and scripts.*

15.1. Event Detection

An important step of the data processing is the *event detection* which is indispensable to normalize time and to compare between trials from the same subject or between subjects. The automatic event detection is performed using an algorithm specially designed by the author in KWON3D XP for the particular task of the study. The algorithm detects 10 events for each trial. Three of them have a computational purpose and seven of them have an analytical purpose (Tables 15.1 and 15.2). The conditions defined in the algorithm were applied to the resultant point velocities of the wrist joint and bottle marker (Figure 15.1.1), which characterize the different steps of the motion task. This algorithm of automatic detection was successful for 5 out of 6 subjects, but in the case of subjects 06 the events had to be interactively detected following the same criteria as the algorithm.

	Event in sequential order	Description
1	START	The subject starts the arm motion. Start of the task.
2	H0_HAND_BOTTLE (H0_HB)	The subject takes the bottle.
3	HX_BOTTLE_HAND (HX_BH)	The subject places the bottle in the target position.
10	H0_HAND_4 (H0_H4)	Arm in arm initial position
5	HX_HAND_BOTTLE (HX_HB)	The subject takes the bottle from the target position.
6	H0_BOTTLE_HAND (H0_BH)	The subject places the bottle in the object initial position.
7	END	The subject ends the arm motion. End of the task.

Table 15.1.: Events' description. Note that the events with a computational purpose do not appear.

Events Computational order		Sequential Order	Purpose	Condition		
				From	To	Method
1	START	1	A	-	H0_HB	Max Resultant Point Velocity of the Wrist Joint
2	H0_HAND_BOTTLE (H0_HB)	2	A	START	-	Resultant Point Velocity of the Bottle > 0.25 m/s
3	HX_BOTTLE_HAND (HX_BH)	3	A	H0_HB	-	Resultant Point Velocity of the Bottle < 0.03 m/s
4	H0_HAND_2 (H0_H2)	5	C	HX_BH	HX_HB	Resultant Point Velocity of the Wrist Joint < 0.3 m/s
5	HX_HAND_BOTTLE (HX_HB)	8	A	HX_BH	-	Resultant Point Velocity of the Bottle > 0.35 m/s
6	H0_BOTTLE_HAND (H0_BH)	9	A	HX_HB	-	Resultant Point Velocity of the Bottle < 0.15 m/s
7	END	10	A	H0_BH	-	Max Resultant Point Velocity of the Wrist Joint
8	H0_HAND_1 (H0_H1)	4	C	HX_BH	H0_H2	Max Resultant Point Velocity of the Wrist Joint
9	H0_HAND_3 (H0_H3)	7	C	H0_H2	HX_HB	Max Resultant Point Velocity of the Wrist Joint
10	H0_HAND_4 (H0_H4)	6	A	H0_H2	H0_H3	Max Resultant Point Velocity of the Wrist Joint

Table 15.2.: Algorithm for automatic event detection. *A)* Analysis purpose. *C)* Computational purpose. For each event, the computational and sequential order, the purpose and the condition are shown.
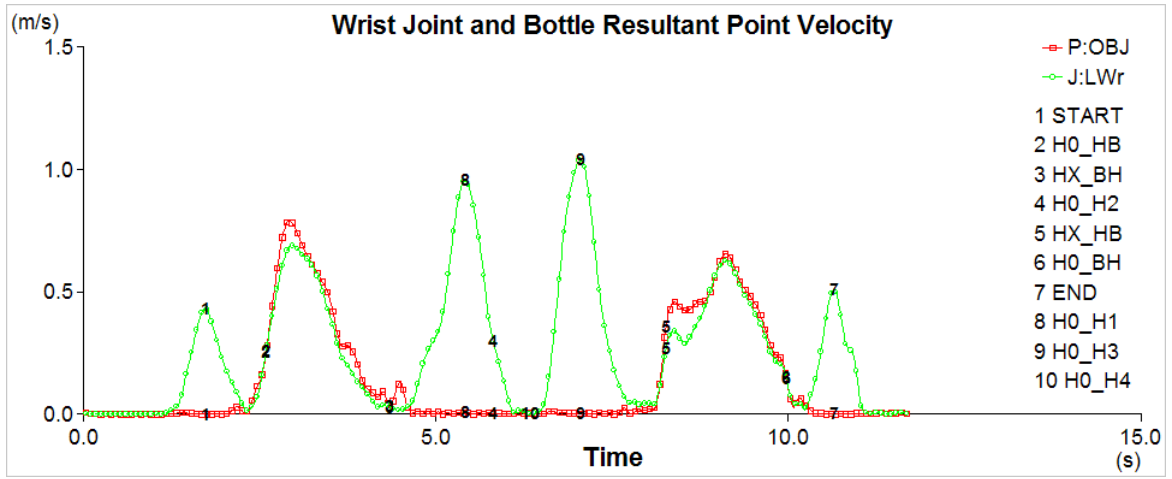
Figure 15.1.1.: Wrist joint (green) and bottle (red) resultant point velocity along time with the detected events. Note that the sequential order does not coincide with the computational order.

Part V.

Results

16. Introduction

This section presents the results obtained from the upper extremity motion analysis. First, the Clinical Report is presented, followed by the Kinematic and Dynamic Analysis. Taking into account the extension limits of this dissertation and the considerable amount of data resulting from the processing, it was necessary to select which data was going to be analyzed and interpreted. In agreement with clinicians (Dr. Frederic Dachs Cardona (head of the Neuro-Orthopedics department) and Manel Ochoa (physical therapist coordinator of the functional rehabilitation department)) from the *Institut Guttmann,* elbow and shoulder flexion-extension were selected because of the interest on this joint rotations for rehabilitation. Therefore, only the Kinematic and Dynamic Analysis of elbow and shoulder flexion-extension are discussed here.

The goal of the Kinematic and Dynamic analysis was to select and highlight biomechanical traits to distinguish between pathological and healthy subjects. The analysis was carried out by means of Exploratory Graphical Analysis which represents a powerful method when dealing with small number of subjects (Wilkinson, 2005). Indicative mean and range values were calculated from the data obtained for the three healthy subjects, but it is important to note that reliable estimates of healthy conditions should be based on the analysis of a large number of subjects, which is outside the scope of this dissertation.

The Kinematic and Dynamic Analysis was performed by comparing each pathological subject (04, 05 and 06) versus the healthy subjects (01, 02 and 03). The first subsection of each chapter describes the results obtained from the healthy subjects (right arm). The rest of subsections present a comparison between one given pathological subject vs. the healthy subjects. Results for Subject 04 are presented and discussed in length, while only those characteristics that are distinct of Subjects 05 and 06 are presented to avoid repetition.

Since the task that is performed by the subjects has two phases that are very similar and the objective of the study was not to examine differences between transport to reach with or without the bottle, only the fist phase of the motion between the START event and the H0_HAND_4 event is presented here. This first phase includes the transport of the bottle to the target position (from 0% to 20%), the placement of the bottle on the target position (from 20% to 60%) and the withdrawal of the arm to the initial position (from 60% to 80%). The rest of the cycle (from 80% to 100%) the arm of the subject remains in the starting position.

The program code created to calculate and plot all the graphics of the Kinematic and Dynamic analysis data is included in Appendix D *Program code: Functions and scripts.*

17. Clinical Report

The *Clinical Report* is created from the data processed with the software KWON3D XP (see section 15 *Data Processing*). The goal of the Clinical Report is to present a summary of objective information on the biomechanics of the motion performed by the subject. The Clinical Report includes 3 main sections: (i) Kinematics, (ii) Kinetics and (iii) Trajectories. The Kinematics section describes the relative angular displacements for each DoF of the 3 arm joints (shoulder, elbow and wrist) and the grasp motion (Figure 17.0.1). The Kinetics section describes the joint moments for each DoF and the muscular power of the 3 arm joints (Figure 17.0.2). The Trajectories section includes 3 graphics (Figure 17.0.3): (i) a 3D view of the biomechanical model in which the clinician can draw the trajectory of any marker or joint of the biomechanical model, (ii) a 2D lateral view with the trajectory of the wrist joint and (iii) a transversal view of the trunk CoM trajectory which gives global information about the motions. A complete Clinical Report is included in Appendix C *Clinical Report*.
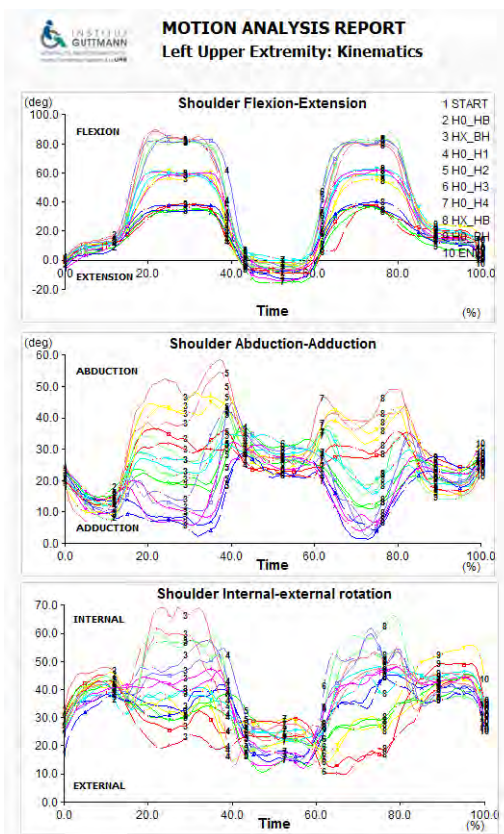
Figure 17.0.1.: Kinematic section of the Clinical Report. On left side the shoulder joint kinematics (flexion extension, abduction-adduction and internal-external rotation).
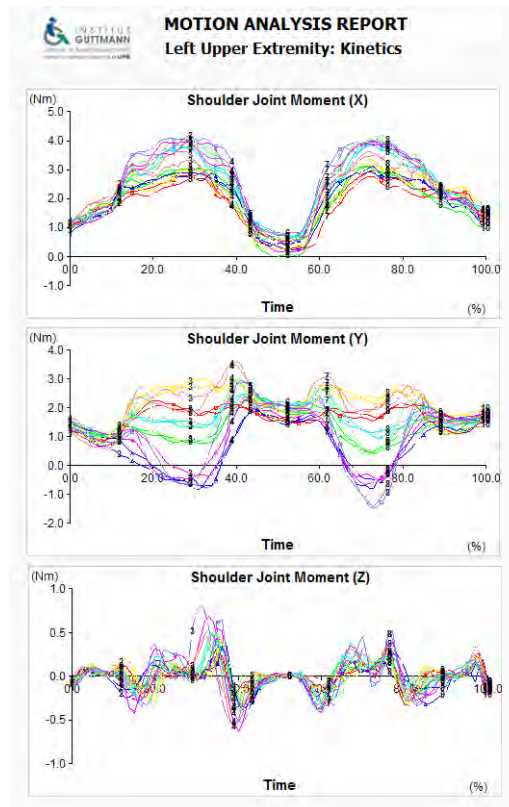
Figure 17.0.2.: Kinetic section of the Clinical Report. Shoulder joint moments for the x, y and z components.
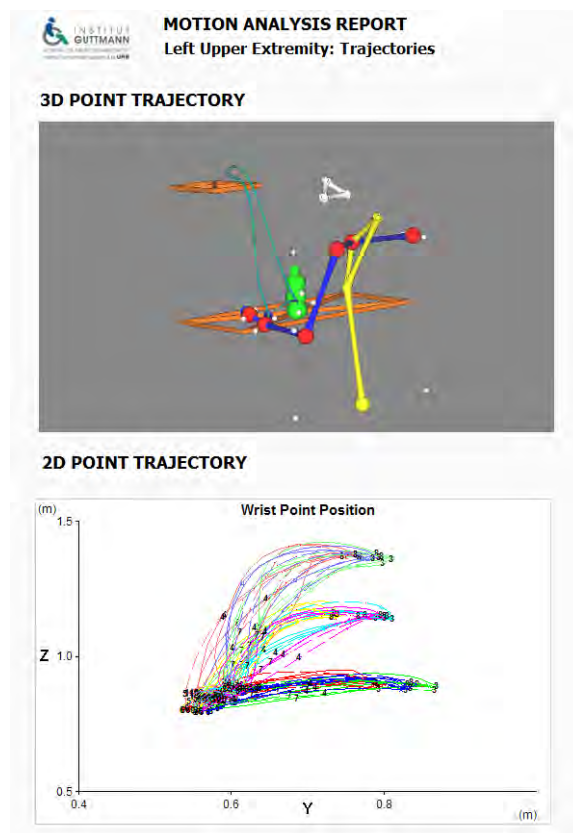
Figure 17.0.3.: Trajectories section of the Clinical Report. 3D view of the biomechanical model stick figure with the wrist joint trajectory represented and 2D representation of the wrist joint trajectory from a lateral view.

18. Kinematic analysis

This section presents the results of the *Kinematic Analysis* of the shoulder and elbow flexion-extension rotations. Three kinematic analysis were performed: (i) elbow and shoulder flexion-extension along time, (ii) relationship between Angular Velocities and Angular Displacements of the shoulder and elbow flexion-extension along time (which are know as Phase Portraits) and (iii) the Phase Angles calculated from the Phase Portraits of shoulder and elbow flexion-extension. Information on the elaboration and interpretation of the Phase Portrait and the Phase Angle graphics can be found in Angulo Barroso et al. (2011) and Angulo Barroso et al. (2010). In what follows, important features for the graphic interpretation are presented.

Important features for graphic analysis

Angular Displacement

The Angular Displacement plot 18.0.1 shows the amount of rotation (expressed in degrees) of the distal body segment relative to the proximal segment along time (expressed in percentage of the cycle). An important feature of the Angular Displacement plot is the Range Of Motion (ROM), between the maximum and minimum values of rotation. The maximum value for the shoulder flexion-extension and the minimum value for the elbow flexion-extension are found at ~50% of the cycle, coinciding with the moment in which the subject finishes placing the bottle at the target position. The minimum value of the shoulder flexion-extension and the maximum value of the elbow flexion-extension are found close to the extremes of the cycle (either 0% or 100%).
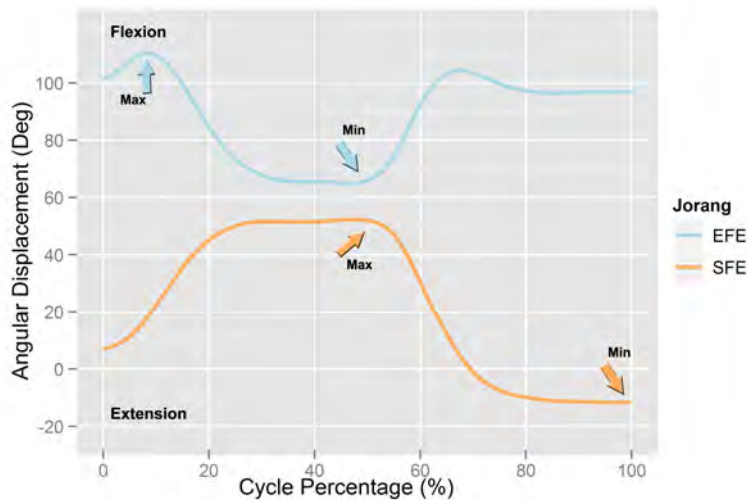
Figure 18.0.1.: Shoulder (red) and elbow (blue) flexion-extension along time. Note that minimum and maximum values of shoulder and elbow flexion-extension are pointed.

Phase Portrait

The Phase Portrait graphic shows the relationship between the angular displacement and the angular velocity along time. The path of this plot provides information on how the joint motion behaves during the analyzed task and shows its general pattern. Important features of the Phase Portrait plot are the shapes of the different sections of the path and the global shape of the path, as well as the maximum angular velocities. In the example of Figure 18.0.2, five path sections of different shapes can be observed (interpretations follow Angulo Barroso et al. (2010)): a) Smooth and round sections indicate a stable and controlled motion. b) Loops that cross at 0 velocity indicate a reversion of the motion (going from flexion to extension). c) Inflexions and protuberances indicate that the motion is (re)starting or stopping. d) An horizontal straight section indicates a period of constant angular velocity and thus 0 angular acceleration. e) Straight sections with an slope different than 0 indicate a period of motion with constant acceleration.

Another important feature of the Phase Portrait is the global shape of the plot. Horizontally elongated plots refer to motions with a large angular displacement and low angular velocities, while vertically elongated plots refer to motions with a short angular displacement and high angular velocities, and circular plots correspond to intermediate situations.

Maximum angular velocities are found at either ~25% or ~75% of the cycle, although ~75% of the cycle is more common because the motion is then in favor of gravity.
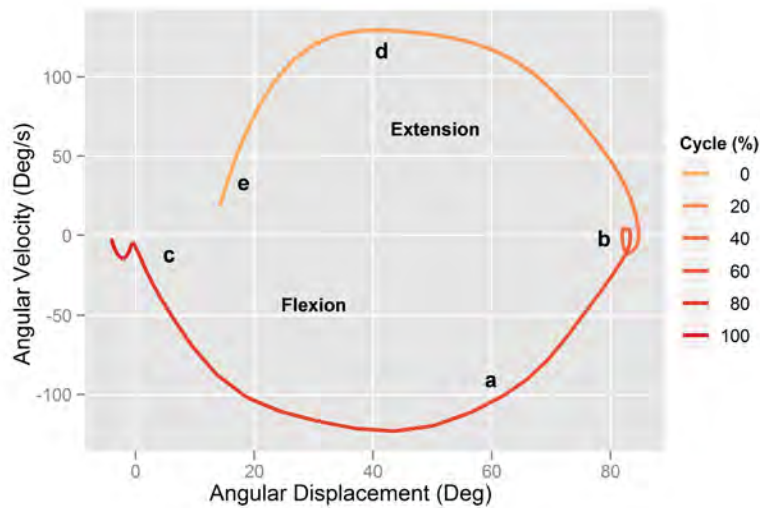
Figure 18.0.2.: Path shapes of a Phase Portrait plot.

Phase Angle

The Phase Angle plot shows the Phase Angle value (Deg) along time (expressed in percentage of the cycle). The Phase Angle values are calculated for each data point of the Phase Portrait (normalized angular displacement - normalized angular velocity) relative to the origin of the polar coordinate system. The Phase Angles must be corrected according to the quadrant in order to have all values ranging between 0° and 180° (first and second quadrant). The path of this plot provides information on how body segments coordinate during the analyzed task. The following interpretations follow Angulo Barroso et al. (2011) an the reader is referred to their article for a complete description on the elaboration of the Phase Angle graphics.

The Phase Angle plot presents a typical alternation of sections (see the example of Figure 18.0.3 a) Inclined linear sections in the paths, with either positive or negative slopes, indicate periods of constant relative change between angular velocity and angular displacement. b) Flat sections in the paths indicate a period during which there is no relative change between angular velocity and angular displacement. c) A change of the slope sign indicates that the segment is reversing the motion (going from extension to flexion or vice versa). Important features in the Phase Angle plot are the relative duration of each section and the smoothness of the line.
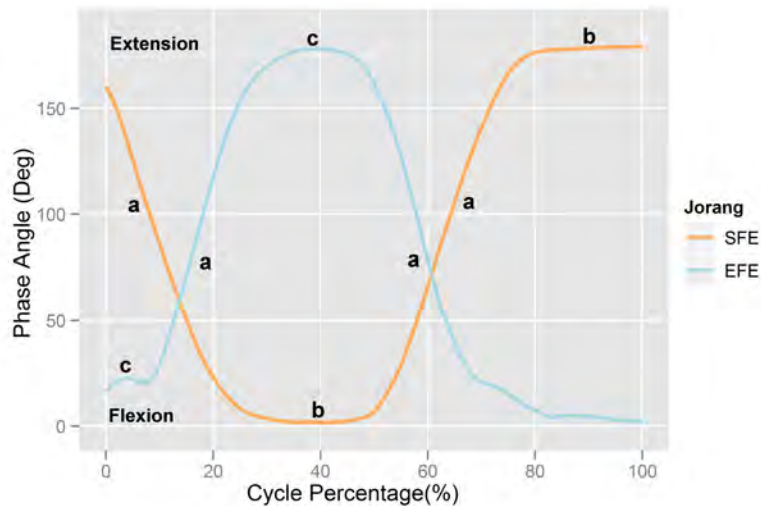
Figure 18.0.3.: Path shapes of a Phase Angle plot.

18.1. Healthy Subjects

Angular Displacement

Figure 18.1.1 shows the angular displacement of the shoulder and elbow flexion-extension. The movement of the elbow starts and ends at 90° of flexion in all cases. At ~50% of the cycle, when the subjects are reaching the target position, the elbow is more extended when the bottle is placed at height H0 (40°) than when it is placed at heights H1 and H2 (60°).

The shoulder starts and ends close to the neutral position ($\backsim 0^o$) in all cases. In contrast to the elbow, the shoulder presents 3 different flexions when placing the bottle depending on the height (H0=40°, H1=60° and H2=80°). This is caused by the fact that the shoulder flexion-extension controls the height of the arm and therefore the reaching height. Moreover, the elbow and the shoulder flexion-extensions present opposite rotation attitude: when the elbow is flexing the shoulder is extending and vice versa.

Phase Portrait

Figures 18.1.2 and 18.1.3 show the relationship between angular velocity and angular displacement along time, for, respectively, elbow and shoulder flexion-extension. Angular velocities and angular displacements of both joint rotations increase with longer paths, and are maximum when the bottle is placed at height H2. The angular velocities of the withdrawal of the arm to the initial position are higher than those of bringing the bottle to the target position, probably because in the former case the direction of the motion is in favor of gravity.

The paths of both joint rotations are smooth, which indicates a stable and controlled motion. Also, the Phase Portraits of Healthy Subjects present loops at the moments of reaching the target position, because of the reversion of the motion between extension and flexion for the elbow, and between flexion and extension for the shoulder. The Phase Portraits of the elbow present loops at the end of the cycle as well, which are not present in the case of the shoulder.

The Phase Portraits indicate that the initial and final angular displacements of the elbow are very similar (Figure 18.1.2), while these values differ in the case of the shoulder (Figure 18.1.2). There is more shoulder extension in the final position than in the initial position, probably because of the inertia of the upper arm during the withdrawal of the arm.

Concerning the shape of the elbow Phase Portraits, more circular shapes are found when the bottle is placed at widths LS (left shoulder) and RS (right shoulder), and more elongated shapes appear when the bottle is placed at widths EXT (external). Shoulder Phase Portraits have similar shapes in all positions.

Phase Angle

In agreement with the findings described in the Angular Displacement section, figure 18.1.4 also shows that the elbow and the shoulder flexion-extensions present opposite rotation attitude (they are out of phase): when the elbow is flexing the shoulder is extending and vice versa.

The alternation between inclined and flat sections of the path mentioned in subsection 18 of *Important Features for Graphic Analysis*, is clearly observable in the Phase Angle plots of Healthy Subjects.

Elbow flexion-extension phase angles show small waves, especially when the bottle is placed at heights H1 and H2, at the start and end of the motion, which indicates that there is a change in the relationship between angular displacement and angular velocity. Apart from these little waves, the plot of the elbow Phase Angle is smooth. Plots of shoulder flexion-extension phase angles are smoother than those of the elbow, because, being a more proximal segment (closer to the trunk), the shoulder flexion-extension motion has a more stable relationship between angular velocity and angular displacement.
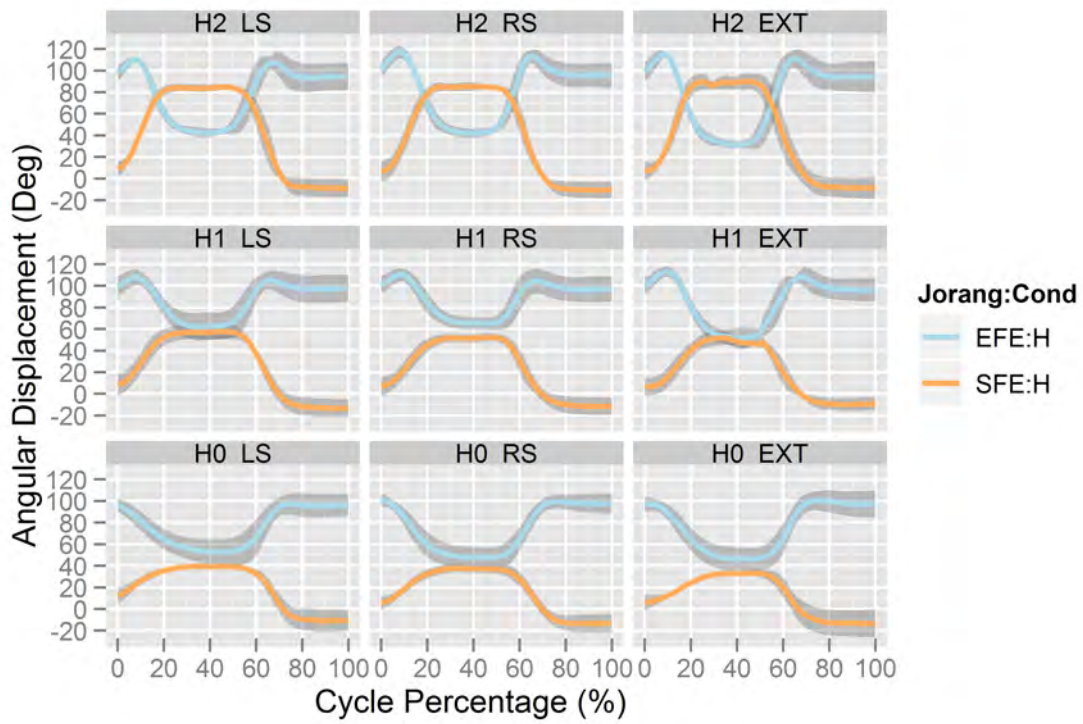
Figure 18.1.1.: Shoulder (red) and elbow (blue) flexion extension of healthy subjects 01, 02 and 03. Mean angular displacement of healthy subjects is represented in faded red and blue. The gray ribbon indicates one standard deviation. The distribution of facet graphics match with the actual spatial distribution of targets.
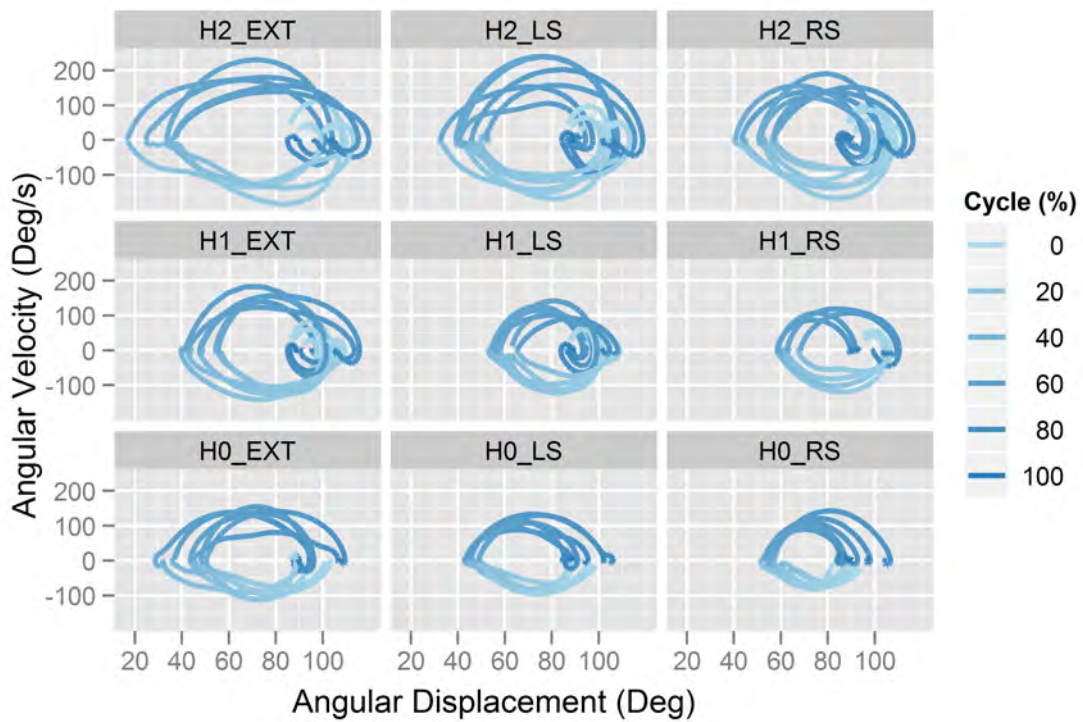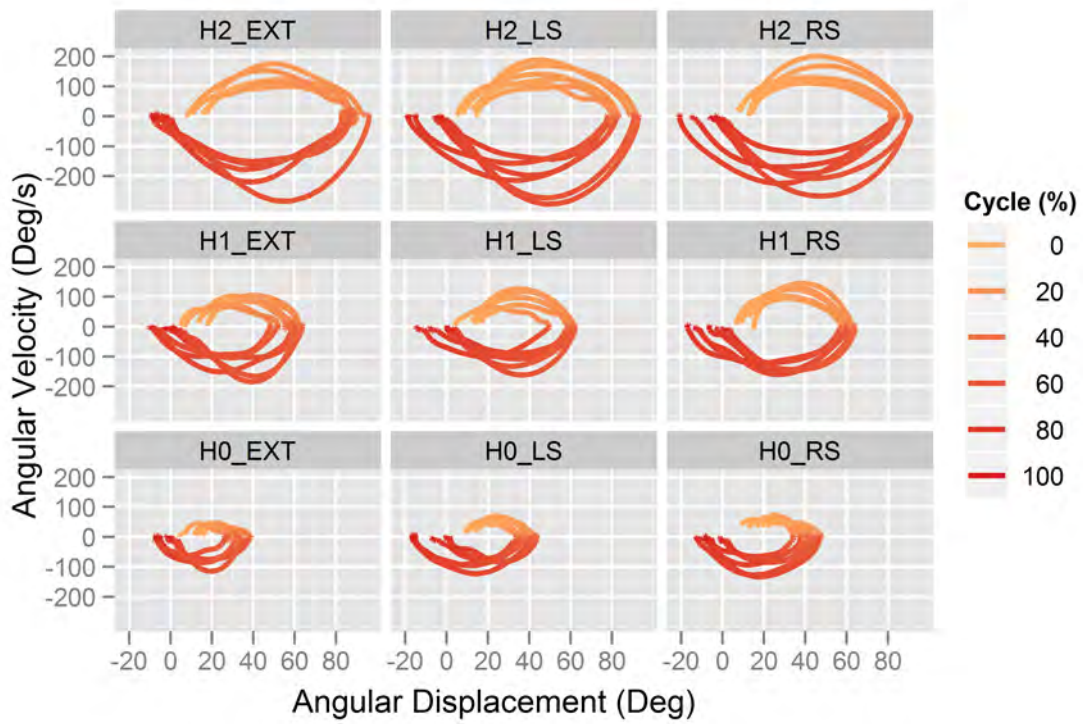

Figure 18.1.2.: Elbow flexion-extension Phase Portrait: relationship between elbow Angular Velocity and elbow Angular Displacement along time of healthy subjects 01, 02 and 03. Time is represented with a color gradient. For all subjects both repetitions are shown. The distribution of facet graphics match with the actual spatial distribution of targets.

Figure 18.1.3.: Shoulder flexion-extension Phase Portrait: relationship between shoulder Angular Velocity and shoulder Angular Displacement along time of healthy subjects 01, 02 and 03. Time is represented with a color gradient. For all subjects both repetitions are shown. The distribution of facet graphics match with the actual spatial distribution of targets.
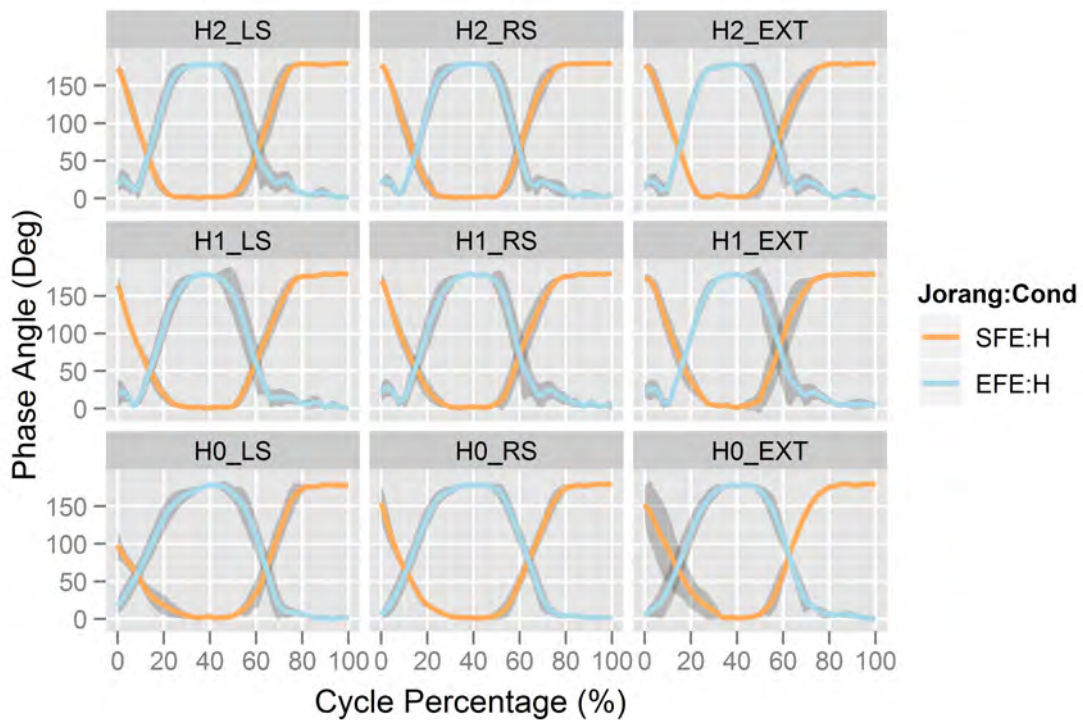
Figure 18.1.4.: Phase Angle of the shoulder (red) and elbow (blue) flexion-extension of healthy subjects 01, 02 and 03. Mean Phase Angle of healthy subjects is represented in faded red and blue. The gray ribbon indicates one standard deviation.The distribution of facet graphics match with the actual spatial distribution of targets.

18.2. Pathological Subject 04

Angular Displacement

Figure 18.2.1 shows that pathological Subject 04 presents a larger elbow extension than the healthy subjects, especially when the bottle was placed at heights H1 and H2. This fact is probably a consequence of the tendon transfer surgery and the subsequent arm rehabilitation. Patients undergoing tendon transfer surgery have their arm immobilized with the elbow completely extended during 2-3 weeks. After this period, the patient needs four months of rehabilitation to regain elbow flexion. Therefore, it is to be expected that these patients tend to extend more the elbow when reaching than healthy patients.

The angular displacement of the shoulder flexion-extension of Subject 04 is very close to that of the healthy subjects.

Phase Portrait

The relationship between elbow Angular Velocity and elbow Angular Displacement along time shown in the Phase Portrait (Figure18.2.2), indicates that the maximum angular velocities of the elbow flexion-extension are higher in pathological Subject 04 than those of the healthy subjects when the bottle was placed at heights H0 and H1. This situation is reversed when the bottle was placed at height H2, probably because of the increased difficulty of the task when the bottle had to be placed at this height.

The Phase Portrait of the shoulder flexion-extension (Figure 18.2.3), shows that the angular velocities of pathological Subject 04 are always lower than those of the healthy subjects. The extra loops (additional to those observed in healthy individuals) at the ending of the path indicate that there was a reversion of the motion while the arm was placed at the initial position. These reversions at the ending of the task are consequence of the motion that Subject 04 had to perform to place the arm at the initial position due to the spasticity on his hands. Inflexions and protuberances are also present during shoulder flexion.

The phase portraits of Subject 04 display elongated shapes while those of healthy subjects present more circular shapes. This difference in shape is very prominent and clearly observable.

Phase Angle

The signal of Phase Angle of Subject 04 presents a saw-tooth shape, both for shoulder and elbow flexion-extension (Figure 18.2.4). This saw-tooth shape is particularly noticeable in the flatter parts of the graph in which the angular velocity gets close to 0 (that is, while the subject is placing the bottle on the target position and when the arm is at its initial position). These irregular, small peaks are caused by the lack of accurate motor control.

The flatter part is wider in the elbow flexion-extension, which implies that Subject 04 spent longer periods of time in the same position (placing the bottle in the target position) than healthy subjects.

Concerning the slopes of the straight segments that appear when the bottle is brought to the target position and during the withdrawal of the arm to the initial position, it is worthwhile noting that these slopes are similar between Subject 04 and the healthy subjects, with the exception of the cases when the bottle is placed at external widths (EXT), for which the slopes of the elbow Phase Angle of Subject 04 are steeper. Steeper slopes indicate that the relative change between angular displacement and angular velocity is larger; realistically, it means faster angular velocities for the same changes in angular displacement.
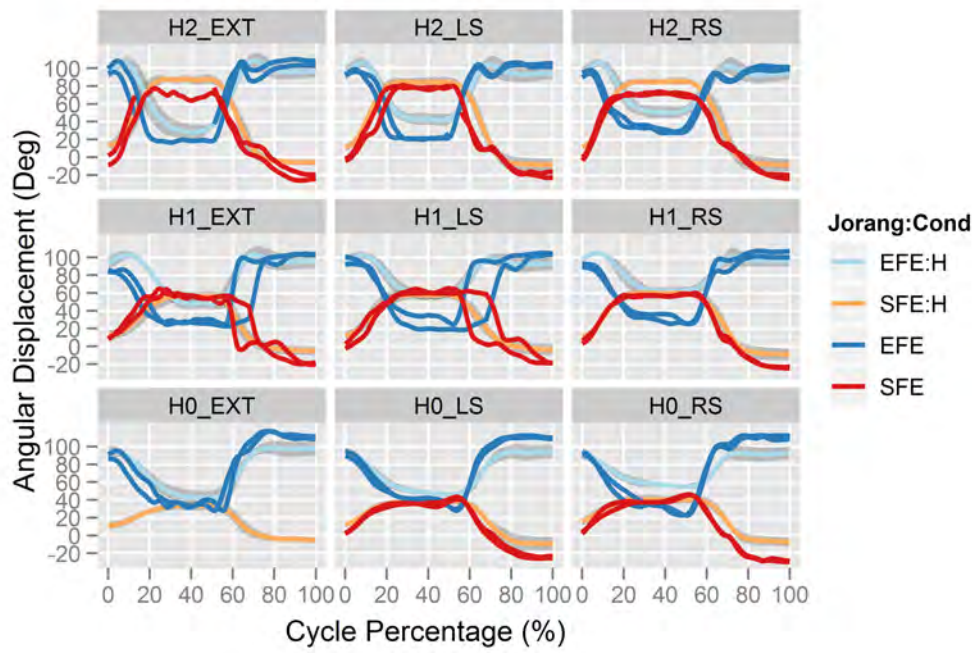
Figure 18.2.1.: Shoulder (red) and elbow (blue) flexion extension of pathological Subject 04 compared to the healthy subjects. Mean angular displacement of healthy subjects is represented in faded colors and the gray ribbon indicates one standard deviation. For pathological Subject 04 both repetitions are shown in bright red and blue. The distribution of facet graphics match with the actual spatial distribution of targets.
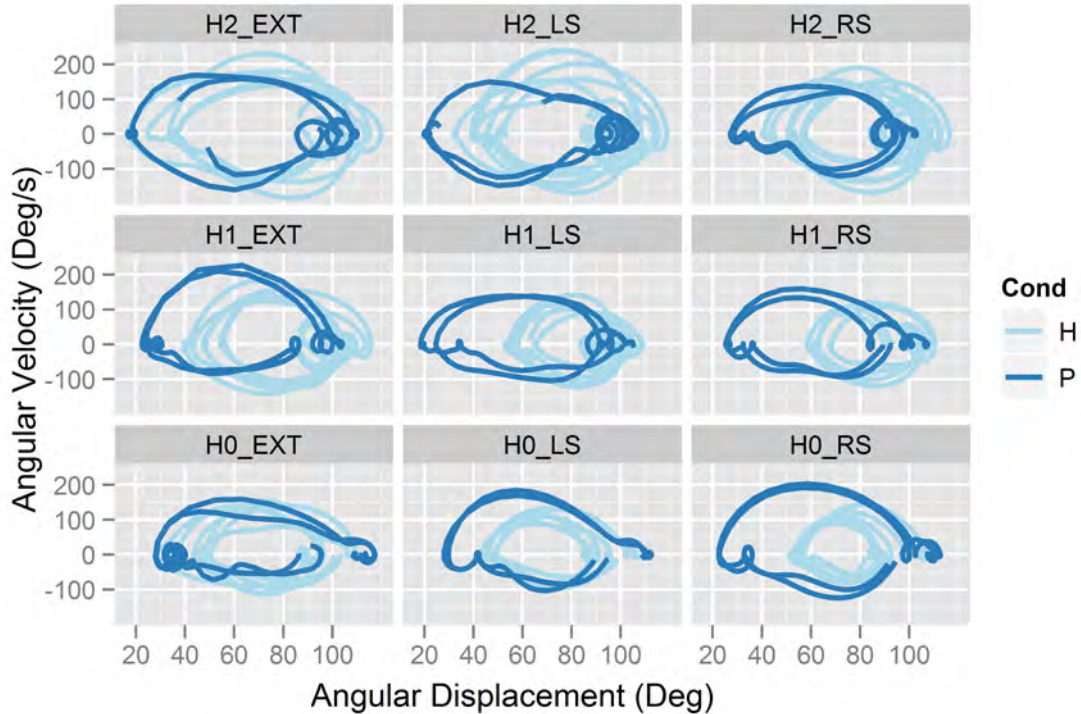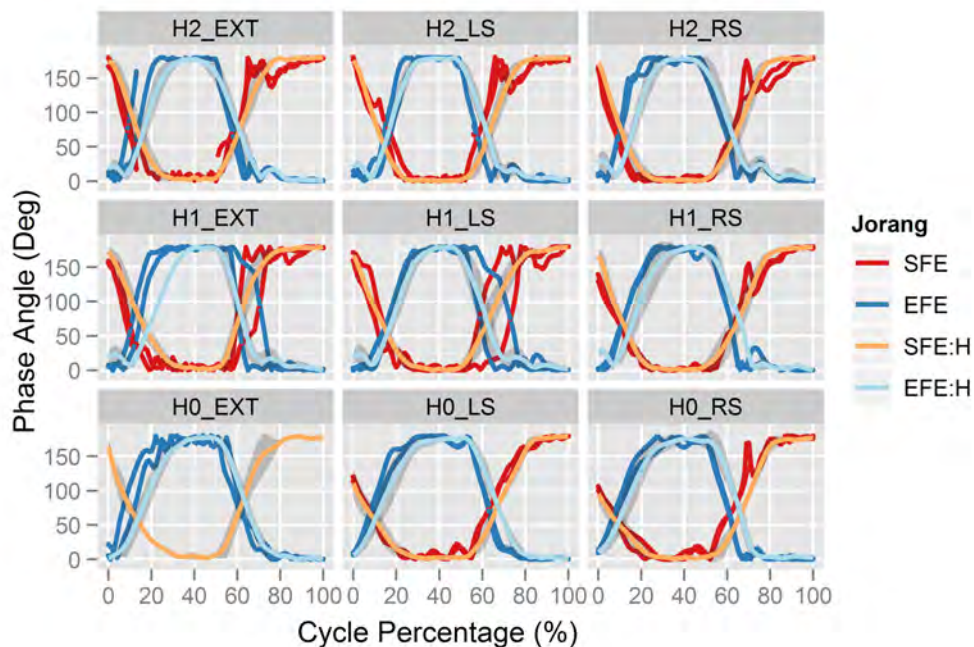

Figure 18.2.2.: Elbow flexion-extension Phase Portrait: relationship between elbow Angular Velocity and elbow Angular Displacement along time of pathological Subject 04 (bright blue) compared to the healthy subjects (faded blue). For all subjects both repetitions are shown. The distribution of facet graphics match with the actual spatial distribution of targets.
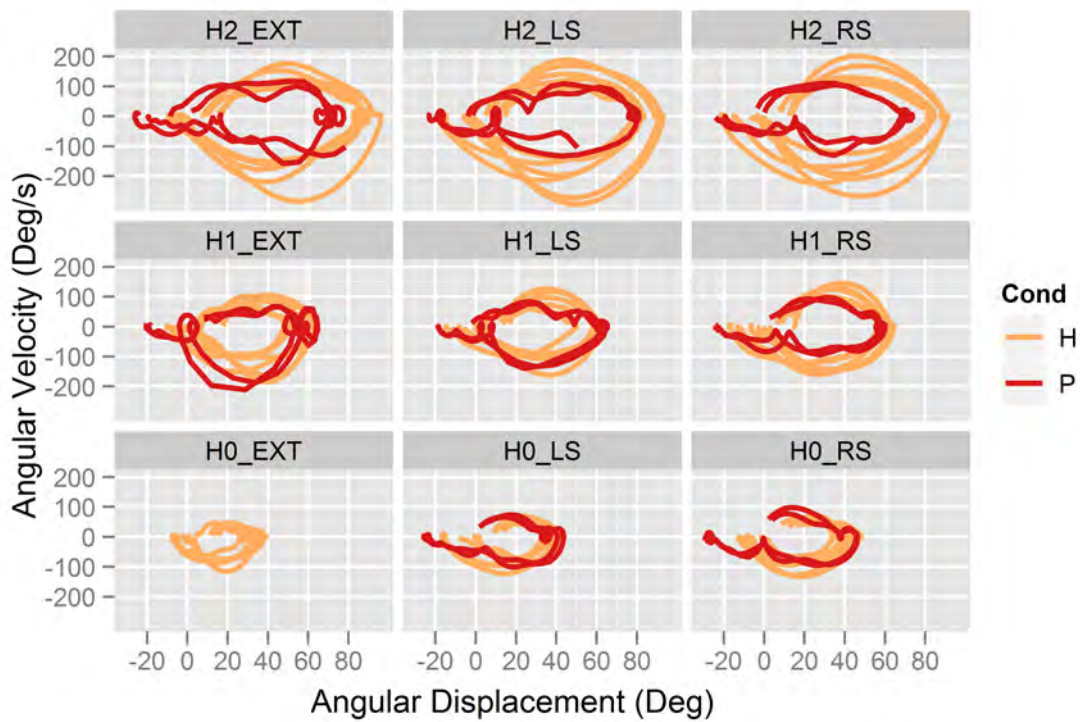
Figure 18.2.3.: Shoulder flexion-extension Phase Portrait: relationship between shoulder Angular Velocity and shoulder Angular Displacement along time of pathological Subject 04 (bright red) compared to the healthy subjects (faded red). For all subjects both repetitions are shown. The distribution of facet graphics match with the actual spatial distribution of targets.
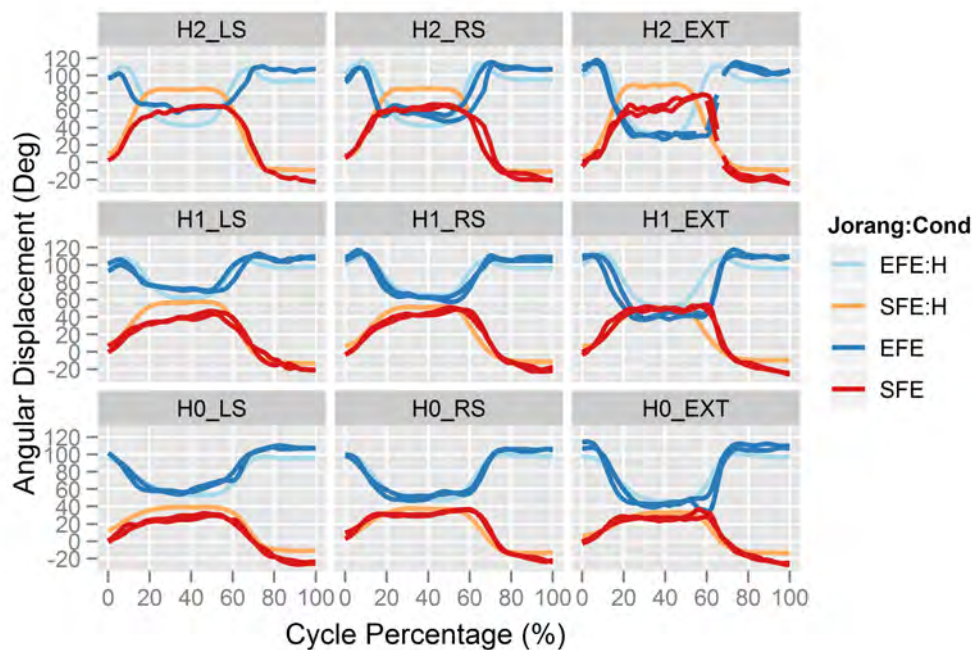

Figure 18.2.4.: Phase Angle of the shoulder (red) and elbow (blue) flexion-extension of pathological Subject 04 compared to the healthy subjects. Mean Phase Angle of healthy subjects is represented in faded colors and the gray ribbon indicates one standard deviation. For pathological Subject 04 both repetitions are shown in bright red and blue. The distribution of facet graphics match with the actual spatial distribution of targets.

18.3. Pathological Subject 05

Angular Displacement

Figure 18.3.1 shows that, in contrast to Subject 04, the elbow flexion-extension of subject 05, which has not undergone tendon transfer surgery, matches the standard motion of the healthy subjects, with the exception of position H2_LS (bottle placed at a height equal to two times that of the shoulder to elbow and at left shoulder width).

The same figure indicates that Subject 05 presents less shoulder extension than the healthy subjects, especially when the bottle was placed at height H2 and at width LS probably because of the increased difficulty of the task.

Phase Portrait

Figure18.3.2, indicates that the the maximum Angular Velocities of the elbow flexion-extension in pathological Subject 05 are a bit lower than those of the healthy subjects in all cases but especially when the bottle was placed at height H2, with the exception of position H0_LS (bottle placed at table height and left shoulder width).

The same conclusion is true for the Phase Portrait of the shoulder flexion-extension (Figure 18.3.3). in addition, this figure presents inflexions and protuberances during flexion, but in contrast to Subject 04, there are no extra loops at the ending of the path.

Shoulder and Elbow Phase Portraits of Subject 05 present circular shapes that are very similar to those of healthy subjects.

Phase Angle

The same comments as for Subject 04 apply, with the difference that steeper slopes are found in almost all cases, which probably indicates that Subject 05 presents a similar elbow-shoulder coordination strategy to perform most of the tasks.

Figure 18.3.1.: Shoulder (red) and elbow (blue) flexion extension of pathological Subject 05 compared to the healthy subjects. Mean angular displacement of healthy subjects is represented in faded colors and the gray ribbon indicates one standard deviation. For pathological Subject 05 both repetitions are shown in bright red and blue. The distribution of facet graphics match with the actual spatial distribution of targets.
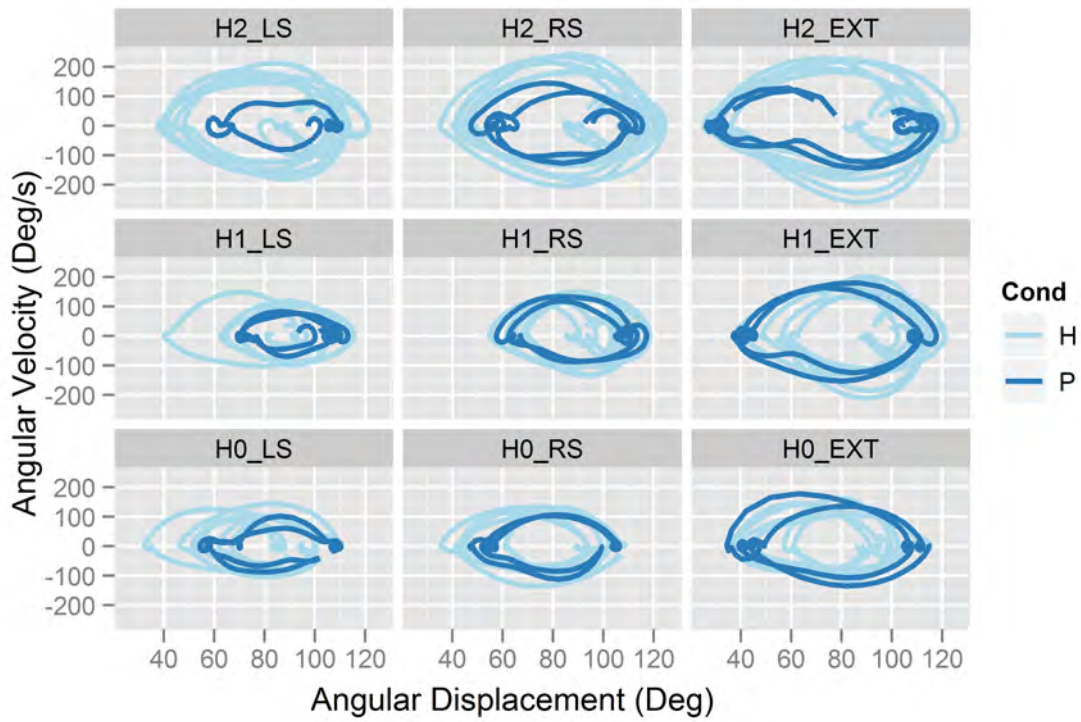
Figure 18.3.2.: Elbow flexion-extension Phase Portrait: relationship between elbow Angular Velocity and elbow Angular Displacement along time of pathological Subject 05 (bright blue) compared to the healthy subjects (faded blue). For all subjects both repetitions are shown. The distribution of facet graphics match with the actual spatial distribution of targets.
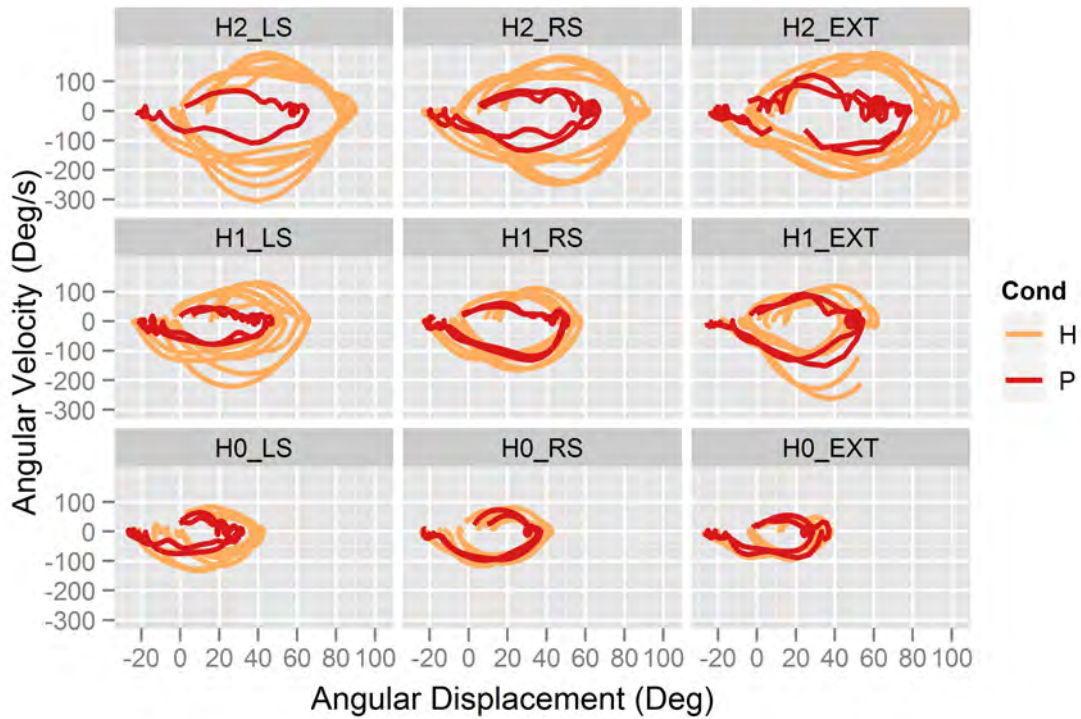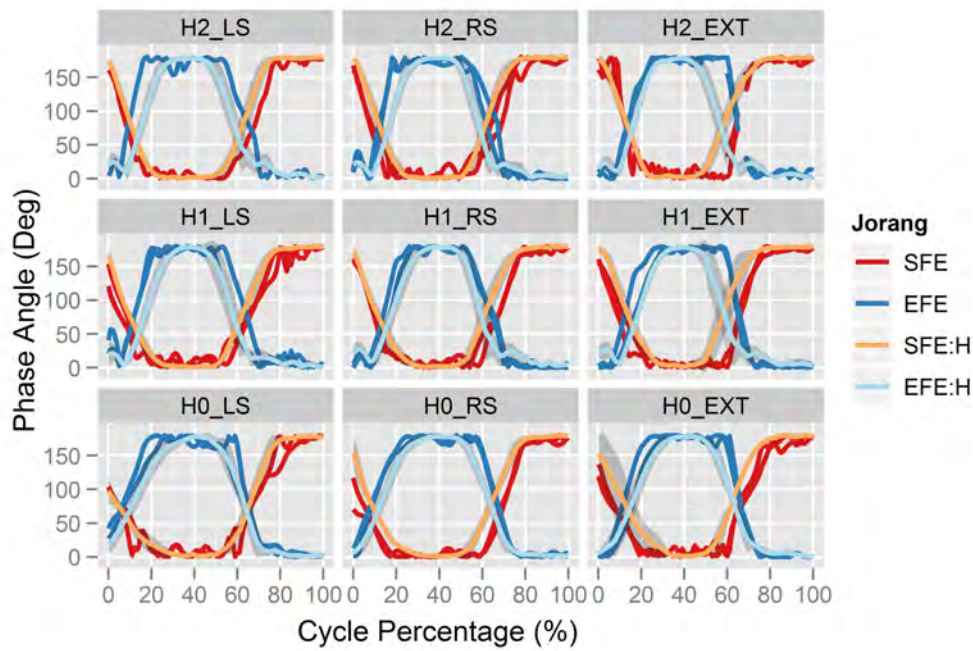

Figure 18.3.3.: Shoulder flexion-extension Phase Portrait: relationship between elbow Angular Velocity and elbow Angular Displacement along time of pathological Subject 05 (bright red) compared to the healthy subjects (faded red). For all subjects both repetitions are shown. The distribution of facet graphics match with the actual spatial distribution of targets.

Figure 18.3.4.: Phase Angle of the shoulder (red) and elbow (blue) flexion-extension of pathological Subject 05 compared to the healthy subjects. Mean Phase Angle of healthy subjects is represented in faded colors and the gray ribbon indicates one standard deviation. For pathological Subject 05 both repetitions are shown in bright red and blue. The distribution of facet graphics match with the actual spatial distribution of targets.

18.4. Pathological Subject 06

Pathological Subject 06 was not able to perform the task for targets placed at height H2. In addition, Subject 06 was not able to perform elbow flexion-extension and thus the rest of target positions were adapted to his maximum arm length.

Angular Displacement

Figure 18.4.1 shows that pathological Subject 06 has very short range of motion in both elbow and shoulder flexion-extension. The Shoulder angular displacement presents a maximum flexion of 40°, and elbow flexion-extension remains close to 100° in all the cycle. Due to the lack of elbow flexion-extension, Subject 06 took advantage of the *trunk flexion-extension* to place the bottle at the target positions (Figure 18.4.2).

Phase Portrait

In agreement with the findings described in the Angular Displacement section, the Phase Portraits of elbow and shoulder flexion-extension (Figures 18.4.3 and 18.4.4) show that the shoulder flexion-extension presents a larger range of motion and higher angular velocities than the elbow flexion-extension, which angular velocities are close to 0 deg/s.

Phase Angle

Because of the very reduced motion of the upper extremity of Subject 06, Phase Angle analysis is irrelevant in this case.
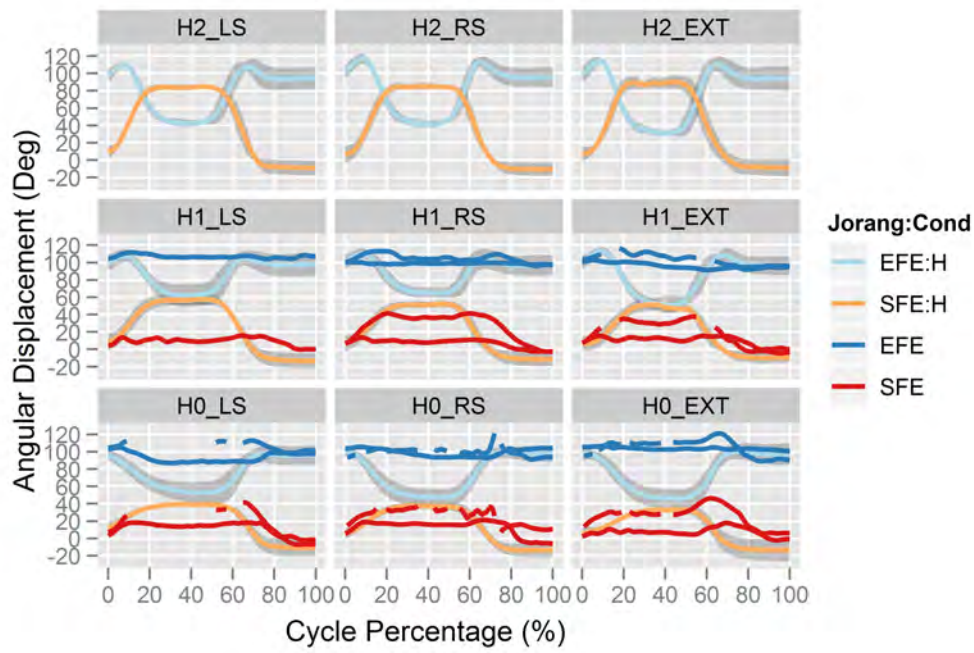
Figure 18.4.1.: Shoulder (red) and elbow (blue) flexion extension of pathological Subject 06 compared to the healthy subjects. Mean angular displacement of healthy subjects is represented in faded colors and the gray ribbon indicates one standard deviation. For pathological Subject 06 both repetitions are shown in bright red and blue. The distribution of facet graphics match with the actual spatial distribution of targets.
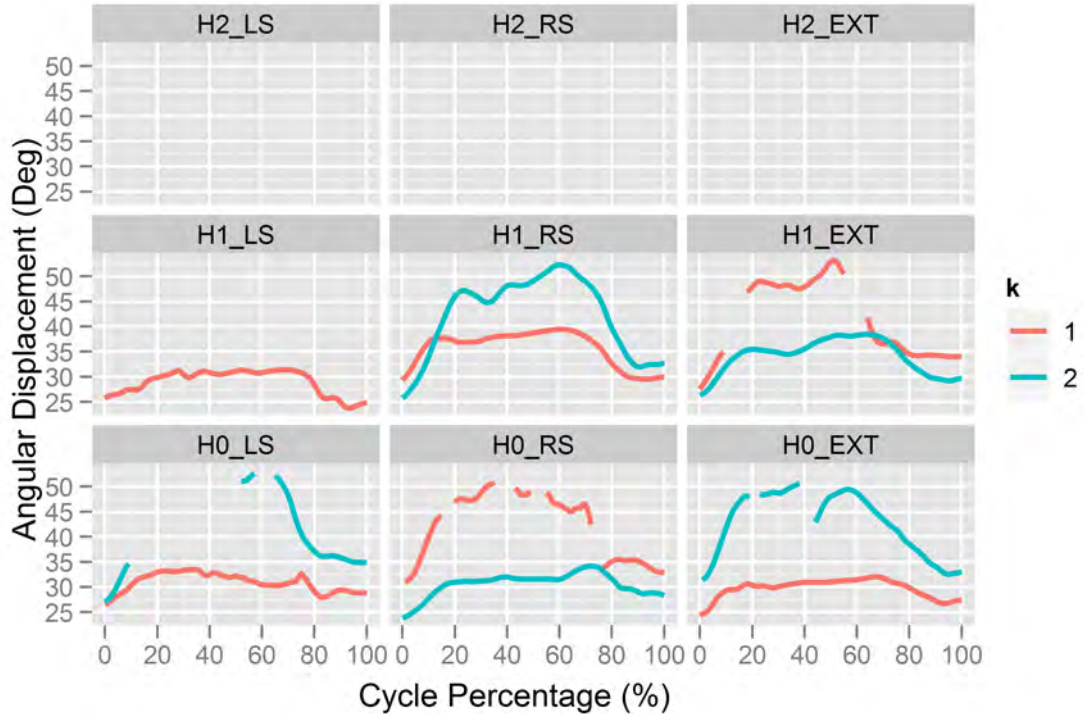
Figure 18.4.2.: Trunk flexion extension of pathological Subject 06. Both repetitions are shown in bright red (k=1) and green(k=2). The distribution of facet graphics match with the actual spatial distribution of targets.
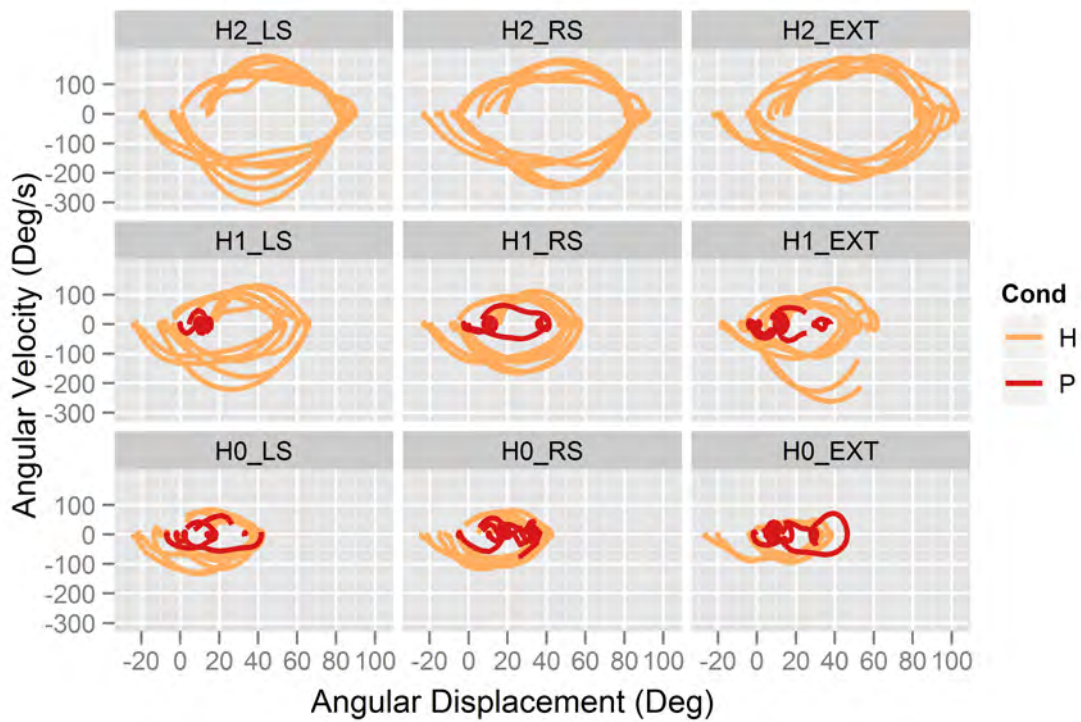
Figure 18.4.4.: Shoulder flexion-extension Phase Portrait: relationship between elbow Angular Velocity and elbow Angular Displacement along time of pathological Subject 06 (bright red) compared to the healthy subjects (faded red). For all subjects both repetitions are shown. The distribution of facet graphics match with the actual spatial distribution of targets.
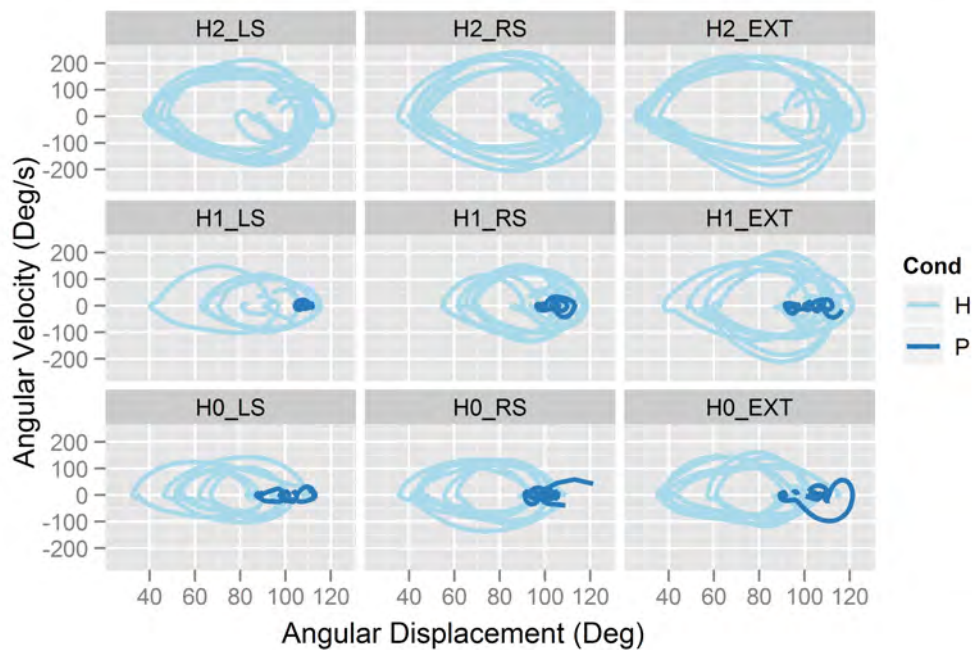
Figure 18.4.3.: Elbow flexion-extension Phase Portrait: relationship between elbow Angular Velocity and elbow Angular Displacement along time of pathological Subject 06 (bright blue) compared to the healthy subjects (faded blue). For all subjects both repetitions are shown. The distribution of facet graphics match with the actual spatial distribution of targets.

19. Dynamic and energetic analysis

This section presents the results of the *Dynamic Analysis* of the upper arm in order to solve the shoulder and elbow flexion-extension moments. The results of such analysis are: (i) elbow and shoulder flexion-extension moments along time and (ii) elbow and shoulder muscular power. It is important to note that the dynamic analysis presents two limitations:

- The model does not have any input on the external forces and moments during the contact between the bottle and the table, which creates a close chain configuration of the system. However, this limitation is not critical as the contact transition represents a small part of the entire cycle ($\sim 5\%$) and the magnitude of the involved contact forces is low.

- The dynamic model assumes that the bottle is attached to the metaphalangeal joint during all the cycle, whereas actually the bottle is only attached during the first phase (while the subject brings the bottle to the target position). This is the part of the analysis that concentrates the clinical interests. The influence of the bottle weight on the dynamic computations during the second phase (while the withdraw of the arm to the initial position) has no significant impact on the results because the bottle weight represents a small part of the total mass of the arm. Furthermore, the software used (KWON3D XP) does not contemplate modifying the system elements within the analysis.

19.1. Healthy Subjects

Joint Moments

Figure 19.1.1 shows the elbow and shoulder flexion-extension joint moments. As described, due to the lack of information during the contact periods, both elbow and shoulder flexion-extension joint moments present small variations around the 50% of the cycle, which do not have any meaningful interpretation and must be neglected. Elbow and shoulder flexion-extension joint moment present a flexor moment during all the cycle which is indicated with the positive sign of each joint moment. The initial values of the joint moment of both joints present similar values (around 1 N·m) while at the end of the cycle the joint moment between both joints present a difference of 1.5 N·m. Note that the shoulder moment is 0 at end of the cycle because the arm is placed at the initial position, while at the same time the elbow moment is 1.5 N·m to maintain the static position of the arm. Shoulder flexion-extension joint moment increases while the arm is bringing the bottle to the target position (shoulder extension), and decreases during the withdrawal of the arm (shoulder extension). To the contrary, the elbow moment decreases while the arm is bringing the bottle to the target position (elbow extension), and increases during the withdrawal of the arm (elbow flexion). Shoulder and elbow flexions decrease the joint moment because the motion is in favor of gravity, and shoulder and elbow extensions increases the joint moment because the motion has to overcome gravity. Amplitude of both signals increase with height, probably because of the increased difficulty of the task: the arm does not have to overcome gravity at height H0, while at height H2 it has to. The joint moments of the shoulder flexion-extension present lower amplitudes when subjects place the bottle at those target positions placed at the external and right shoulder widths (EXT and RS), because other joint rotations (i.e. shoulder abduction-adduction or shoulder internal-external rotations) exert shoulder moments. This change of amplitude is especially notable for target positions placed at the external width where shoulder abduction-adduction is more relevant.

Muscular Power

Figure 19.1.2 shows the resultant muscular power at the elbow and shoulder joints. As described in Section 7.5 *Interpretation of the rigid body dynamics and energetics,* , the muscular power becomes positive if the joint torque and the angular velocity of the motion have the same direction, suggesting concentric contraction of the muscle. A negative muscular power means eccentric contraction of the muscle. Thus, while the arm is bringing the bottle to the target position, the flexor muscles of the shoulder are performing a concentric contraction while the extensor muscles of the elbow are performing an eccentric contraction. Instead, withdrawal of the arm implies that flexor muscles of the shoulder perform an eccentric contraction and the extensor muscles of the elbow perform a concentric contraction. The analyzed motion is cyclic and thus the net change of the mechanical energy due to energy transfer between the proximal and distal segments at the end of the cycle must be 0. Accordingly, Figure 19.1.2 shows that the muscular power of both joints have similar positive and negative areas underneath the curves, which suggest a 0 net change of the mechanical energy.
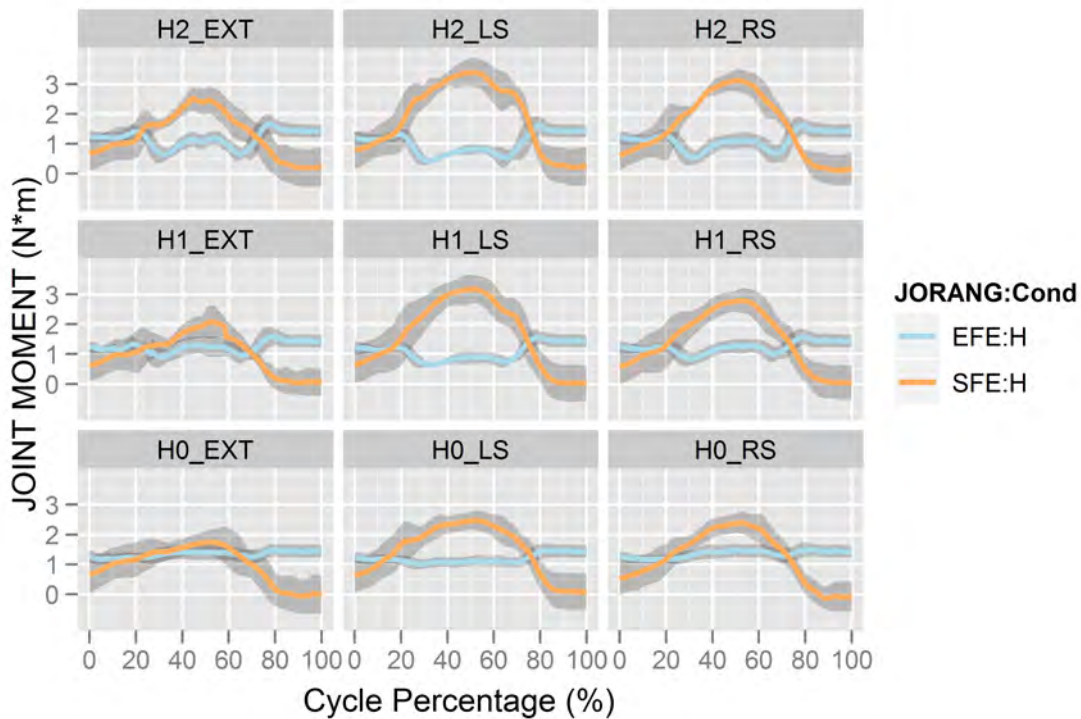
Figure 19.1.1.: Shoulder (red) and elbow (blue) joint moments of flexion extension of healthy subjects 01, 02 and 03. Mean joint moment of healthy subjects is represented in faded red and blue. The gray ribbon indicates one standard deviation. The distribution of facet graphics match with the actual spatial distribution of targets.
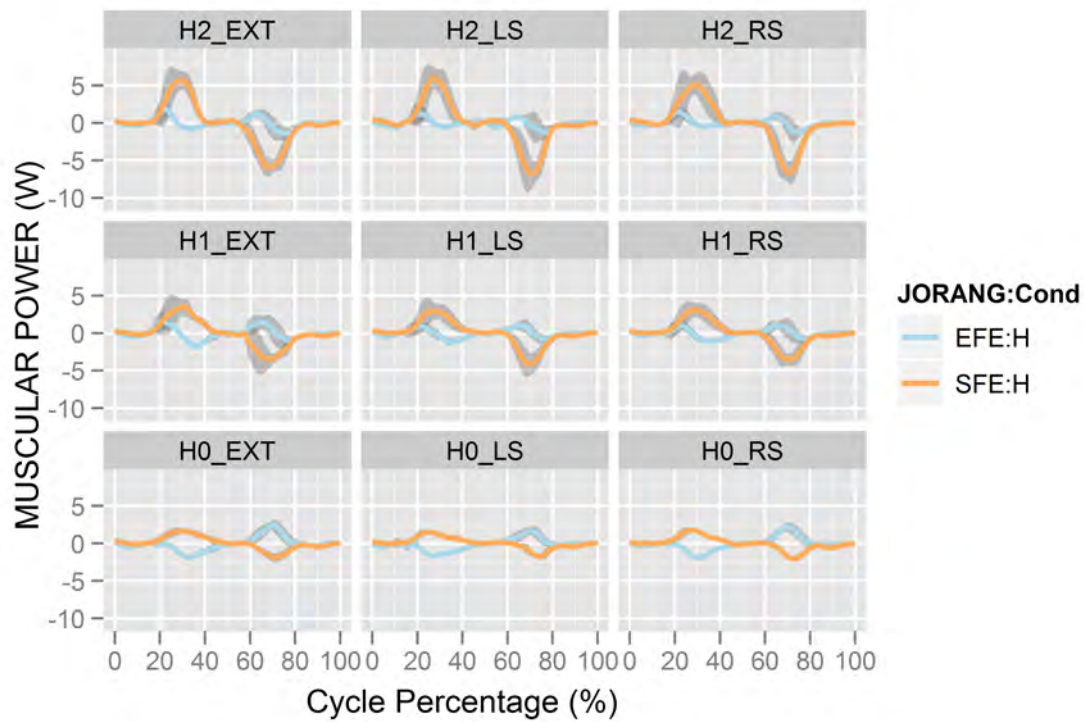
Figure 19.1.2.: Shoulder (red) and elbow (blue) muscular power of healthy subjects 01, 02 and 03. Mean muscular power of healthy subjects is represented in faded red and blue. The gray ribbon indicates one standard deviation. The distribution of facet graphics match with the actual spatial distribution of targets.

19.2. Pathological Subject 04

Joint Moments

Figure 19.2.1 shows that joint moments of Subject 04 are similar to those of healthy subjects. But with lower flexor moments for both shoulder and elbow flexion-extension. Some saw-tooth line shape is also observable.

The amplitude of the joint moments of Subject 04 increases with height, especially for the shoulder flexion-extension joint moment.

When Subject 04 places the bottle at target positions placed at height 0 (H0), the shoulder moment at the end of the cycle becomes negative meaning an extensor moment.

Muscular Power

Figures 19.2.2 and 19.2.3 show that the muscular power of pathological Subject 04 at the shoulder and elbow joints present a saw-tooth shape, which indicates lack of accurate motor control. Since the muscular power is calculated as the product of the joint moment and the relative angular velocity, the small peaks of both signals are amplified when the muscular power is computed.

The amplitudes of the muscular power of the shoulder joint of pathological Subject 04 are lower than those of healthy subjects.
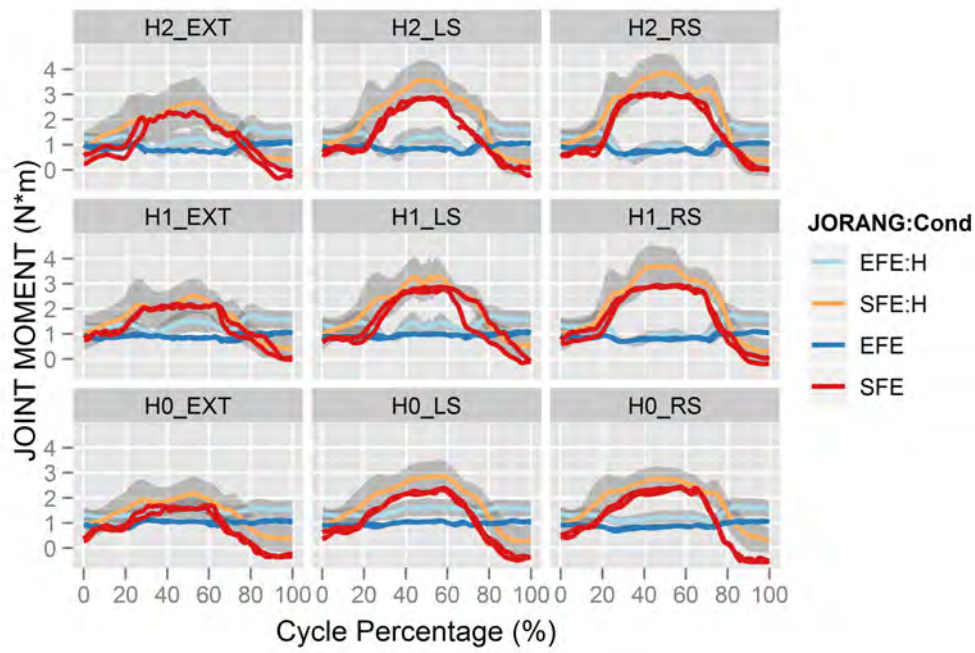
Figure 19.2.1.: Shoulder (red) and elbow (blue) joint moments of flexion extension of pathological Subject 04 compared to the healthy subjects. Mean joint moment of healthy subjects is represented in faded red and blue. The gray ribbon indicates one standard deviation. For pathological Subject 04 both repetitions are shown in bright red and blue. The distribution of facet graphics match with the actual spatial distribution of targets.
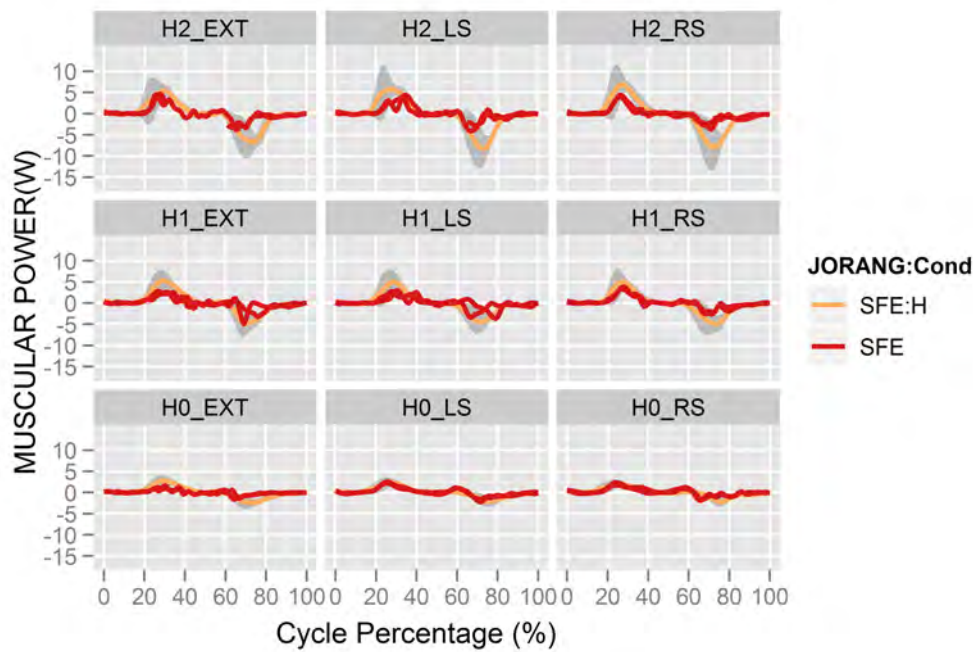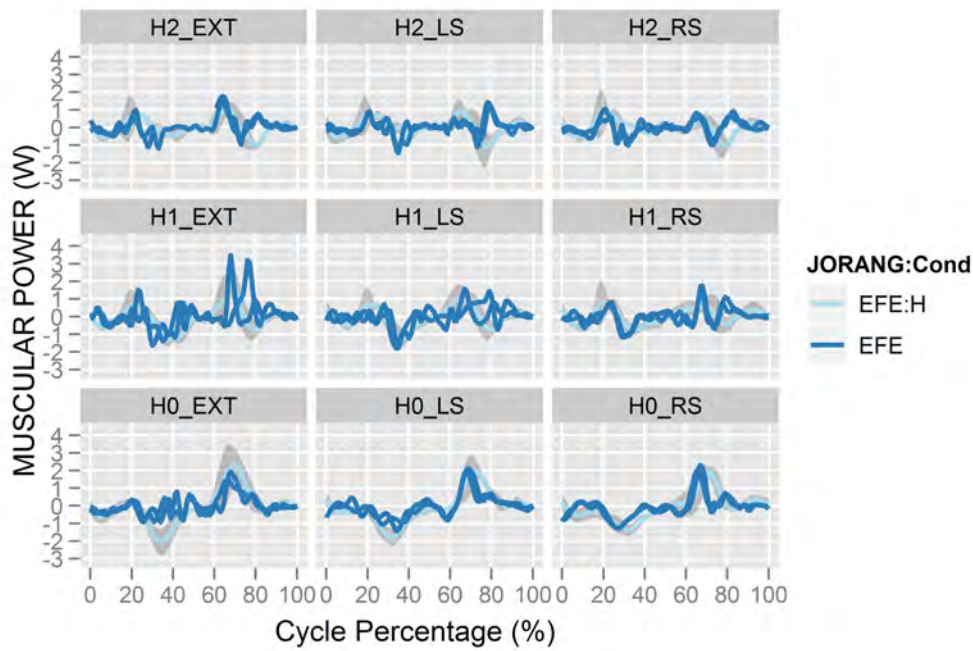

Figure 19.2.2.: Shoulder muscular power of pathological Subject 04 compared to the healthy subjects. Mean muscular power of healthy subjects is represented in faded red, and the gray ribbon indicates one standard deviation. For Subject 04 both repetitions are shown in bright red. The distribution of facet graphics match with the actual spatial distribution of targets.

Figure 19.2.3.: Elbow muscular power of pathological Subject 04 compared to the healthy subjects. Mean muscular power of healthy subjects is represented in faded blue, and the gray ribbon indicates one standard deviation. For Subjects 04 both repetitions are shown in bright blue. The distribution of facet graphics match with the actual spatial distribution of targets.

19.3. Pathological Subject 05

Joint Moments

The joint moments of pathological Subject 05 are also similar to but lower than those of healthy subjects, and also lower than in the case of Subject 04 (Figure 19.3.1). The high frequency variability is also more pronounced in Subject 05, indicating less motor control.

A delay of the shoulder and elbow moments signals respect to those of healthy subjects is observable (especially when bringing the bottle to the target position), but this is caused by the time normalization and is meaningless.

Muscular Power

Figure 19.3.2 and 19.3.3 show that the muscular power of pathological Subject 05 at the shoulder and elbow joints present a saw-tooth shape as in the case of Subject 04.

The amplitudes of the muscular power of the shoulder joint of pathological Subject 05 are also lower than those of healthy subjects. The same delay of the shoulder and elbow muscular power signals as in the case of the joint moments is observable here, but again this is just caused by the time normalization and is meaningless.
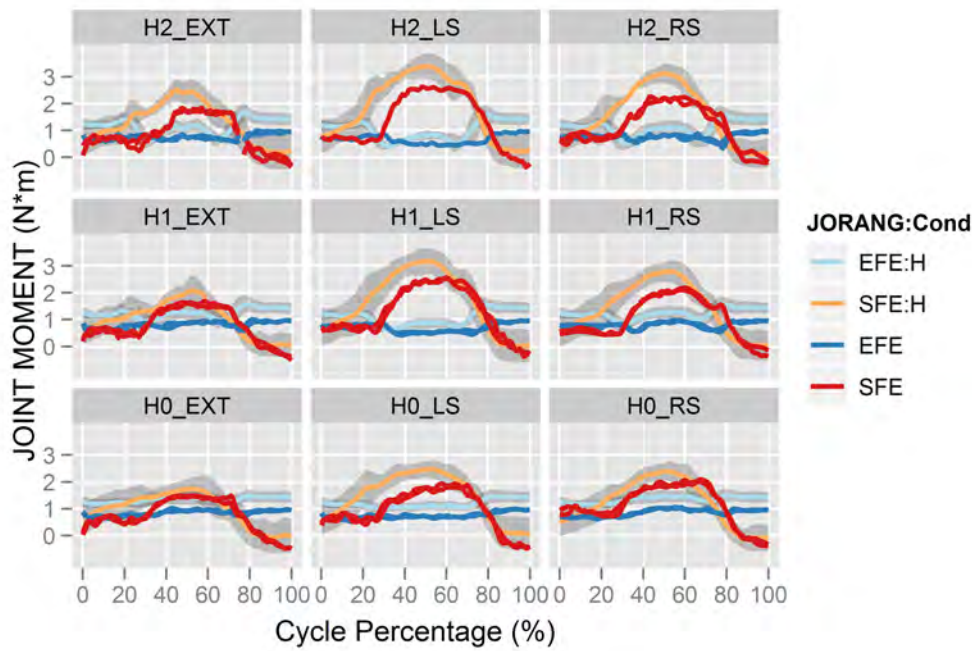
Figure 19.3.1.: Shoulder (red) and elbow (blue) joint moments of flexion extension of pathological Subject 05 compared to the healthy subjects. Mean joint moment of healthy subjects is represented in faded red and blue. The gray ribbon indicates one standard deviation. For pathological Subject 05 both repetitions are shown in bright red and blue. The distribution of facet graphics match with the actual spatial distribution of targets.
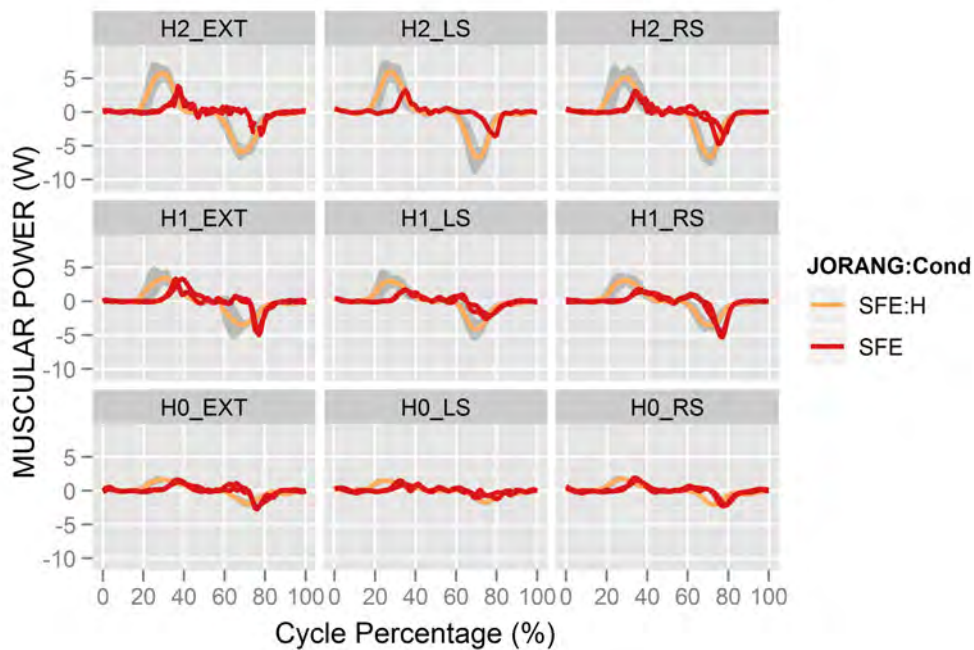

Figure 19.3.2.: Shoulder muscular power of pathological Subject 05 compared to the healthy subjects. Mean muscular power of healthy subjects is represented in faded red, and the gray ribbon indicates one standard deviation. For Subject 05 both repetitions are shown in bright red. The distribution of facet graphics match with the actual spatial distribution of targets.
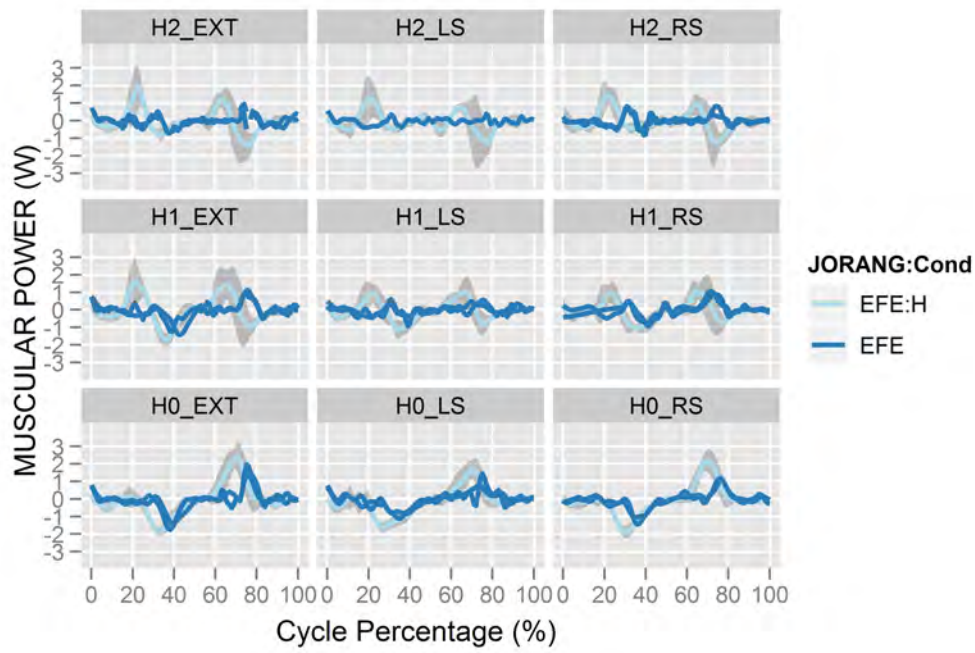
Figure 19.3.3.: Elbow muscular power of pathological Subject 05 compared to the healthy subjects. Mean muscular power of healthy subjects is represented in faded blue, and the gray ribbon indicates one standard deviation. For Subjects 05 both repetitions are shown in bright blue. The distribution of facet graphics match with the actual spatial distribution of targets.

19.4. Pathological Subject 06

Because of the very reduced motion of the upper extremity of Subject 06, Dynamic analysis is irrelevant in this case.

Part VI.

Conclusions and Future Work

20. Conclusions

Conclusions from the Internship

1. Interacting with patients and clinic specialists is essential to understand how neurological disorders impact on the patient's Activities of Daily Living and thus state a meaningful work plan for any engineering study on this field. The experience gained thanks to my participation in the activities of the Functional Rehabilitation Department at the *Institut Guttmann* indicated that:

   a) The progression of the patients through the complex rehabilitation process has to be evaluated systematically.

   b) Nowadays, clinical assessment of functional capacity of the upper extremities is based on subjective, qualitative observational motion analysis, which is solely dependent on the physician's experience and intuitive understanding of human motion.

   c) Objective quantification of rehabilitation progress is necessary for the improvement of clinical treatment methods and rehabilitation strategies, and to prevent injury.

Conclusions from the Literature Review

1. The literature review indicates a general agreement on the need to standardize the upper extremity motion analysis protocol in order to achieve a better communication among researchers and clinicians. A significant step towards standards to define joint coordinate systems of various joints for the reporting of human joint motion has been made by the ISB (Wu et al., 2005), and these standards have been followed in this study. In addition, Kontaxis et al. (2009) presented a proposal of a framework for the definition of standardized protocols for upper extremity motion analysis.

Conclusions from the Development of the Project

1. The marker model and the reaching task defined in this project are appropriate for acquiring motion data of the upper extremity of patients with neurological disorders through an Optoelectronic System. This success is based on a design that has taken into account daily experience in rehabilitation facilities and has benefited from interaction with specialized personnel: the marker model has been designed for specific patients with neurological disorders and for a particular motion capture system. The task that is performed by the subjects for the motion capture is an abridged summary of basic Activities of Daily Living, agreed with rehabilitation personnel after numerous assays and approved by clinicians. The following remarks must be highlighted in this context:

   a) There is a trade-off between the signal accuracy when using joint markers (Method 1) and the more comprehensive but noisier register when using segment markers (Method 2). This study presents a well suited combination of segment markers with joint markers, which requires an static trial to register the relative relations between the positions of segment markers (marker cuffs) and those joint markers that are removed in the dynamic trial. The joint marker location follows ISB recommendations.

   b) The registered signals of the joint markers (Method 1) present higher SNR values than segment markers (Method 2) for those frequencies providing meaningful information (0Hz - 3Hz). SNR values of Method 2 approach those of Method 1 if the signal is processed with a Butterworth filter and a cut-off frequency of 3Hz.

   c) Marker cuffs (Method 2) are subject to displacements by skin motions during segment rolling (internal rotation) and muscular contraction, and should be placed at the proximal part of the segments to reduce this problem. This method should be only used when occlusion problems occur during the recording of the segments' motion.

2. The presented Rigid Body Biomechanical Model provides a convenient simplification of the upper extremity motion, while keeping the necessary detail for rehabilitation monitoring of subjects with neurological disorders

   a) In contrast to previous upper extremity models, the presented model is able to analyze the grasp motion between the first phalange of thumb and the first phalange of the index finger. It is important to take into account that the grasp motion represents an essential motion for the subject to interact with the environment, and thus information about the progress of the grasp function is considered as crucial by clinicians.

   b) The presented model makes possible the kinematic analysis of 10 segments (lower and upper trunk, head, right and left clavicule, upper arm, forearm, palm, thumb and fingers) with a total of 20 DoF during the reaching task. The shoulder internal-external rotation presents inaccurate results due to skin motion artifacts produced by the use of marker cuffs.

   c) The presented model makes possible the dynamic analysis of 6 segments (lower and upper trunk, head, upper arm, forearm and palm) and 3 joints (wrist, elbow and shoulder) during the reaching task. Even though the model does not have any input on the external forces and moments during the contact between the bottle and the table, which creates a close chain configuration of the system, the dynamic results are not significantly altered.

3. Fast reporting of biomechanical properties calculated by the model (joint kinematics and dynamics, and trajectories of the joints and segment CoM), which follows clinical standards, provides valuable information for clinicians to achieve a thorough understanding of the patients' upper extremity motion.

   a) The 2D and 3D trajectories of the joints represent valuable information for clinicians and can be used as biofeedback for patients.

4. Comprehensive graphic analysis of Kinematic and Dynamic properties of the elbow and shoulder flexion-extensions has proven able to highlight biomechanical differences between healthy and pathological subjects.

   a) The normalization of the Phase Portraits makes the comparison between subjects possible, but also distorts the shape of the path and therefore the dynamics of the joint motion. The analysis of the Phase Portraits must be carried out without normalization to compare the actual joint motion between healthy and pathological subjects. The normalization is appropriate to extract the Phase Angles.

   b) The Phase Angle plots were useful to compare the differences on the motor control between healthy and pathological subjects.

   c) As the shapes of the paths in the phase portraits are easy to perceive and very distinct between subjects, we propose that this feature could be an important diagnostic trait and could be used to identify dysfunctional patterns of the reaching motion.

20.1. Improvements

- Effort should be made to solve the lack of information on the external forces and moments during the contact between the bottle and the table, which implies that the resulting dynamic data for these contact periods have a lower quality, even if this contact transition represents only a small part of the entire cycle. An optional solution would be to place a 3D force plate at the target position in order to register the external forces and moments during the contacts.

- Clinical indicators should be calculated from the kinetic and dynamic analyses in order to summarize different aspects of the motion.

20.2. Applicability and Future Work

An interesting follow-on of this work would be to use the presented biomechanical model to identify dysfunctional patterns within different pathologies, through the systematic registration of a large number of subjects at different moments of the rehabilitation process. In this case, a large number of healthy subjects should be studied also in order to provide a background reference with statistical significance.

Another interesting application of the biomechanical analysis resulting from this model, is that it can be used to guide the design and control of an upper extremity active orthosis aimed for neuro-rehabilitation in subjects with neurological disorders. Actually, my intention is to follow-up this study at the Technische Universiteit of Delft (TU Delft, The Netherlands) in collaboration with the *Institut Guttmann* in this line.

Acknowledgments

Bibliography

Anatomists, I. C. o.: 1961, *Nomina anatomica: Revised by the International Anatomical Nomenclature Committee appointed by the Fifth International Congress of Anatomists held at Oxford in 1950, and approved by the Sixth and Seventh International Congresses of Anatomists, held in Paris, 1955 and New York, 1960*. Excerpta Medica.

Anglin, C. and U. P. Wyss: 2000, 'Review of arm motion analyses'. *Proceedings of the Institution of Mechanical Engineers, Part H: Journal of Engineering in Medicine* **214**(5), 541–555.

Angulo Barroso, R., A. Busquets Faciabén, and E. Mauerberg deCastro: 2010, 'El retrato de fase como una herramienta de análisis del comportamiento motor'. *Apunts. Educación Física y Deportes* **102**, 49–61.

Angulo Barroso, R., A. Busquets Faciabén, and E. Mauerberg deCastro: 2011, 'El ángulo de fase y la fase relativa continua para la investigación de la coordinación motora'. *Apunts: Educación física y deportes* **103**, 38–47.

Belanger, E. and A. D. O. Levi: 2000, 'The acute and chronic management of spinal cord injury'. *Journal of the American College of Surgeons* **190**(5), 603–618.

Brown, A., E. Elovic, S. Kothari, S. Flanagan, and C. Kwasnica: 2008, 'Congenital and Acquired Brain Injury. 1. Epidemiology, Pathophysiology, Prognostication, Innovative Treatments, and Prevention'. *Archives of Physical Medicine and Rehabilitation* **89**(3), S3–S8.

C3D.ORG: 2011, 'The 3D Biomechanics Data Standard'. http://www.c3d.org/.

Centre, T. G.: 2011, 'Multi-Sensory Therapy for brain repair'. http://gordonpomarescentre.com/multi-sensory-therapy/brain_tools_functions/.

Davis, R. B., S. Õunpuu, D. Tyburski, and J. R. Gage: 1991, 'A gait analysis data collection and reduction technique'. *Human Movement Science* **10**(5), 575–587.

de Leva, P.: 1996, 'Adjustments to Zatsiorsky-Seluyanov's segment inertia parameters'. *Journal of Biomechanics* **29**(9), 1223–1230.

Dentalarticles: 2011, 'Dental Articles'. http://www.dentalarticles.com/.

Elbaum, J. and D. Benson: 2007, *Acquired Brain Injury: An Integrative Neuro-Rehabilitation Approach*. Springer, 1 edition.

for Surgery of the Hand, A. S.: 2011, 'Tendon Transfer Surgery'. http://www.assh.org/Public/HandConditions/Pages/TendonTransferSurgery.aspx.

Gamage, S. S. H. U. and J. Lasenby: 2002, 'New least squares solutions for estimating the average centre of rotation and the axis of rotation'. *Journal of Biomechanics* **35**(1), 87–93. PMID: 11747887.

Guttmann, I.: 2011, 'Institut Guttmann'. http://www.guttmann.com/.

Hingtgen, B., J. R. McGuire, M. Wang, and G. F. Harris: 2006, 'An upper extremity kinematic model for evaluation of hemiparetic stroke'. *Journal of Biomechanics* **39**(4), 681–688.

Hyder, A. A., C. A. Wunderlich, P. Puvanachandra, G. Gururaj, and O. C. Kobusingye: 2007, 'The impact of traumatic brain injuries: A global perspective'. *NeuroRehabilitation* **22**(5), 341–353.

Jenkins, D.: 1991, *Hollinshead's functional anatomy of the limbs and back*. Philadelphia: Saunders, 6th ed. edition.

Kontaxis, A., A. Cutti, G. Johnson, and H. Veeger: 2009, 'A framework for the definition of standardized protocols for measuring upper-extremity kinematics'. *Clinical Biomechanics* **24**(3), 246–253.

Kwon, Y.: 1998, 'Theoretical Foundation'. http://www.kwon3d.com/theories.html.

Lu, T. W. and J. J. O'Connor: 1999, 'Bone position estimation from skin marker co-ordinates using global optimisation with joint constraints'. *Journal of Biomechanics* **32**(2), 129–134. PMID: 10052917.

Mackey, A. H., S. E. Walt, G. A. Lobb, and N. S. Stott: 2005, 'Reliability of upper and lower limb three-dimensional kinematics in children with hemiplegia'. *Gait & Posture* **22**(1), 1–9.

Nakae, A., K. Nakai, K. Yano, K. Hosokawa, M. Shibata, and T. Mashimo: 2011, 'The Animal Model of Spinal Cord Injury as an Experimental Pain Model'. **2011**. PMID: 21436995 PMCID: 3062973.

Netter, F.: 1997, *Atlas of human anatomy*. East Hanover N.J.: Novartis, 2nd ed. edition.

Petuskey, K., A. Bagley, E. Abdala, M. A. James, and G. Rab: 2007, 'Upper extremity kinematics during functional activities: Three-dimensional studies in a normal pediatric population'. *Gait & Posture* **25**(4), 573–579.

Rab, G., K. Petuskey, and A. Bagley: 2002, 'A method for determination of upper extremity kinematics'. *Gait & Posture* **15**(2), 113–119.

Rau, G., C. Disselhorst-Klug, and R. Schmidt: 2000, 'Movement biomechanics goes upwards: from the leg to the arm'. *Journal of Biomechanics* **33**(10), 1207–1216.

Rettig, O., L. Fradet, P. Kasten, P. Raiss, and S. I. Wolf: 2009, 'A new kinematic model of the upper extremity based on functional joint parameter determination for shoulder and elbow'. *Gait & Posture* **30**(4), 469–476.

Robinson, M. A., G. J. Barton, A. Lees, and P. Sett: 2010, 'Analysis of tetraplegic reaching in their 3D workspace following posterior deltoid-triceps tendon transfer'. *Spinal Cord: The Official Journal of the International Medical Society of Paraplegia* **48**(8), 619–627. PMID: 20065989.

Roux, E., S. Bouilland, A. P. Godillon-Maquinghen, and D. Bouttens: 2002, 'Evaluation of the global optimisation method within the upper limb kinematics analysis'. *Journal of Biomechanics* **35**(9), 1279–1283.

Schmidt, R., C. Disselhorst-Klug, J. Silny, and G. Rau: 1999, 'A marker-based measurement procedure for unconstrained wrist and elbow motions'. *Journal of Biomechanics* **32**(6), 615–621.

Silva, M. P. T. and J. A. C. Ambrósio: 2004, 'Sensitivity of the results produced by the inverse dynamic analysis of a human stride to perturbed input data'. *Gait & Posture* **19**(1), 35–49.

Slavens, B. A. and G. F. Harris: 2008, 'The Biomechanics of Upper Extremity Kinematic and Kinetic Modeling: Applications to Rehabilitation Engineering'. **36**(2-3), 93–125.

Slavens, B. A., P. F. Sturm, and G. F. Harris: 2010, 'Upper extremity inverse dynamics model for crutch-assisted gait assessment'. *Journal of Biomechanics* **43**(10), 2026–2031.

Snell, R. S.: 2000, *Clinical Anatomy for Medical Students*. Lippincott Williams & Wilkins, sixth edition.

Stokdijk, M., J. Nagels, and P. M. Rozing: 2000, 'The glenohumeral joint rotation centre in vivo'. *Journal of Biomechanics* **33**(12), 1629–1636. PMID: 11006387.

Team, R. D. C.: 2011, *R: A Language and Environment for Statistical Computing*. Vienna, Austria: R Foundation for Statistical Computing.

van der Kooij, H., B. Koopman, and F. C. van der Helm: 2008, 'Human Motion Control Reader for Delft University course wb2407 and Twente University course 115047'. *Springer Experimental Brain Research* **152**.

Waring, W. P., F. Biering-Sorensen, S. Burns, W. Donovan, D. Graves, A. Jha, L. Jones, S. Kirshblum, R. Marino, M. Mulcahey, R. Reeves, W. M. Scelza, M. Schmidt-Read, and A. Stein: 2010, '2009 Review and Revisions of the International Standards for the Neurological Classification of Spinal Cord Injury'. **33**(4), 346–352. PMID: 21061894 PMCID: 2964022.

Whittle, M.: 2007, *Gait analysis : an introduction*. Edinburgh ;;New York: Butterworth-Heinemann, 4th ed. edition.

Wickham, H.: 2009, *ggplot2: elegant graphics for data analysis*. Springer New York.

Wilkinson, L.: 2005, *The Grammar of Graphics*. Springer, 2nd edition.

Williams, S., R. Schmidt, C. Disselhorst-Klug, and G. Rau: 2006, 'An upper body model for the kinematical analysis of the joint chain of the human arm'. *Journal of Biomechanics* **39**(13), 2419–2429.

Wu, G., F. C. van der Helm, H. (DirkJan) Veeger, M. Makhsous, P. Van Roy, C. Anglin, J. Nagels, A. R. Karduna, K. McQuade, X. Wang, F. W. Werner, and B. Buchholz: 2005, 'ISB recommendation on definitions of joint coordinate systems of various joints for the reporting of human joint motion–Part II: shoulder, elbow, wrist and hand'. *Journal of Biomechanics* **38**(5), 981–992.

Yang, N., M. Zhang, C. Huang, and D. Jin: 2002, 'Synergic analysis of upper limb target-reaching movements'. *Journal of Biomechanics* **35**(6), 739–746.

Projecte Final d'Estudis
MÀSTER EN ENGINYERIA BIOMÈDICA

Projecte Final d'Estudis presentat el dia   de   de 200
amb la següent Comissió Avaluadora:

Dr.   President

Dr.   Vocal 1

Dr.   Vocal 2

Dr.   Secretari

Amb la qualificació de: